KU LEUVEN

ARENBERG DOCTORAL SCHOOL
Faculty of Engineering Science

centralelille

Univ. Lille, CNRS, Centrale Lille,
UMR 9189 CRIStAL
Ecole Doctorale SPI 072

Design tools for the robust decentralised control of large-scale systems with time-delays

Deesh Dileep

Supervisors:
Prof. dr. Wim Michiels
Prof. dr. Jean-Pierre Richard
Dr. Laurentiu Hetel

Dissertation presented in partial fulfillment of the requirements for the joint-degree of Doctor in Engineering Science (PhD): Computer Science at KU Leuven and Doctor in Control systems, Computing Engineering, Data processing and Images at Centrale Lille.

6 March 2020

Design tools for the robust decentralised control of large-scale systems with time-delays

Deesh Dileep

Thesis committee:
Prof. dr. Carlo Vandecasteele, chairman
Prof. dr. Stefan Vandewalle
Prof. dr. Irinel-Constantin Morărescu
Prof. dr. Maria Domenica Di Benedetto
Dr. Catherine Bonnet
Dr. Goele Pipeleers
Dr. Luca Zaccarian
Supervisors:
Prof. dr. Wim Michiels
Prof. dr. Jean-Pierre Richard
Dr. Laurentiu Hetel

Dissertation presented in partial fulfillment of the requirements for the degree of Doctor in Engineering Science (PhD): Computer Science at KU Leuven and Doctor in Control systems, Computing Engineering, Data processing and Images at Centrale Lille.

6 March 2020



This project has received funding from the European Union's EU Framework Programme for Research and Innovation Horizon 2020 under Grant Agreement No 675080.

All rights reserved. No part of the publication may be reproduced in any form by print, photoprint, microfilm, electronic or any other means without written permission from the publisher.

"*If you want to find the secrets of the universe, think in terms of energy, frequency and vibration.*"

- Nikola Tesla

अनेकसंशयोच्छेदि, परोक्षार्थस्य दर्शकम् ।
सर्वस्य लोचनं शास्त्रं, यस्य नास्त्यन्ध एव सः ॥

It blasts many doubts, foresees what is not obvious |
Science is the eye of everyone, one who hasn't got it, is like a blind ||

- Sanskrit verse from Hitopadesha, 800-950 CE

Acknowledgement

This thesis is a result of my three year expedition to the field of control theory. Even though this period of my life has been challenging, it has also been the most fruitful and exciting so far. First of all, I would like to thank all my supervisors, Prof. Wim Michiels, Prof. Jean-Pierre Richard, and Dr. Laurentiu Hetel, for believing in me, even though my knowledge in control and time-delay systems was limited at the time when I was offered this opportunity. I would also like to thank the European Union for funding this research and providing numerous opportunities to potential researchers.

My first thanks goes to Prof. Wim Michiels for introducing me to the world of control theory with utmost patience. I will forever be indebted to him, since he was kind to share his ideas and provide me with constructive comments in a continuous manner which enabled us to produce many results during this period. I would like to thank Dr. Laurentiu Hetel for supervising and guiding me in the endeavour to networked control systems, LMI techniques, and switched systems. Additionally, his insights on making our papers more attractive to researchers were extremely useful. I would like to thank Prof. Jean-Pierre Richard for supervising me and helping me throughout my stay in Centrale Lille and France. His continuous support, participation in the meetings, and feedback on our results were extremely valuable. His charismatic presentation and courses inspired me to work harder while pursuing my PhD. In the end, I cannot express in words, how honoured and lucky I feel to be supervised by these three well-known experts in their respective domains of systems and control theory.

A part of this thesis, on automated vehicle platooning, was the result of a collaboration with TNO, Helmond, Netherlands. This would not have been possible without fruitful discussions with M. Fusco, J. Verhaegh, and J. Zegers. Guidance from Mauro and Jan, enabled us to formally present the results at a conference. I would like to thank Prof. N. v. d. Wouw for our fruitful discussions on ways to improve the results on sampled-data control and automated vehicular platoons. Furthermore, I would like to thank my thesis committee members, Prof. S. Vandewalle, Dr. G. Pipeleers, Dr. L. Zaccarian, Prof. I.-C. Morãrescu, Dr. C. Bonnet, Prof. M. D. Di Benedetto, and Prof. C. Vandecasteele for accepting the role while sacrificing their valuable time and for their constructive feedback on the thesis.

I am grateful to my colleagues and fellow early stage researchers of the UCoCoS project, Francesco, Pieter, Koen, Dan, Ruben, Youness, Xinyong, Ayush, Marco, Jijju, Haik, Kirill, Libo, Luca, Quentin, and Yanling, who helped me navigate through the world of control theory. I was lucky to be a part of the project along with them. Our visits to multiple bars in different cities, where we discussed about politics, history, science, and analysis and control of dynamical systems for hours elevated my belongingness to the project. Without them, our project meetings could have been far less enjoyable and relaxing. I believe that every PhD candidate should enrich their personal life with social activities or hobbies. For me, this was easy, thanks to SIAM student chapter of KU Leuven and PhD society Leuven. I would like to thank all my friends in Leuven for all the times they joined me for a few beers on the weekends (especially during the bad weather) overcoming their laziness. I am glad that I was able to meet all my colleagues during this endeavour from the VALSE and SHOC teams of the CRIStAL lab and the NUMA unit of KU Leuven. I would like to thank them for organising seminars, social events, and discussing various topics during our meet-ups for lunch which made me feel at home. In addition, I would also like to express my gratitude to the staff of the Computer Science Department, KU Leuven (especially Margot Peeters) for their support.

Finally, I would like to dedicate this thesis to my family. Especially to my mother, Shaja Dileep Kumar, my wife, Gauthami, my brother, Nideesh, my father, S. Dileep Kumar, and my late grand father, K. Krishnankutty.

Contents

Contents i

1 General introduction 1

1.1 Context . . . 1
1.2 Control architectures . . . 6
1.3 Literature on design of decentralised controllers . . . 9
1.4 LTI time-delay systems . . . 11
1.5 Stabilisation and fixed-order controller design . . . 15
1.5.1 Traditional methods for controller design . . . 17
1.5.2 Robust spectral abscissa optimisation . . . 18
1.5.3 Strong $\mathcal{H}_\infty$ norm optimisation . . . 21
1.6 General problem setting . . . 24
1.6.1 Systems with network structure . . . 25
1.6.2 Challenges . . . 26
1.7 Structure of the thesis . . . 27

2 Design of decentralised controllers 31

2.1 Introduction . . . 31
2.2 Design of structurally constrained controllers . . . 35
2.3 Exploiting network structure of systems . . . 39
2.3.1 Decoupling for the stabilisation problem . . . 41
2.3.2 Decoupling for the $\mathcal{H}_\infty$ optimisation problem . . . 42
2.3.3 Discussion . . . 45
2.3.4 Generalisations to distributed controllers . . . 46

2.3.5 Numerical examples . . . 48
2.4 Extension to a scalable algorithm . . . 59
2.4.1 Controller design approach . . . 60
2.4.2 Numerical example . . . 62
2.5 Conclusions . . . 67

3 Decentralised controllers in a network of sampled-data systems 69
3.1 Introduction . . . 69
3.2 MIMO plant and decentralised controllers . . . 72
3.2.1 Sampled-data decentralised control . . . 74
3.2.2 A feedback interconnection interpretation . . . 76
3.3 Stability criterion: generic case . . . 83
3.4 Controller design . . . 86
3.4.1 Generic case . . . 86
3.4.2 Network structure exploitation . . . 88
3.5 Numerical example . . . 93
3.6 Conclusions . . . 101

4 Application to cooperative adaptive cruise control 103
4.1 Introduction . . . 103
4.2 Vehicle model . . . 105
4.3 One vehicle look-ahead platoon with CACC . . . 107
4.4 Stability and performance objectives . . . 110
4.4.1 Platoon stability: spectral abscissa . . . 110
4.4.2 Motivation for string stability . . . 112
4.4.3 Platoon string stability . . . 114
4.4.4 Platoon stability: pseudospectral abscissa . . . 117
4.4.5 Investigating a robust string stabilising controller . . . 118
4.5 Simulation-based studies . . . 119
4.6 Conclusions . . . 122

5 General conclusions 125
5.1 Summary . . . 125
5.2 Future work . . . 127

A Frequently used network topologies **129**

B Small gain theorem **134**

C Well posedness of the systems considered **136**

D Consensus problem in a ring network topology **138**

E Upper-bound for the operators **141**

Bibliography **145**

Abbreviations

CACC	Cooperative Adaptive Cruise Control
DDAE	Delay Differential Algebraic Equation
HANSO	Hybrid Algorithm for Non-Smooth Optimisation
LMI	Linear Matrix Inequality
LTI	Linear Time-Invariant
MIMO	Multiple Input Multiple Output
NCS	Networked Control System
TDS	Time-Delay System

Nomenclature

$A = [a_{i,j}]_{i,j=1}^{n}$	A is a square matrix with element $a_{i,j}$ at i^{th} row and j^{th} column, for all $i = 1, ..., n$ and $j = 1, ..., n$
A^{-1}	inverse of matrix A
$A^{\top}$	transpose of matrix A
A^{*}	complex conjugate transpose of matrix A
$A \otimes B$	Kronecker product of matrices A and B
$[A]_{(i,j)}$	element from i^{th} row and j^{th} column of matrix A
$\text{blkdiag}\{A_1, .., A_n\}$	block diagonal matrix with $A_1, ..., A_n$ as its diagonal blocks
$\mathcal{B}(\bar{\tau}, \epsilon)$	an open ball of radius $\epsilon \in \mathbb{R}_0^+$ centred at $\bar{\tau}$, $\mathcal{B}(\bar{\tau}, \epsilon) := \{\bar{\theta} \in \mathbb{R}^m \, \|\bar{\theta} - \bar{\tau}\| < \epsilon\}$
$\mathcal{C}([a, b]; \mathbb{R}^n)$	banach space of continuous functions mapping $[a, b]$ to $\mathbb{R}^n$
$\mathbb{C}$	set of all complex numbers
$\det(A)$	determinant of matrix A
$\Delta : \mathcal{L}_{2e}(a, b) \to \mathcal{L}_{2e}(c, d)$	operator Δ receives an input belonging to $\mathcal{L}_{2e}(a, b)$ and produces an output belonging to $\mathcal{L}_{2e}(c, d)$
$\mathcal{L}_{2e}(a, b)$	extended $\mathcal{L}_2$ space of all square integrable and Lebesgue measurable functions defined on interval (a, b), with $\mathcal{L}_2$ norm defined as $\|\|q\|\|_2^2 = \int_a^b q(s)^* q(s) \mathrm{d}s$

∘

$\lambda_{\max}(A)$	maximum eigenvalue of matrix A
$\mathbb{N}$	set of all natural numbers
$\mathbb{N}_0$	set of all natural numbers including zero
$\mathbb{R}$	set of all real numbers
$\mathbb{R}^n$	n-dimensional real coordinate space
$\mathbb{R}^+(\mathbb{R}^-)$	set of all positive (negative) real-numbers
$\mathbb{R}_0^+(\mathbb{R}_0^-)$	set of all non-negative (non-positive) real-numbers
$\mathfrak{R}(\lambda)$	real part of complex number λ
$\sigma_i(A)$	i-th singular value of matrix A
trace$[A]$	trace of matrix A
$\text{vec}(A), A = [a_1 \vert \cdots \vert a_n]$	vectorisation of matrix A, $\text{vec}(A) = [a_1 \top \cdots a_n^\top]^\top$
$\mathbb{Z}^+$	set of all positive integers
$\mathbb{Z}$	set of all integers
$\vert\vert \cdot \vert\vert$	euclidean vector norm
$\vert\vert \cdot \vert\vert_2$	$\mathcal{L}_2$ norm of a signal or induced-$\mathcal{L}_2$ gain
$\vert\vert \cdot \vert\vert_{\mathcal{H}_\infty}(\vert\vert \cdot \vert\vert_{\mathcal{H}_2})$	$\mathcal{H}_\infty$ ($\mathcal{H}_2$) norm of an LTI system
$\vert\vert\phi\vert\vert_s$	supremum norm of $\phi \in \mathcal{C}([-\tau_{\max}, 0]; \mathbb{R}^n)$, $\vert\vert\phi\vert\vert_s = \sup_{\tilde{\theta}\in[-\tau_{\max},0]} \vert\vert\phi(\tilde{\theta})\vert\vert_2$

Abstract

The presented thesis is devoted to the design of structured dynamic Linear Time-Invariant (LTI) feedback controllers (such as decentralised, distributed, and overlapping controllers) for linear time-delay systems. Scalable and computationally efficient algorithms are proposed for robust control design. The proposed algorithms use frequency domain-based techniques, grounded in necessary and sufficient conditions for stability.

An approach is initially proposed to design decentralised, distributed, and overlapping fixed-order controllers for generic Multiple-Input Multiple-Output (MIMO) plants with time-delays modelled using Delay Differential Algebraic Equations (DDAEs) (which are flexible in modelling interconnected systems).

As a next step, the approach for generic systems is extended to the case when more information about the interconnection between (sub-)systems is known: a structure exploiting method is proposed. The systems considered are delay coupled identical systems arranged in some network topology, which are to be controlled by identical fixed-order decentralised, distributed, or overlapping controllers. By using the structure exploiting approach, we improve the computational efficiency for the controller design with the number of subsystems. This structure exploiting method reduces the overall design problem to a robust or simultaneous controller design problem for one parameterised subsystem, where the allowable values of the parameter are related to the network topology (eigenvalues of the adjacency matrix of the network graph). We suggest treating these parameters as perturbations (contained in specific intervals or regions in the complex plane) determined by the topology of the network. By using

state-of-the-art (frequency domain-based) optimisation tools for robust control design, we ensure that the achieved stability property, robustness property, and the computational complexity of the controller design problem are independent of the number of subsystems and the network topology.

An extension to design decentralised controllers which are robust against communication imperfections (such as model uncertainties, time-varying delays, aperiodic sampling, and asynchrony) is presented. An input-output $\mathcal{L}_2$ stability criterion is proposed. The approach is based on rewriting the plant and sampled-data controllers as a feedback interconnection of a continuous-time closed-loop system and an uncertainty block (which represents the errors induced by the communication). Furthermore, an efficient (and scalable) control design approach is proposed for a network of quasi-identical sampled-data systems (with non-identical uncertainties and communication imperfections) through structure exploitation.

Finally, an application of the automated heterogeneous (parameter) vehicular platoon using Cooperative Adaptive Cruise Control (CACC) is considered. An approach is proposed to design stabilising controllers that achieve strict $\mathcal{L}_2$ string stability. The predecessor-follower topology of the platoon with CACC is exploited to ensure that the overall computational complexity (for designing identical controllers) is independent of the number and combination of the heterogeneous vehicles in the platoon.

Samenvatting

Dit proefschrift beschrijft het ontwerp van gestructureerde dynamische feedback regelaars zoals gedecentraliseerde, gedistribueerde en overlappende regelaars- voor lineaire tijdsinvariante (LTI) systemen. Er wordt gefocust op algoritmen voor robuust regaal ontwerp met een beperkte rekencomplexiteit en een goede schaalbaarheid. Deze algoritmen zijn gebaseerd op het frequentiedomein en de noodzakelijke en voldoende voorwaarden worden gebruikt voor stabiliteit. Eerst wordt een aanpak voorgesteld om gedecentraliseerde, gedistribueerde en overlappende regelaars met vaste orde te ontwerpen voor generieke meerdere-invoer meerdere-uitvoer (MIMO) -systemen met tijdvertragingen. Deze systemen worden gemodelleerd met behulp van differentiaal-algebraïsche vergelijkingen met vertragingen (DDAEs), omdat deze toelaten om gekoppelde systemen eenvoudig te modelleren.

In een volgende stap wordt een gespecialiseerde methode voorgesteld voor systemen met een bepaalde structuur. De beschouwde systeemklasse bestaat uit netwerken van gekoppelde (deel)systemen met vertraging in de koppeling, aangestuurd door identieke gedecentraliseerde, gedistribueerde of overlappende regelaars, met een vooraf vastgelegde dimensie. Door de netwerkstructuur uit te buiten verbeteren we de rekenefficiëntie voor het regelaar ontwerp met betrekking tot het aantal subsystemen. De methode reduceert het algehele ontwerpprobleem tot een robuust of simultaan regelaar ontwerp voor één geparametriseerd deelsysteem. De toegestane waarden van de parameter zijn gerelateerd aan de netwerkstructuur. Meer specifiek, ze zijn gelijk aan de eigenwaarden van de verbindingsmatrix van de netwerkgraaf. In deze scriptie stellen we voor

om deze parameters te behandelen als verstoringen met waarden in specifieke intervallen of gebieden in het complexe vlak, bepaald door de topologie van het netwerk. Door gebruik te maken van state-of-the-art (frequentiedomein gebaseerde) optimalisatietechnieken voor een robuust controllerontwerp zorgen we ervoor dat het bereikte niveau van de stabiliteit, de robuustheid en de rekencomplexiteit van het ontwerpprobleem van de regelaars onafhankelijk zijn van het aantal deelsystemen en van de netwerkstructuur.

In dit proefschrift presenteren we ook een uitbreiding om gedecentraliseerde regelaars die robuust zijn tegen communicatie-imperfecties, zoals modelonzekerheid, tijdsafhankelijke vertragingen, niet-periodieke bemonstering en a-synchroniteit, te ontwerpen. Hiervoor wordt een input-output $\mathcal{L}_2$ stabiliteitscriterium voorgesteld dat het systeem en de sample data- controllers modelleren als een feedback interconnectie tussen een continue gesloten kring systeem en een onzekerheid, die de imperfecte communicatie voorstelt. Verder wordt een efficiënte (en schaalbare) ontwerpmethode voor sample-data controllers voorgesteld voor een netwerk van quasi-identieke systemen met niet-identieke onzekerheden en communicatie-imperfecties.

Ten slotte beschouwen we het regelen van een heterogene groep voertuigen met behulp van Cooperative Adaptive Cruise Control (CACC). We stellen een aanpak voor om stabiliserende controllers te ontwerpen die strikte $\mathcal{L}_2$ stringstabiliteit garanderen. De voorganger-volger topologie van het peloton met CACC wordt benut om de algehele rekencomplexiteit van het controllerontwerpprobleem te verminderderen. Bovendien is de rekencomplexiteit van het voorgestelde algoritme onafhankelijk van het aantal voertuigen en de volgorde van de voertuigen in het peloton.

Résumé

Cette thèse est consacrée à la conception de contrôleurs dynamiques structurés (décentralisés, distribués, ou imbriqués) pour la commande à base de modèles linéaires à retards (LTI, pour Linear Time-Invariant). Des algorithmes de conception efficaces et extensibles en dimension sont proposés pour garantir la robustesse du contrôle, y compris dans le cas d'un réseau comportant un grand nombre de sous-systèmes. Ils utilisent des techniques du domaine fréquentiel, reposant sur des conditions nécessaires et suffisantes de stabilité.

Une approche est d'abord proposée pour concevoir des contrôleurs d'ordre fixe décentralisés, distribués et imbriqués, pour des processus à retards et à entrées et sorties multiples (MIMO, pour multi-input / multi-output) modélisés grâce à des équations différentielles algébriques avec retard (DDAE), permettant de représenter des systèmes interconnectés génériques. Dans un deuxième temps, cette approche générique est approfondie pour des cas mieux spécifiés : lorsqu'on dispose de davantage d'informations sur l'interconnexion entre sous-systèmes, un procédé d'exploitation de structure est proposé. On considère en particulier que les sous-systèmes sont identiques, couplés par les liens à retards, disposés selon une topologie de réseau donnée, et qu'ils doivent être commandés par des contrôleurs (décentralisés, distribués ou imbriqués) identiques et d'ordre fixe. En exploitant la structure, nous améliorons l'efficacité calculatoire pour la conception du contrôleur, ce qui devient un atout important lorsque le nombre de sous-systèmes augmente. Cette méthode d'exploitation de la structure réduit le problème de conception global à un problème de conception simultanée d'un contrôleur robuste pour un seul sous-système paramétré, où les valeurs

paramétriques autorisées sont liées à la topologie du réseau (valeurs propres de la matrice d'adjacence du graphe de réseau). Nous suggérons de traiter ces paramètres comme des perturbations déterminées par la topologie du réseau et contenues dans des intervalles ou des régions spécifiques du plan complexe. En utilisant des outils récents pour l'optimisation à partir du domaine fréquentiel, nous garantissons que la propriété de stabilité obtenue, la propriété de robustesse et la complexité de calculatoire du problème de conception du contrôleur, sont indépendantes du nombre de sous-systèmes et de la topologie du réseau.

Nous présentons ensuite une extension à la conception de contrôleurs décentralisés robustes vis-à-vis des incertitudes de modèles (par exemple, lorsque le modèle unique des sous-systèmes n'est qu'une approximation) et des imperfections de communication (retards variables, échantillonnage apériodique, asynchronisme, bruit). Un critère de stabilité entrée/sortie $\mathcal{L}_2$ est proposé. Cette approche repose sur la réécriture du processus et de ses contrôleurs échantillonnées sous la forme d'une interconnexion entre un système en boucle fermée et en temps continu d'une part, et d'un bloc d'incertitude qui représente les imperfections induites par la communication, d'autre part. Comme précédemment, cette approche générique est ensuite considérée en exploitant des informations de structure du réseau, pour conduire à la conception d'un contrôle structuré, efficace et extensible en dimension. On considère ainsi un réseau de systèmes échantillonnés quasi-identiques (c'est-à-dire avec des incertitudes différentes autour d'un modèle de base identique), en tenant compte des imperfections de communication.

Pour finir, ces résultats sont appliqués à la conduite coopérative de véhicules hétérogènes (hétérogénéité paramétrique) utilisant un régulateur de vitesse coopératif adaptatif (CACC, pour Cooperative Adaptive Cruise Control). Une approche est proposée pour concevoir des contrôleurs stabilisants assurant la stabilité chaînée (strict string $\mathcal{L}_2$ stability) d'un convoi de véhicules (platooning). Lorsqu'on considère le problème de la conception de contrôleurs identiques, l'exploitation de la topologie prédécesseur-suiveur du convoi sous CACC permet de garantir que la complexité informatique globale est indépendante du nombre et de la combinaison des véhicules hétérogènes du convoi.

Chapter 1

General introduction

This thesis is dedicated to the topic of distributed control for large scale systems with time-delays. We propose approaches to design distributed controllers for generic time-delay systems. Furthermore, we consider the special case where the systems are composed of a group of subsystems with time-delays (strongly) interacting with each other. For this special case, we propose scalable and computationally efficient algorithms to design distributed controllers which guarantee global objectives while acting and sensing locally. In the following sections within this chapter, we present the context of this thesis, the concept of structurally constrained controllers, linear time-delay systems, and existing tools for the design of centralised and structurally constrained controllers for linear time-delay systems. These concepts are essential to understand the problems considered in this thesis (described at the end of this chapter) and our approaches to tackle them.

1.1 Context

Challenges are arising in science, society, and industry induced by the overgrowing complexity of systems in the hyper-connected world. In general, systems are entities composed of well-defined components. Complexity emerges



Figure 1.1: Some examples of complex systems.

as a result of the interactions (and, in particular, the resulting feedback loops) of the components within the system, which are generally not based on a predetermined plan. The conventional methods used to define a system with reference to its individual components become less reliable. The complexity defies the definition on an element basis as interactions between the elements play a bigger role than the behaviour of the elements themselves.

Electricity transmission and distribution, traffic flow, global banking system, and communication networks are some examples that clearly pose challenges

which include encountering problems that are beyond classical scientific or engineering knowledge. These networks of man-made systems are reaching complexity levels that are beyond the level of human understanding (Aström et al., 2011). Many researchers are focusing on understanding these systems and are trying to develop models that can capture their behaviour accurately. Some examples of the complex systems are also shown in Figure 1.1.

Control theory could be utilised to give a relevant and helpful perspective on understanding and controlling such complex systems. Key concepts in control theory are dynamical system modelling, feedback, adaptation, and robustness. System models for control purposes do not aim at accuracy or exhaustiveness of the representations (which, in complex systems, is neither possible nor desirable), but balance the following trade-offs:

- an abstraction level which is sufficiently rich to catch the complexity and sufficiently simple to be traceable;
- analysis and control methods which are robust enough to compensate for modelling errors and varied enough to suggest constructive ways for understanding/influencing the stability and performance of the complex systems.

In this context, the motivation for this work relies on the fact that the classical controller design methodologies used for such complex systems are, in general, computationally cumbersome and not scalable. Also, for large networks, it is expensive, if not impossible (for example in vehicular platoons), to control all the (sub-)systems using mainstream centralised control strategies.

In the 1990s, distributed control architectures[1] were generally preferred over centralised control due to their practicality and costs involved (Lunze, 1992; Siljak, 2013). This trend seemed to change for some time in the 2000s with the popularisation and development of internet and other wireless communication technologies resulting in Networked Control Systems (NCS) (Bemporad et al., 2010; Donkers et al., 2011; Hetel et al., 2017) which aided centralised control

[1]The terms related to control architectures will be explained in Seciton 1.2. Distributed control architectures include decentralised and overlapping control architectures.

strategies. However, in the recent years, distributed control architectures are gaining popularity (again) resulting from the overgrowing complexity in systems (mainly due to the hyper-connectivity and the enormous amounts of sensors employed). Many researchers acknowledge the need to develop scalable and computationally efficient algorithms that are decentralised and deployable at huge distributed scales which are supported by local decisions and global coordination, see (Lamnabhi-Lagarrigue et al., 2017) and the references therein.

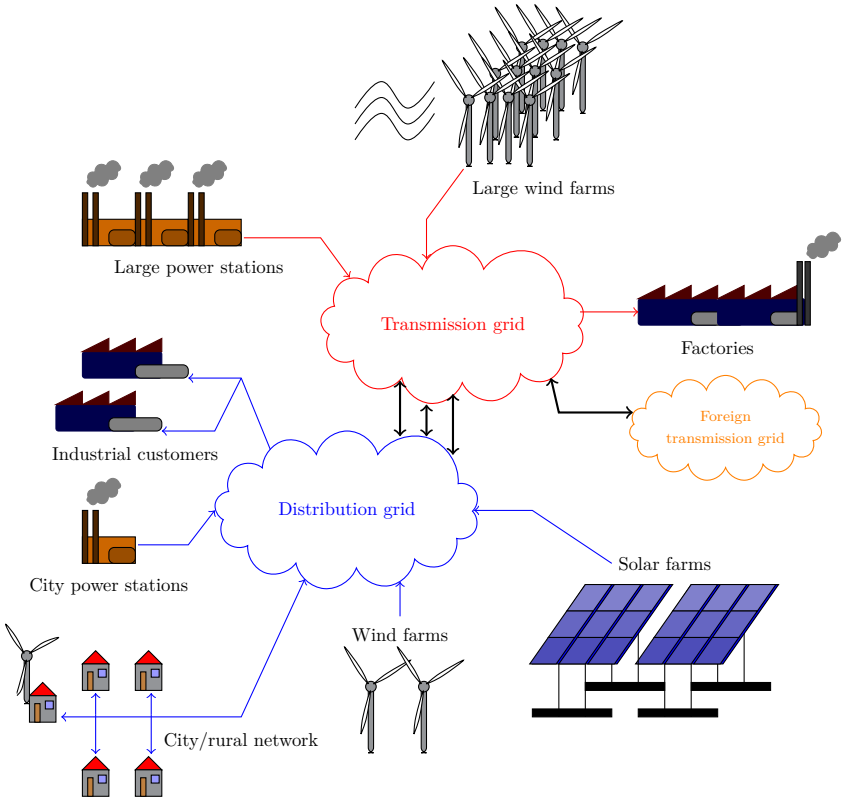

Figure 1.2: A simple layout of modern electricity grids.

Distributed controllers are relevant for many applications. For example, in the application of power systems, distributed and cooperative control techniques have been receiving large attention, see (Arioua et al., 2014; Wang et al., 2015) and the references therein. This is mainly due to the emergence of

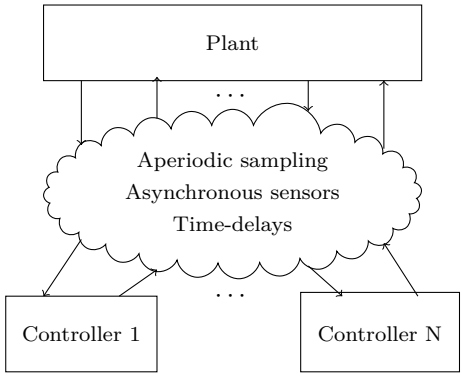

(a) Networked (decentralised) control system

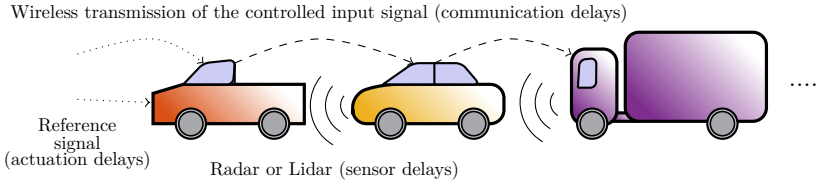

(b) Car following model (CACC configuration)

Figure 1.3: Illustration of the examples for *complex* time-delay systems considered in this thesis.

distributed generating stations, HVDC links, and smart grids, as a result of the environmental concerns, which generate electricity closer to users or loads, see Figure 1.2. This is in contrast to the classical setting wherein large amounts of power were produced at a few locations and transmitted through long distances to cities or industries. Therefore, it is necessary that the distributed controllers implemented in such settings cooperate to ensure that unwanted disturbances are not introduced into the power system due to their individual actions (undesirable counteractions).

Consider, as another application, the control of a platoon of vehicles using Cooperative Adaptive Cruise Control (CACC) technique, see (Darbha et al., 2019; Ploeg et al., 2014a) and the references therein. This is an automated

vehicle following system based on inter-vehicular exchange of data through wireless communication and radar or lidar (see Figure 1.3). One of the main objectives of the controllers is to ensure that the vehicle follows a trajectory or the vehicle in front. Another important objective is to prevent the amplification of disturbances in the upstream direction of vehicles. Again, for this application, it is desirable to design a distributed controller for each vehicle in the platoon. The application to CACC in automated platoon is discussed in more detail within Chapter 4 of this thesis.

Despite their ubiquitous use, designing distributed controllers may be challenging as they have to collectively meet global objectives while acting (and sensing) locally with actuators (and sensors) which may not be reliable all the time. Additionally, time-delays arise in a wide range of applications (such as engineering, natural, or social sciences) due to transport, communication, measurement, control or computation delays (Michiels et al., 2017). Including such time-delays in the system models make them infinite-dimensional (Richard, 2003). In general, state-of-the-art methods for decentralised control do not carry over easily to systems with time-delays. Hence, a shift of the control paradigm is needed, which is the goal of this thesis.

1.2 Control architectures

Automatic control is essential for complex systems such as intelligent transportation systems, robotic systems, manufacturing systems, and many industrial operations. In this thesis, we call the objects (or a group of objects that interact with each other) to be controlled a *plant*. We refer to the overall system that includes both the plant and the control system as the *closed-loop system*. Note that the plant may also be referred to as a system: for instance, in the vehicle platooning problem (Ploeg et al., 2014b), the vehicle (a multi-physical system) is considered to be a plant whose trajectory needs to be controlled in relation to other vehicles.

We consider Linear Time-Invariant (LTI) plants with time-delays in this thesis (Gu et al., 2012). The adopted LTI model implies the assumption that the

superposition principle holds. In general, this assumption corresponds to the local approximation (around some equilibria) or to the use of active linearisation (by feedback control). This assumption may be supported by the fact that we consider systems with delay effects. In the presence of time-delays, most of the constructive stability algorithms are developed in the LTI framework (Fridman, 2014; Gu et al., 2012; Michiels and Niculescu, 2014; Richard, 2003).

A commonly used control architecture is that of the feedback control (also referred to as the closed-loop control architecture). Feedback control system maintains a prescribed relationship between the measured output from sensors and the reference input by comparing them and using the difference as a means of control through actuators. Such means of control enable the system to adjust its performance to meet a desired output response (Ogata, 2010). Alternatively, there are open-loop control architectures wherein the measured output or other plant signals have no effect on the control action. However, this thesis focuses on the design of LTI feedback control systems.

Feedback control of large scale systems may be seen as a feedback control of Multiple Input Multiple Output (MIMO) plants with large number of states, inputs and outputs.

In general, engineers select control architectures in an ad-hoc manner. Hence, there are plenty of control architectures available to study. However, in this thesis, we focus on a few generic architectures (such as decentralised, distributed, and overlapping controllers) which are commonly used, see (Bakule, 2008; Siljak, 2013; van Schuppen and Villa, 2014).

The classical approach would be to design centralised controllers for such systems. This is a simple conceptual framework with one controller and one system. Many procedures are already available for the design of centralised controllers for linear systems. However, the centralised control configuration is often impractical to implement for large-scale systems which could be due to the large costs involved in implementing the communication links, the large delays in communication, or the large computational costs and lack of scalability (such as in power systems (Wang et al., 2015) and automated vehicular platoons (Darbha et al., 2019; Ploeg et al., 2014b)). Model-based controller synthesis can become cumbersome

if the system model is large and the corresponding structure is not exploited. This calls for alternative control strategies such as distributed, decentralised, or overlapping control. Illustrations of some generic control configurations such as centralised, decentralised, distributed, and overlapping control (in the same order) are shown in Figure 1.4. Now we categorize some of the commonly used control configurations, similar to (Bakule, 2008), as follows.

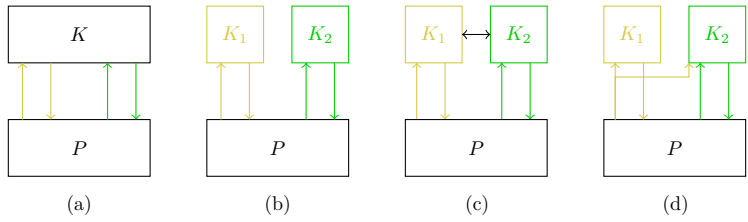

Figure 1.4: Overview of (a) centralised, (b) decentralised, (c) distributed, and (d) overlapping control configurations for the MIMO plant. Here, P is the MIMO plant and K, K_1, and K_2 are the controllers.

Centralised controllers: A MIMO plant is said to have a centralised controller when it receives (sends) all the actuator (sensor) information from (to) the controller (see Figure 1.4-(a)).

Decentralised controllers: A MIMO plant is said to have a decentralised controller when it is controlled by multiple (local) controllers that do not communicate with each other. Also, the corresponding actuator (controlled input) and sensor (measured output) information are unique for each controller (see Figure 1.4-(b)).

Distributed controllers: A MIMO plant is said to be controlled using a distributed controller when a collection of local controllers (of a decentralised controller) communicate some information between each other (see Figure 1.4-(c)). The information shared between sub-controllers may include controller state, measured output, or controlled input.

Overlapping controllers: A MIMO plant is said to have an overlapping controller when the local controllers (of a decentralised controller) share some of the sensor information (measured output) between each other (see Figure 1.4-(d)). Unlike distributed controllers, overlapping controllers do not share any information on controller state or controlled input.

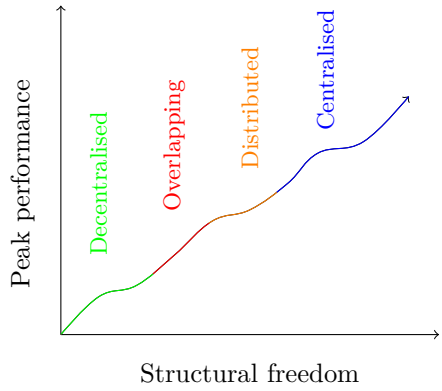

Figure 1.5: A qualitative analysis of the peak performance for the different control configurations considered in this thesis.

Notice that decentralised, overlapping, and distributed controllers can be seen (from a mathematical perspective) as special cases of centralised controllers with some fixed structure (due to constraints in communication), see Figure 1.5. These controllers are structured in the sense that some elements of the corresponding gain or coefficient matrices may have a fixed value (such as zero). Structure for the controller may also arise from predetermined conditions or from other given structures such as a PID controller.

The communication or implementation costs and time-delays involved when using (localised) decentralised controllers may be minimal in comparison to other control configurations. However, the lack of interaction between the controllers and the lack of consideration of any information from neighbouring sensors or actuators could limit their achievable performance. Therefore, distributed or overlapping controllers maybe preferred over decentralised controllers for some applications such as power systems and intelligent transportation systems.

1.3 Literature on design of decentralised controllers

In this section, some of the techniques available to design LTI decentralised feedback controllers for LTI plants (without time-delays) are presented from

the rich literature on the topic. We focus on these works due to their relevance to this thesis. We refer to (Lunze, 1992; Siljak, 2013) for a general overview of the concept of decentralised feedback control. Distributed and decentralised control was a popular research topic in the 90s (Davison and Chang, 1990; Geromel et al., 1999; Ikeda et al., 1993). Recently, the topic of decentralised and distributed control has (again) received the attention of many researchers, see (Alavian, 2017; Alavian and Rotkowitz, 2015a; Bakule, 2008; Bauer et al., 2013; Thomas et al., 2018; van Schuppen and Villa, 2014) and the references therein, due to the overgrowing hyper-connectivity of modern large-scale systems and the enormous amounts of sensors employed.

In (Savastuk and Siljak, 1994), an optimal decentralised control using the classical method of Lagrange was presented. The authors in (Savastuk and Siljak, 1994) formulated the decentralised information structure constraints as differential equations, which were added to the equations of motion to form a suitable set of constraints for the minimization of a cost functional.

In (Stankovic et al., 2000), an overlapping control law was proposed for an automated vehicular platoon. It was obtained by using the inclusion principle, that is, by decomposing the original system model using an appropriate input or state expansion. The Linear Quadratic (LQ) control technique was applied to these locally extracted subsystems. The local quadratic criteria directly reflected the desired system performance. However, optimization was carried out by using a sequential algorithm adapted to the lower block triangular structure of the closed-loop system model, which was specific to the application. Contraction to the original space provided a decentralised controller for the application which preserved the asymptotic stability and the steady-state behaviour of the controller obtained in the expanded space.

In (Zecevic and Siljak, 2004), an approach was proposed to design decentralised controllers in the time domain using Lyapunov-based stability conditions expressed in terms of Linear Matrix Inequalities (LMIs). The resulting control was robust with respect to uncertainties, and was based on imposing several types of information structure constraints on the LMIs.

In (Lavaei et al., 2008), a design approach for decentralised controller was

proposed which consisted of local estimators so that each controller estimates the state of the whole formation. It was noted that due to the cooperation between these decentralised controllers, the overall control structure could be considered as a centralised controller.

The tuning of a decentralised PID controller for a large flexible space structure in (Shi et al., 2016) uses the frequency domain-based direct optimisation approach. In (Shi et al., 2016) and (Davison et al., 2009), a performance index was proposed which was motivated by *optimal transient shaping* and the index was minimised by tuning PID controller gains under the constraint that the system is stable for systems.

Additionally, in (Alavian and Rotkowitz, 2013), (Alavian and Rotkowitz, 2015b), (Alavian, 2017) and the references therein, it is shown that for particular combinations of LTI plants and admissible controllers, the $\mathcal{H}_\infty$ design problem can still be recast as a convex optimisation problem.

1.4 LTI time-delay systems

The goals of this thesis include the design of decentralised controllers for time-delay systems. Hence, in this section, we (briefly) introduce time-delay systems and some of the existing tools available to design (centralised) controllers for them. We refer to (Fridman, 2014; Gu et al., 2012; Michiels and Niculescu, 2014; Richard, 2003) and the references therein for more detail on time-delay systems and their properties. Time-delays are inherent to various complex systems and often deteriorate the system performances. Systems with time-delays are often known as time-delay systems, hereditary systems, systems with after-effect, and systems with time-lag (Gu et al., 2012). Analysis of time-delay systems has become attractive to researchers due to their prevalence in applications such as chemical processes, engine cooling systems, aircraft systems, hydraulic systems, irrigation channels, supply networks, communication channels, electrical power systems, and metallurgical processing systems (Alanis and Sanchez, 2017). Time-delays may arise in these systems due to transport, communication, measurement, control, or computation delays. The time-delays

may be known or unknown, constant or time-varying, deterministic or stochastic depending on the system that is considered (Alanis and Sanchez, 2017). Delays represent a versatile modeling tool for communication effects, since it can gather distance, packet loss, sampling, and asynchronism phenomena into one unique time effect (Kruszewski et al., 2012; Richard and Divoux, 2007; Zhang et al., 2014). In this thesis, the applications of sampled data control system and automated vehicle following system are considered in Chapters 3 and 4, respectively. Many other examples of time-delay systems include congestion control in communication networks, neural networks, populations dynamics, epidemics, control of turbulent flows, and pressure control, see (Anthonis et al., 2007; Erneux, 2009; Feingesicht et al., 2017; Foley and Mackey, 2009; Fridman, 2014; Hollot et al., 2002; Kolmanovskii and Myshkis, 1999; Sipahi et al., 2011)

In this work, we consider linear time-invariant plants with constant time-delays described by Delay Differential Algebraic Equations (DDAEs), see (Gumussoy and Michiels, 2011; Michiels, 2011) and the references therein, in the most general form

$$\mathcal{P}: \begin{cases} E_p \dot{x}_p(t) & = A_{p0}x_p(t) + \sum_{i=1}^{m} A_{pi}x_p(t-\tau_i) + B_{p1}u(t) + B_{p2}w(t), \\ y(t) & = C_{p1}x_p(t), \\ z(t) & = C_{p2}x_p(t), \end{cases} \tag{1.1}$$

where $x_p(t) \in \mathbb{R}^{n_p}$ is the instantaneous state (solution) vector at time t. The time-delays are assumed to be time-invariant and satisfy $0 < \tau_i \leq \tau_{\max}$. The state of system (1.1) is a function $x_{p,t}$ corresponding to the past time-interval $[t - \tau_{\max}, t]$. That is, $x_{p,t}(\tilde{\theta}) = x_p(t + \tilde{\theta})$, $-\tau_{\max} \leq \tilde{\theta} \leq 0$, then let $x_{p,0} = \phi$, and $x_p(\tilde{\theta}) = \phi(\tilde{\theta})$, $-\tau_{\max} \leq \tilde{\theta} \leq 0$. Similarly, $u(t) \in \mathbb{R}^{n_u}$ and $y(t) \in \mathbb{R}^{n_y}$ are instantaneous controlled input and measured output vectors at time t, whereas the instantaneous exogenous input and the instantaneous exogenous (or controlled) output are represented as $w(t) \in \mathbb{R}^{n_w}$ and $z(t) \in \mathbb{R}^{n_z}$ respectively. We use the notations $\mathbb{R}$, $\mathbb{R}_0^+$ and $\mathbb{R}^+$ to represent sets of real numbers, non-negative real numbers and strictly positive real numbers respectively, and $x_p \in \mathbb{R}^{n_p}$ is a short notation for $(x_{p1}, ..., x_{pn_p})$.The measured output y is made available to the controller for feedback computation. Throughout the thesis, A,

B, C, D and E (with or without subscript) will be used to represent constant real-valued matrices. We allow the leading matrix E_p in (1.1) to be singular. For well-posedness of system (1.1), we consider the following assumption throughout out this thesis which is satisfied in most practical cases of interest.

Assumption 1 *There exist a pair of matrices U and V such that matrix $U^T A_{p0} V$ is invertible, where the columns of U and V form a minimal basis for the left and right null spaces of matrix E_p respectively.*

Assumption 1 ensures that DDAE (1.1) without inputs is semi-explicit (differentiation index equal to 1) (Fridman, 2002; Gumussoy and Michiels, 2011). This assumption is satisfied by retarded and neutral type time-delay systems considered in this thesis.

For the purpose of defining the solution of system (1.1), we consider its inputs to be zero ($u \equiv 0$ and $w \equiv 0$). Then, a forward solution of (1.1) on the interval $[0, t_0]$, $\forall\ t_0 > 0$, with an initial condition ϕ, is an absolutely continuous function that satisfies the differential equation (1.1) almost everywhere on the interval $[0, t_0]$ (Michiels, 2011). Let us consider the initial condition $\phi \in \mathcal{X}$,

$$\mathcal{X} := \left\{ \phi \in \mathcal{C}([-\tau_{\max}, 0]; \mathbb{R}^{n_p}) : U^{\mathrm{T}} A_{p0} \phi(0) + \sum_{i=1}^{m} U^{\mathrm{T}} A_{pi} \phi(-\tau_i) = 0 \right\},$$

where $U \in \mathbb{R}^{n_p \times \nu}$ is a minimal basis for the right nullspace of E_p (with $\mathrm{rank}(E_p) = n_p - \nu$), such that $U^{\mathrm{T}} E_p = 0$. Then, it is shown in (Fridman, 2002) that for every initial condition $\phi \in \mathcal{X}$, $t_0 > 0$, a forward solution for $(x_p(\phi))(t)$ exists and is uniquely defined on the interval $[0, t_0]$. Here, we use the notation $(x_p(\phi))(t)$ to show that the forward solution in time is dependent on the initial condition ϕ.

Even without the presence of the feed-through terms, input delays, or output delays, the model given by (1.1) allows to describe LTI systems with discrete delays in their most general form, including systems of retarded and neutral type, delays in input and output, non-trivial feed-through, and delayed interconnections of subsystems. This is portrayed below with the help of a simple example.

Example 1.4.1 *Let us consider the presence of time-delays at the controlled input, the measured output and the first-order derivative of the state vector in an LTI system (a neutral type time-delay system),*

$$\begin{cases} \dot{\psi}(t) + e_1\dot{\psi}(t-\theta_1) &= a\psi(t) + b_0u(t) + b_1u(t-\theta_2), \\ y(t) &= c_0\psi(t) + c_1\psi(t-\theta_3) + du(t), \end{cases} \tag{1.2}$$

where a, b_0, b_1, e_1, d, c_0 and c_1 are constants, θ_1, θ_2 and θ_3 are constant time-delays, ψ is the instantaneous state, u is the input, and y is the output. Using dummy variables γ_ψ, γ_u and γ_y, we can rewrite the system as

$$\begin{aligned} \dot{\gamma}_\psi(t) &= a\psi(t) + b_0\gamma_u(t) + b_1\gamma_u(t-\theta_2), \\ 0 &= -\gamma_\psi(t) + \psi(t) + e_1\psi(t-\theta_1), \\ 0 &= -\gamma_u(t) + u(t), \\ 0 &= -\gamma_y(t) + c_0\psi(t) + c_1\psi(t-\theta_3) + d\gamma_u(t), \\ y(t) &= \gamma_y(t). \end{aligned} \tag{1.3}$$

The dummy variables γ_ψ, γ_u and γ_y , defined by the 2nd-4th equations in (1.3), allow to move a delay in the derivative of the state variable (inherent to a neutral type system), in the input and the output to a delay in a (pseudo) state variable, and then remove the feed-through term from the output equation. That is, by defining the new state vector as $x_p(t) = [\gamma_\psi^T(t)\ \psi^T(t)\ \gamma_u^T(t)\ \gamma_y^T(t)]^T$, the LTI system (1.2) can be turned into form (1.1). ∘

Furthermore, as differential equations and algebraic equations modelling connections can be directly included in (1.1), the latter is very amendable for modelling interconnected systems. Due to the generality of system description (1.1), it is possible to consider classes of non-causal systems and systems with impulsive solutions. In order to exclude such systems, Assumption 1 has been consider for well-posedness (Gumussoy and Michiels, 2011). The following section recalls some of the techniques available to analyse and design fixed-order controllers for time-delay systems of the form (1.1).

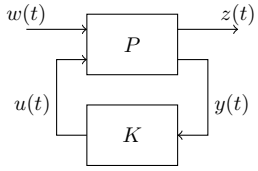

Figure 1.6: The closed-loop system of plant and controller.

1.5 Stabilisation and fixed-order controller design

The system described in (1.1) is to be controlled using a feedback controller with prescribed order "n_c",

$$\mathcal{K}: \begin{cases} \dot{x}_c(t) = A_c x_c(t) + B_c y(t), \\ u(t) = C_c x_c(t) + D_c y(t), \end{cases} \tag{1.4}$$

where $x_c(t) \in \mathbb{R}^{n_c}$ is the controller state vector. Here, the case of $n_c = 0$ corresponds to a static or proportional controller of the form $u(t) = D_c\ y(t)$. The other cases of $n_c \geq 1$ correspond to a dynamic controller as given in (1.4), where A_c is a matrix of size $n_c \times n_c$. Throughout this thesis, we assume that plants of the form (1.1) can be stabilised using a fixed-order controller of the form (1.4). The feedback interconnection of plant (1.1) and controller (1.4) can be described, when defining $x = [x_p^{\mathrm{T}} u^{\mathrm{T}} \gamma_w^{\mathrm{T}} x_c^{\mathrm{T}} y^{\mathrm{T}}]^{\mathrm{T}}$, by the following DDAE (see Figure 1.6),

$$\begin{cases} E\dot{x}(t) &= A_0 x(t) + \sum_{i=1}^{m} A_i x(t-\tau_i) + B w(t), \\ z(t) &= C x(t), \end{cases} \tag{1.5}$$

where

$$E = \begin{bmatrix} E_p & 0 & 0 & 0 & 0 \\ 0 & 0 & 0 & 0 & 0 \\ 0 & 0 & 0 & 0 & 0 \\ 0 & 0 & 0 & I & 0 \\ 0 & 0 & 0 & 0 & 0 \end{bmatrix},\ A_0 = \begin{bmatrix} A_{p0} & B_{p1} & B_{p2} & 0 & 0 \\ C_{p1} & 0 & 0 & 0 & -I \\ 0 & 0 & -I & 0 & 0 \\ 0 & 0 & 0 & A_c & B_c \\ 0 & -I & 0 & C_c & D_c \end{bmatrix}, \tag{1.6}$$

and, for $i = 1, ..., m$, we have

$$A_i = \begin{bmatrix} A_{pi} & 0 & 0 & 0 & 0 \\ 0 & 0 & 0 & 0 & 0 \\ 0 & 0 & 0 & 0 & 0 \\ 0 & 0 & 0 & 0 & 0 \\ 0 & 0 & 0 & 0 & 0 \end{bmatrix}, \; B = \begin{bmatrix} 0 \\ 0 \\ I \\ 0 \\ 0 \end{bmatrix}, \; C^{\mathrm{T}} = \begin{bmatrix} C_{p2} \\ 0 \\ 0 \\ 0 \\ 0 \end{bmatrix}.$$

Now we outline two popular classes of techniques to perform stability analysis of linear TDSs. First, using frequency domain-based techniques, necessary and sufficient conditions for exponential stability are generally expressed in terms of the position of the characteristic roots (eigenvalues) of the system post-Laplace transformation (Apkarian and Noll, 2018; Michiels and Niculescu, 2014; Partington and Bonnet, 2004). Second, using time domain-based techniques, sufficient conditions for exponential stability are generally expressed in terms of LMI using Lyapunov-Krasovskii and Lyapunov-Razumikhin stability conditions (Fridman, 2014).

Note that for well-posedness of the closed-loop system (1.5), Assumption 1 changes to the following assumption.

Assumption 2 *Matrix $U^T(A_{p0} + B_{p1}D_cC_{p1})V$ is invertible.*

Assumption 2 rephrases Assumption 3.1 in (Gumussoy and Michiels, 2011) (see appendix for proof), which ensures that DDAE (1.1) without inputs is semi-explicit (differentiation index equal to 1) and that this property is not altered by the feedback. We refer to (Gumussoy and Michiels, 2011) for more details.

The direct optimisation approach of (Michiels, 2011) and (Gumussoy and Michiels, 2011) may be used to stabilise and subsequently optimise the robustness of the closed-loop system in the frequency domain. In this case, it is possible to directly optimise stability and performance measures as a function of the

parameter vector $\bar{p}$, containing the tunable parameters of the controller, that is,

$$\bar{p} = \text{vec}\left(\left[\begin{array}{c|c} A_c & B_c \\ \hline C_c & D_c \end{array}\right] \right) \tag{1.7}$$

for a non-structured controller of dimension n_c. Notice in (1.6) that all the controller parameters are contained in matrix A_0, which can be emphasized by using the notation $A_0(\bar{p})$. The frequency domain-based direct-optimisation approach is adequate for the design of structurally constrained controllers. We say that an LTI controller is structurally constrained if its coefficient matrices have elements that are fixed (hence, they are not available for design). However, the traditional design methods using LMI approach cannot be (easily) adapted to the case of structurally constrained output-feedback controllers.

First, we briefly discuss the traditional methods available for control design and provide a reasoning for not adopting them. Then, the concepts of the adopted frequency domain-based optimisation technique are recalled.

1.5.1 Traditional methods for controller design

Traditional methods for designing stabilising and optimal $\mathcal{H}_\infty$ controllers for LTI MIMO plants with time-delays are grounded in the Riccati equation and LMI framework (see (Fridman, 2014) and references therein) using sufficient conditions for stability. In general, controllers designed by these methods are not structured and their dimension is equal or larger than the order of the plant (full order controllers).

The classical approach for control design based on matrix inequalities with an unknown output-feedback static controller gain matrix gives rise to a bilinear (non-convex) optimisation problem. Several attempts to solve this optimisation problem can be found in the literature (Chen and Zheng, 2006; Fridman and Shaked, 2002; Li and de Souza, 1997; Zeng et al., 2015; Zhang et al., 2005). For example, in (Barreau et al., 2018), an iterative LMI procedure which takes advantage of the elimination lemma was introduced to solve the bilinear optimisation problem. Intuitively, the problem does not become simpler for the

design of robust and stabilising structured (for decentralised, overlapping, or distributed controllers) or fixed-order controllers for systems with multiple delays at input, output, and state. Therefore, this thesis focuses on using frequency domain-based direct optimisation techniques of (Michiels, 2011) and (Gumussoy and Michiels, 2011) grounded in necessary and sufficient conditions for stability which are adequate for designing structured (decentralised, distributed, PID, and overlapping) and lower-order (or fixed-order) controllers. However, using this approach implies that only LTI systems with constant time-delays can be considered for control design. Then, some nonlinear and time-varying properties of the (linearised) systems may be treated later, on the basis of the resulting LTI controller, using techniques from robust control theory (which are generally conservative). The objective functions used for optimisation of the controller parameters in the frequency domain are described in the following subsections.

1.5.2 Robust spectral abscissa optimisation

In this thesis, we focus on (strong) exponential stability of LTI systems with constant time-delays. The notion of exponential stability (of the null solution) is defined as follows for (1.1) when the inputs are zero (Michiels and Niculescu, 2014).

Definition 1.5.1 *(Exponential stability) The null solution of (1.1), when* $u \equiv 0$ *and* $w \equiv 0$*, is exponentially stable if and only if there exist constants* $\alpha_1 > 0$ *and* $\alpha_2 > 0$ *such that,*

$$\forall\ \phi \in \mathcal{X},\ \forall\ t \geq 0,\ ||(x_p(\phi))(t)|| \leq \alpha_1 \mathrm{e}^{-\alpha_2 t}||\phi||_s,$$

where $||\cdot||_s$ *is the supremum norm,* $||\phi||_s = \sup_{\tilde{\theta}\in[-\tau_{\max},0]} ||\phi(\tilde{\theta})||_2$.

However, plant (1.1) need not be stable and we would like to design a controller that guarantees the exponential stability of the closed-loop system (1.5). For this purpose, the frequency domain-based direct optimisation technique is adopted for the reasons mentioned in Section 1.5.1. The spectral abscissa of

the closed-loop system (1.5) with $w \equiv 0$ is defined as follows,

$$c(\bar{p};\bar{\tau}) = \sup_{\lambda\in\mathbb{C}}\{\mathfrak{R}(\lambda) : \det M(\lambda,\bar{p};\bar{\tau}) = 0\}, \tag{1.8}$$

where $\bar{p}$ is defined in (1.7),

$$M(\lambda,\bar{p};\bar{\tau}) = \lambda E - A_0(\bar{p}) - \sum_{i=1}^{m} A_i \mathrm{e}^{-\lambda\tau_i},$$

$\bar{\tau} \in (\mathbb{R}^+)^m$ is the vector of time-delays ($\bar{\tau} = [\tau_1 \ .... \ \tau_m]^{\mathrm{T}}$), and $\mathfrak{R}(\lambda)$ is the real part of the complex number λ. Notice that we stress the dependence of functions on $\bar{\tau}$ and $\bar{p}$ only when necessary. However, for the optimisation problem, the objective function only has controller parameters ($\bar{p}$) as variables. We use the notation $m(a;b)$ throughout this thesis to express m as a function of variable a, depending on parameter b. The exponential stability of the null solution of (1.5) is equivalent to the condition $c(\bar{p};\bar{\tau}) < 0$ (see (Michiels, 2011)). However, the function $\bar{\tau} \mapsto c(\bar{p};\bar{\tau})$ might not be continuous and could be sensitive to infinitesimal delay changes (in general, as neutral time-delay system could be included in model (1.1)). Therefore, we define the *robust spectral abscissa* $C(\bar{p};\bar{\tau})$ in the following way:

$$C(\bar{p};\bar{\tau}) := \lim_{\epsilon\to 0^+} \sup_{\bar{\tau}_\epsilon\in\mathcal{B}(\bar{\tau},\epsilon)} c(\bar{p};\bar{\tau}_\epsilon). \tag{1.9}$$

In (1.9), $\mathcal{B}(\bar{\tau},\epsilon)$ is an open ball of radius $\epsilon \in \mathbb{R}_0^+$ centred at $\bar{\tau}$, $\mathcal{B}(\bar{\tau},\epsilon) := \{\bar{\theta} \in \mathbb{R}^m : ||\bar{\theta} - \bar{\tau}|| < \epsilon\}$. The sensitivity of the spectral abscissa with respect to infinitesimal delay perturbations has been resolved by considering the robust spectral abscissa, since this function can be shown to be a continuous function of the delay parameters (and also parameters in $\bar{p}$), see (Michiels, 2011). We use the following neutral type example taken from (Michiels, 2011) to show that $C(\bar{p})$ may be greater than $c(\bar{p})$.

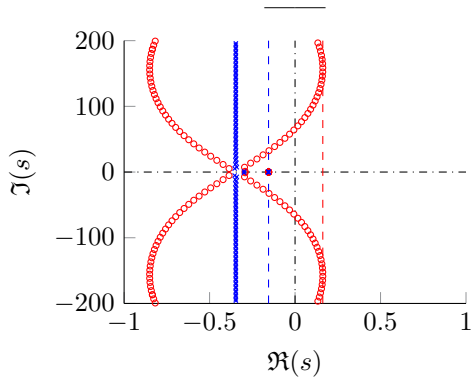

Figure 1.7: Characteristic roots of (1.10) for delays $(\tau_1, \tau_2) = (1, 2)$ (indicated with blue 'x') and $(\tau_1, \tau_2) = (0.99, 2)$ (indicated with red 'o').

Example 1.5.2 *Consider the system*

$$\begin{bmatrix} 1 & 0 \\ 0 & 0 \end{bmatrix} \dot{x}(t) = \begin{bmatrix} 0 & -\frac{1}{8} \\ -1 & 1 \end{bmatrix} x(t) + \begin{bmatrix} 0 & 0 \\ 0 & -\frac{3}{4} \end{bmatrix} x(t-\tau_1) + \begin{bmatrix} 0 & 0 \\ 0 & \frac{1}{2} \end{bmatrix} x(t-\tau_2). \quad (1.10)$$

In Figure 1.7, we plot the rightmost characteristic roots for two sets of delay values: $(\tau_1, \tau_2) = (1, 2)$ *and* $(\tau_1, \tau_2) = (0.99, 2)$*. The blue dashed line corresponds to the spectral abscissa and the red dashed line corresponds to the robust spectral abscissa of system (1.10) with delays* $(\tau_1, \tau_2) = (1, 2)$*. Thus, although the zero solution is asymptotically stable for* $(\tau_1, \tau_2) = (1, 2)$*, the stability is not robust to an infinitesimal delay perturbation.*

We now define the concept of strong exponential stability.

Definition 1.5.3 *The null solution of (1.5) when* $w \equiv 0$ *is strongly exponentially stable if there exists a number* $\epsilon > 0$ *such that the null solution of*

$$E\dot{x}(t) = A_0 x(t) + \sum_{i=1}^{m} A_i x(t - (\tau_i + \delta\tau_i)))$$

is exponentially stable for all $\delta\bar{\tau} \in \mathbb{R}^m$ *satisfying* $||\delta\bar{\tau}|| < \epsilon$ *and* $\tau_i + \delta\tau_i \geq 0,\ i = 1, ..., m.$

In (Michiels, 2011) it has been shown that the null solution is strongly exponentially stable iff $C(\bar{p}) < 0$. To obtain a strongly exponentially stable closed-loop system and to maximise the exponential decay rate of the solutions, the tunable controller parameters (in $\bar{p}$) are tuned for minimising robust spectral abscissa, that is, they are obtained by minimising

$$\min_{\bar{p}} C(\bar{p}). \tag{1.11}$$

1.5.3 Strong $\mathcal{H}_\infty$ norm optimisation

The $\mathcal{H}_\infty$ norm was introduced in the 1970s and early 1980s, see (Helton, 1978; Tannenbaum, 1980; Zames, 1981). Subsequently, the $\mathcal{H}_\infty$ methods were developed and are now routinely used for control design. The $\mathcal{H}_\infty$ norm may be used for designing systems with optimal (energy) gain from input disturbances w to some output signal z. Additionally, the robustness of stability for systems with parametric uncertainties can be recast in terms of the $\mathcal{H}_\infty$ norm. In this thesis, the system performance levels are expressed in terms of the $\mathcal{H}_\infty$ norm.

The transfer function matrix from w to z of the system represented by (1.5) is given by

$$G(\lambda, \bar{p}; \bar{\tau}) := C\Big(\lambda E - A_0(\bar{p}) - \sum_{i=1}^{m} A_i \mathrm{e}^{-\lambda \tau_i}\Big)^{-1} B. \tag{1.12}$$

Under assumption of internal stability, the $\mathcal{H}_\infty$ norm of the transfer function matrix given in (1.12) can be expressed as

$$||G(j\omega, \bar{p}; \bar{\tau})||_{\mathcal{H}_\infty} = \sup_{\omega \in \mathbb{R}} \sigma_1(G(j\omega, \bar{p}; \bar{\tau})), \tag{1.13}$$

where σ_1 is the maximum singular value

$$\sigma_1(G(j\omega, \bar{p}; \bar{\tau})) = \sqrt{\lambda_{\max}(G(j\omega)^* G(j\omega))}, \tag{1.14}$$

of the matrix $G(j\omega)$, where $\lambda_{\max}$ is the maximum eigenvalue of a matrix. If $G(s)$ is a scalar function, then $||G||_{\mathcal{H}_\infty} = \sup_{\omega \in \mathbb{R}} |G(j\omega)|$. The $\mathcal{H}_\infty$ norm can also be defined in the time domain. For this purpose, let $\mathcal{L}_2[0, \infty)$ be the $\mathcal{L}_2$ space of all square integrable and Lebesgue measurable functions defined on

the time interval $[0, \infty)$. Additionally, let the $\mathcal{L}_2$ norm be defined as

$$||w||_{\mathcal{L}_2} = \sqrt{\int_0^\infty w(t)^* w(t) \mathrm{d}t}. \tag{1.15}$$

Then, it can be shown that the following equality holds (Fridman, 2014)

$$||G||_{\mathcal{H}_\infty} = \sup \left\{ \frac{||z||_{\mathcal{L}_2}}{||w||_{\mathcal{L}_2}} : \ w \ \in \ \mathcal{L}_2[0, \infty), \ w \neq 0 \right\}. \tag{1.16}$$

Therefore, the $\mathcal{H}_\infty$ norm reflects a worst case energy amplification ratio of the output signal energy $||z||_{\mathcal{L}_2}$ to the input signal energy $||w||_{\mathcal{L}_2}$.

Similar to the spectral abscissa function, the function $\bar{\tau} \in (\mathbb{R}^+)^m \mapsto ||G(j\omega, \bar{p}; \bar{\tau})||_{\mathcal{H}_\infty}$ might not be continuous and could be sensitive to infinitesimal delay changes (in general, inherited from the behaviour of the transfer function at high frequencies). We use the following example taken from (Gumussoy and Michiels, 2011) to illustrate this behaviour.

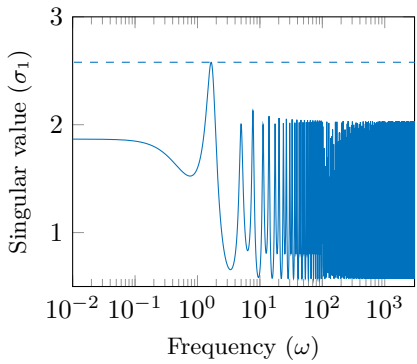

Figure 1.8: The maximum singular value plot of $G(j\omega)$ in (1.17) for $(\tau_1, \tau_2) = (1, 2)$ as a function of ω.

Example 1.5.4 *Consider the transfer function*

$$G(\lambda; \bar{\tau}) = \frac{\lambda + 2.1}{(\lambda + 0.1)(1 + 0.25\mathrm{e}^{-\lambda\tau_1} + 0.5\mathrm{e}^{-\lambda\tau_2})}. \tag{1.17}$$

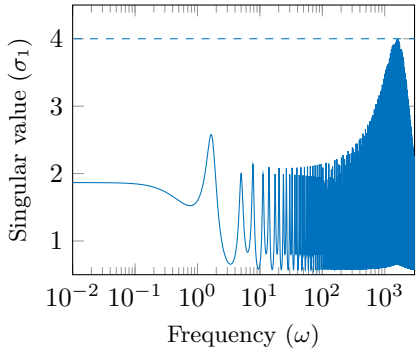

Figure 1.9: The maximum singular value plot of $G(j\omega)$ in (1.17) for $(\tau_1, \tau_2) = (0.999, 2)$ as a function of ω.

We plot the maximum singular values for two sets of delay values: $(\tau_1, \tau_2) = (1, 2)$ *(in Figure 1.8) and* $(\tau_1, \tau_2) = (0.999, 2)$ *(in Figure 1.9) as a function of* ω*. The dashed line in Figures 1.8-1.9 correspond to the* $\mathcal{H}_\infty$ *norms of system (1.17) with delays* $(\tau_1, \tau_2) = (1, 2)$ *and* $(\tau_1, \tau_2) = (0.999, 2)$*, respectively. This example illustrates that the* $\mathcal{H}_\infty$ *norm of the transfer function* G *may be sensitive to small delay perturbations. It has been shown in (Gumussoy and Michiels, 2011) that the* $\mathcal{H}_\infty$ *norm is not continuous in the delays at* $(\tau_1, \tau_2) = (1, 2)$ *for this example and, hence, sensitive with respect to infinitesimal delay perturbations.*

Therefore, under the assumption of strong exponential stability of the null solution, we define the strong $\mathcal{H}_\infty$ norm $|||G(j\omega, \bar{p}; \bar{\tau})|||_{\mathcal{H}_\infty}$ as follows.

$$|||G(j\omega, \bar{p}; \bar{\tau})|||_{\mathcal{H}_\infty} := \lim_{\epsilon \to 0+} \sup_{\bar{\tau}_\epsilon \in \mathcal{B}(\bar{\tau}, \epsilon)} ||G(j\omega, \bar{p}; \bar{\tau}_\epsilon)||_{\mathcal{H}_\infty} \tag{1.18}$$

Contrary to the (standard) $\mathcal{H}_\infty$ norm, the strong $\mathcal{H}_\infty$ norm continuously depends on the delay parameter. The continuous dependence also holds with respect to the elements of the system matrices, which include the elements in $\bar{p}$, as shown in (Gumussoy and Michiels, 2011).

To improve the robustness or performance levels expressed in terms of the $\mathcal{H}_\infty$ norm of (1.13), tunable controller parameters (in $\bar{p}$) can be optimised by solving

the problem

$$\min_{\bar{p}} |||G(j\omega, \bar{p})|||_{\mathcal{H}_\infty}. \tag{1.19}$$

Finally, note that if the closed-loop system corresponds to a delay system of the retarded type, then the robust spectral abscissa and strong $\mathcal{H}_\infty$ norm reduce to the standard spectral abscissa and $\mathcal{H}_\infty$ norm (see (Michiels, 2011) and (Gumussoy and Michiels, 2011)).

1.6 General problem setting

The work in this thesis is dedicated to the following problem:

"Develop scalable and computationally efficient algorithms for the design of robust and stabilising LTI decentralised, distributed, and overlapping feedback controllers for LTI time-delay systems".

More precisely, we provide methods to design a (structured) controller for the following cases.

- The generic case where the plant to be controlled is a Multiple-Input Multiple-Output LTI time-delay system as in (1.1).
- A special case where not only the controller but also system (1.1) is *structured*. The special case addressed corresponds to system (1.1) composing of identical or quasi-identical (identical subsystems with non-identical uncertainties) subsystems or nodes arranged in some network topology.

For the generic case, the approaches to design (structured) controllers will be based on translating the structure into an appropriate sparsity pattern on the controller coefficient matrices. For the special case, the approaches to design structured controllers will be based on a decoupling transformation. The latter problem for structured systems is formulated using some concepts from graph theory (Bapat, 2010) in the following subsection.

1.6.1 Systems with network structure

Consider that the system of form (1.1) is composed of a network, corresponding to the interconnection of subsystems, where the interconnections are described by a directed graph $\mathcal{G} = \{\mathcal{V}, \mathcal{E}, A_M\}$ with a set of nodes $\mathcal{V} = \{1, 2, 3, ..., n\}$ and a set of edges $\mathcal{E} \subset \mathcal{V} \times \mathcal{V}$. The edge $(i, j) \in \mathcal{E}$ connects from node $j \in \mathcal{V}$ to node $i \in \mathcal{V}$. The graph $\mathcal{G}$ need not be strongly connected. The weighted adjacency matrix, denoted by

$$A_M = [a_{Mi,j}]_{i,j=1}^{n},$$

has zero diagonal entries and non-negative off-diagonal entries such that $a_{Mi,j} > 0$ if and only if the corresponding edge $(i, j) \in \mathcal{E}$. For more details on graph theory and adjacency matrices, we refer to (Bapat, 2010).

Each of the n subsystems or nodes hosts a dynamical system described by a DDAE as

$$\begin{cases} \hat{E}_p \dot{x}_{pi}(t) = & \hat{A}_{p0} x_{pi}(t) + \sum_{k=1}^{m} \hat{A}_{pk} x_{pi}(t - \tau_k) \\ & \quad + \hat{B}_{p1} u_i(t) + \hat{B}_{p2} w_i(t) + \hat{B}_{p3} u_{ci}(t), \\ y_i(t) = & \hat{C}_{p1} x_{pi}(t), \\ z_i(t) = & \hat{C}_{p2} x_{pi}(t), \\ y_{ci}(t) = & \hat{C}_{p3} x_{pi}(t), \qquad i = 1, \ldots, n, \end{cases} \tag{1.20}$$

where $x_{pi} \in \mathbb{R}^{\hat{n}_p}$ is the instantaneous state, $u_i \in \mathbb{R}^{\hat{n}_u}$ is the controlled input, $y_i \in \mathbb{R}^{\hat{n}_y}$ is the measured output, $w_i \in \mathbb{R}^{\hat{n}_w}$ is the exogenous input, and $z_i \in \mathbb{R}^{\hat{n}_z}$ is the exogenous output of node "i". The additional input $u_{ci} \in \mathbb{R}^{n_{uc}}$ and output $y_{ci} \in \mathbb{R}^{n_{yc}}$ are related to the coupling with other nodes or subsystems in the network, described by

$$u_{ci}(t) = \sum_{j=1}^{n} a_{Mi,j} y_{cj}(t), \quad i = 1, \ldots, n. \tag{1.21}$$

For the same reason as that of (1.1), DDAE (1.20) allows to describe LTI subsystems in their most general form. Throughout this thesis, the word "node" is used interchangeably with "subsystem", since each node under

consideration is a dynamical subsystem. Notice that the system (1.20)-(1.21) is a special case of the system (1.1) with $x_p(t) = [x_{p1}(t)^\top \ \dots \ x_{pn}(t)^\top]^\top$, $y(t) = [y_1(t)^\top \ \dots \ y_n(t)^\top]^\top$, $u(t) = [u_1(t)^\top \ \dots \ u_n(t)^\top]^\top$, $w(t) = [w_1(t)^\top \ \dots \ w_n(t)^\top]^\top$, and $z(t) = [z_1(t)^\top \ \dots \ z_n(t)^\top]^\top$.

For simplicity of the presentation in this section, analysis is performed on the network topologies assuming that they have a kind of *normalised* adjacency matrix based on the concept of *normalised* Laplacian matrices in (Graham and Chung, 1996). In this thesis, we consider a *normalised* adjacency matrix to satisfy the row sum condition $\sum_{j=1}^{n} a_{Mi,j} = 1 \ \forall \ i = 1, ..., n$, whenever the in-degree of row i is not zero[2]. Let the spectrum of the adjacency matrix A_M be denoted by $\{\lambda_{a1}, ..., \lambda_{an}\}$. A *normalised* adjacency matrix has the property that all its eigenvalues have modulus smaller than or equal to 1 independent of its dimension ($|\lambda_{ai}| \in [0, 1]$, since $\sum_{j=1}^{n} a_{Mi,j} = 1, \ i = 1, ..., n$). This will play a significant role in the scalable design of distributed controllers (more details on why will be presented in Chapter 2). Some frequently used network topologies for large-scale or complex systems (with n nodes) are described in Appendix A.

1.6.2 Challenges

All the works mentioned in Section 1.3 were focused on designing LTI decentralised (feedback) controllers for non-delayed systems. However, their techniques do not carry over easily to systems with time-delays, as the system models become infinite-dimensional. The control design problem addressed in this thesis is characterised by three main challenges. First, with the aforementioned classical control design approaches imposing constraints on the structure or order of the controller gives (typically) rise to non-convex bilinear matrix inequalities, which are difficult to solve (Barreau et al., 2018). Second, by including delays the system models become infinite-dimensional (Michiels et al., 2017), hence, any controller design problem involving tuning of finitely many

[2]Note that we can "normalise" an arbitrary adjacency matrix A_M when its row sum $\sum_{j=1}^{n} a_{Mi,j} = d_g, \ i = 1, ..., n, \ d_g > 0$. That is, we can rewrite $y_{ci}(t) = d_g \hat{C}_{p3} x_{pi}(t)$ and $u_{ci}(t) = d_g^{-1} \sum_{j=1}^{n} a_{Mi,j} y_{cj}(t), \ i = 1, ..., n$ in (1.20)-(1.21).

controller parameters can be considered as a reduced-order controller design problem. Also, it is difficult to implement full order controllers for time-delay systems, hence, they are generally avoided in applications. Furthermore, as the number of subsystems increase in (1.20), there is a large increase in the computational complexity of the corresponding controller design problem. That is, it may not always be possible to solve the (non-convex) controller design (optimisation) problem for very large number of subsystems due to the large computation time required.

A few researchers have proposed methods to design structured controllers for time-delays systems. In (Özer and İftar, 2015), a method was proposed to design decentralised controllers for systems with time-delays as an extension of the decentralised pole assignment algorithm in (Davison and Chang, 1990), where the centralised controller design algorithm was used to design a controller for each agent at each step. However, at each step all the tunable parameters were therefore not (simultaneously) considered. Alternatively, in (Apkarian and Noll, 2018), $\mathcal{H}_\infty$ controller synthesis was proposed for decentralised control by imposing structure in the controller design algorithm. They used the Nyquist stability criterion and grid-based optimisation technique for $\mathcal{H}_\infty$ controller synthesis. The method proposed in this thesis complements the approach in (Apkarian and Noll, 2018).

In general, the design of structurally constrained (decentralised, distributed, and overlapping) controllers for time-delay systems, in a scalable and computationally efficient manner, is a largely open problem in the literature. Hence, one of the main goals of this thesis will be to solve this open problem. Furthermore, we propose scalable or computationally efficient methods to design control for networked systems (with aperiodic sampling and time-varying delays using the small gain theorem recalled in Appendix B) and automated platoons of heterogeneous (parameter) vehicles.

1.7 Structure of the thesis

The remainder of this thesis is organised as follows.

Chapter 2

A methodology is proposed in Chapter 2 for the design of robust structurally constrained controllers for linear time-delay systems, focusing on decentralised and overlapping fixed-order controllers for MIMO plants. The methodology is grounded in a direct optimisation approach and relies on the minimisation of the spectral abscissa and $\mathcal{H}_\infty$ cost functions, as a function of the controller or design parameters. First, an approach applicable to generic MIMO time-delay systems is presented, which is based on imposing a suitable sparsity pattern with the possibility of fixing elements in the controller parametrisation. Second, we show that if the delay system to be controlled has by itself the structure of a network of coupled identical subsystems, this structure can then be exploited by an improved algorithm for the design of decentralised (or overlapping) fixed-order controllers for the infinite-dimensional system, thereby increasing the computational efficiency and scalability with the number of subsystems. Several numerical examples are used to illustrate the effectiveness of the methodology, as well as its extension towards consensus type problems. Furthermore, an extension to a scalable algorithm, which has an exponential stability condition that is independent of the number of nodes, using a novel structure exploiting tool is presented for the design of decentralised controllers. The results of this chapter have been presented in (Dileep et al., 2018a), (Dileep et al., 2018b), and (Dileep et al., 2018c).

Chapter 3

In Chapter 3, a methodology is proposed for the design of sampled-data fixed-order decentralised controllers for MIMO LTI time-delay systems with asynchronous sensors and actuators, time-varying transmission delays, and aperiodic sampling. We model the errors induced by the network imperfections using an operator approach leading to an $\mathcal{L}_2$ stability criterion. First, the proposed method is applied to generic MIMO LTI systems with time-delays. Second, when the delay system to be controlled has the structure of a network of coupled quasi-identical subsystems, we use a scalable algorithm to design identical decentralised controllers through network structure exploitation. Quasi-identical subsystems are identical subsystems that have non-identical uncertainties or network imperfections. By exploiting the structure, we increase

the computational efficiency and scalability with the number of subsystems. Finally, the effectiveness of the methodology is illustrated using a numerical example. The results of this chapter have been presented in (Dileep et al., 2020).

Chapter 4

In Chapter 4, the application of heterogeneous vehicular platoons with Cooperative Adaptive Cruise Control (CACC) configuration, based on the problem formulation of TNO (Helmond, Netherlands), is presented. We consider Linear Time Invariant (LTI) models with constant time-delays at state, input, and output for the vehicles. The closed-loop systems of (identical) local controllers and heterogeneous parameter vehicles are modelled by a system of delay differential algebraic equations. The design problem of stabilising (identical) controllers achieving $\mathcal{L}_2$ string stability for one vehicle look-ahead platoon is reduced to a simultaneous controller design problem for a parameterised (sub)system, where the allowable values of the parameters correspond to heterogeneity (including time-delays) of the vehicles. By treating the heterogeneity in parameters as perturbations contained in specific intervals or regions, we determine the values for pseudo-spectral abscissa and robust induced-$\mathcal{L}_2$ norm. Hence, we ensure that the achieved exponential stability and string stability properties along with the overall computational complexity (of designing the controller) are independent of the number of vehicles. The effectiveness of the approach is validated by numerical experiments using the MATLAB software. The results of this chapter have been presented in (Dileep et al., 2019).

Chapter 5

Finally, Chapter 5 presents the general conclusions of this thesis and some directions for future work.

Chapter 2

Design of decentralised controllers

2.1 Introduction

In this chapter, we address the design of structurally constrained stabilising and $\mathcal{H}_\infty$ optimal controllers for large-scale linear systems with time-delays, including systems having a network structure. For large-scale MIMO plants it is often infeasible to implement centralised controllers (see (Lamnabhi-Lagarrigue et al., 2017; Lunze, 1992; Siljak, 2013) and the references therein). As a consequence, structurally constrained controllers, in particular decentralised or distributed (PID) controllers, are favourable for industrial applications (McMillan, 2012).

The methodology used in this chapter is grounded in the direct optimisation approach for controller design, where objective functions specifying performance criteria are directly optimised as a function of the available controller or design parameters. More specifically, the stabilisation and robust controller design problem for the delay system are translated into solving the, in general, non-smooth non-convex optimisation problems of minimising the spectral abscissa function and $\mathcal{H}_\infty$ norms (see (Michiels, 2011) and (Gumussoy and Michiels,

2011) respectively) using dedicated optimisation algorithms. This approach generalises the one underlying the HIFOO package (Burke et al., 2006) and the one underlying the MATLAB function `hinfstruct` (Apkarian and Noll, 2006), both for finite-dimensional LTI systems.

The subject-matter of this chapter is three-fold. First, the direct optimisation approach for designing fixed-order $\mathcal{H}_\infty$ optimal controller for time-delay systems is extended towards a more general class of structured controllers for MIMO plants, which includes decentralised and overlapping controllers (recalling from (Dileep et al., 2018b)). We assume that controllers are overlapping when they consider measured output from neighbouring subsystems. Hereby the structural constraints are translated into sparsity patterns for the controller parameterisation, as done in (Ozer and Iftar, 2015) for the stabilisation problem. The approach starts from a state space representation and fully exploits properties of delay systems. Particularly for neutral type systems with multiple delays, it explicitly takes into account the fragility (problem) of potential sensitivity of the spectral abscissa and $\mathcal{H}_\infty$ norms with respect to infinitesimal delay perturbations (Hale and Verduyn Lunel, 2002; Michiels et al., 2009b). The adopted approach complements the approach for infinite-dimensional systems in (Apkarian and Noll, 2018), which is based on appropriately sampling the frequency response.

Second, we consider systems which have themselves a network structure. We show how in the design of classes of decentralised and distributed fixed-order controllers, the structure of the overall system can be exploited by a refined method, in order to arrive at a higher computational efficiency, and improved scalability with respect to the number of subsystems. More precisely, we will assume that the MIMO plant consists of a network of coupled identical subsystems, each of them having an identical local controller to be designed. The key will be a decoupling transformation reducing the overall design problem into a robust or simultaneous controller design problem for one parameterised subsystem, where the allowable values of the parameter are related to the adjacency matrix of the network graph (Col et al., 2018; Rejeb et al., 2018). The same kind of transformation has been used for the design of full order distributed controllers for delay-free systems in (Massioni and Verhaegen, 2009),

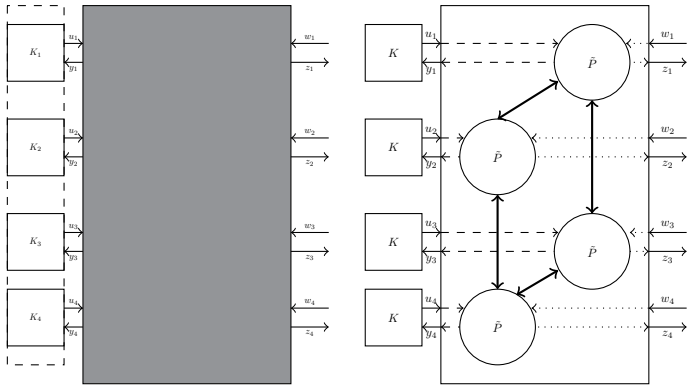

(a) MIMO plant and structurally constrained controller.

(b) Structured plant with identical subsystems and controllers.

Figure 2.1: Classes of systems under consideration. Section 2.2 presents an approach for the design of structured controllers for generic MIMO plants (shown in Fig. 2.1a for the special case of decentralised feedback control). In Section 2.3 a particularised approach is presented for a class of systems having a network structure (Fig. 2.1b).

within an LMI framework. It has also proven its usefulness in the analysis of linear consensus problems (see, e.g. (Morarescu et al., 2016; Olfati-Saber and Murray, 2004) and the references therein), and of network synchronisation, as it lays at the basis of the so-called Master Stability Function (Pecora and Carroll, 1998).

Third, we focus on network topologies that have the (eigenvalue) parameter related to the network topology confined to a specific subset Ω of the complex plane (an interval on the real axis, a circle,...), which can be chosen independently of the number of nodes. In such a case, sufficient conditions for stability, achieving a desired level of performance of the network, can be obtained by taking a robust control point of view and handling the network related parameter as an uncertain parameter confined to the full set Ω. Note that if the (Hausdorff) distance between the spectrum of the adjacency matrix and Ω goes to zero when the number of systems goes to infinity, the conservatism of the sufficient conditions disappears in the limit. In this chapter, we illustrate this approach by means of the decentralised stabilisation problem for network

topologies for which the set Ω is an interval on the real axis. The robust stabilisation problem of a system, affected by *uncertainty* confined to an interval on the real axis, fits within the framework of the (real structured) pseudospectral abscissa optimisation. The novel method proposed in (Borgioli and Michiels, 2018) for the computation of the pseudospectral abscissa of a delay system (see Section 2.4 for the definition) is able to fully exploit the structure of the uncertainty. Hence, the related robust stability conditions are necessary and sufficient. The method in (Borgioli and Michiels, 2018) is based on the discretisation of a gradient flow maximising the real part of the right most eigenvalue in the space of perturbations. The optimisation of the pseudospectral abscissa as a function of the controller parameters, which may be a non-convex and non-smooth function, is performed with the HANSO algorithm (Hybrid Algorithm for Non-Smooth Optimisation, see (Overton, 2009)). The final contribution of this chapter consists of combining the ingredients spelled out above, the decomposition approach of networks and the pseudospectral abscissa optimisation, which allows us to design stabilising decentralised fixed-order controllers for network of coupled systems, with computational complexity independent of the number of nodes.

The presented algorithms for structurally constrained controller design, with the possibility of network exploitation, have been integrated in the existing software tool `tds_hopt` for fixed-order $\mathcal{H}_\infty$ optimisation of delay systems corresponding to the article (Gumussoy and Michiels, 2011). The updated software tool (`tds_hopt-nse`, see (Dileep and Michiels, 2018b)) allows the designer to select the sub-controller input-output interactions and specify their orders. Additionally, the user can also specify the adjacency matrix and other matrices corresponding to the input or output signals exchanged between coupled subsystems.

Both presented methods start from system models in terms of linear delay-differential algebraic equations (DDAEs), which are very flexible and general as they allow a systematic description of (sub)-systems, controllers and their interconnections. DDAE models include delay systems of both retarded and neutral type and preserve linearity of system matrices with respect to the controller parameters in the closed-loop system description. We will also

illustrate how, relying on the DDAE framework mentioned in Section 1.4, the applicability of the design method can be extended towards synchronisation and consensus type problems in networks of delay-coupled systems. This involves the design of feedback controllers acting on output measurements, relative with respect to the output of other subsystems. The targeted classes of systems, related to the main contributions of this chapter as mentioned above, are illustrated in Fig. 2.1.

The remainder of this chapter is organised as follows. Section 2.2 presents a direct optimisation approach to design structurally constrained controllers for time-delay systems with multiple inputs and multiple outputs. Section 2.3 addresses the application to networks of interconnected systems, and the exploitation of the network structure. Some numerical examples are presented in Section 2.3.5, where an example of a consensus-type problem is considered. Then, an extension to a scalable algorithm for the design of stabilising decentralised controllers and the corresponding numerical example is presented in Section 2.4. Finally, some concluding remarks are given in Section 2.5. The results of this chapter have been presented in (Dileep et al., 2018a), (Dileep et al., 2018b), and (Dileep et al., 2018c).

2.2 Design of structurally constrained controllers

In this section, we formalise the design problem of structured controllers for generic time-delay systems of the form (1.1). Several kinds of structurally constrained controllers can be obtained by enforcing constraints on elements of the controller coefficient matrices contained in

$$P_M := \left[\begin{array}{c|c} A_c & B_c \\ \hline C_c & D_c \end{array}\right]$$

and only use the free parameters as variables in the optimisation problem described in the previous section (see (Dileep et al., 2018b) for more details). For decentralised and overlapping controllers this amounts to introducing a sparsity pattern, as can be portrayed with the help of the following example.

Example 2.2.1 *Consider a MIMO plant containing two control inputs and two measured outputs, and a controller parameterised in the following way:*

$$\begin{bmatrix} \dot{x}_{c1} \\ \dot{x}_{c2} \\ u_1 \\ u_2 \end{bmatrix} = \overbrace{\left[\begin{array}{cc:cc} a_{c_{11}} & 0 & b_{c_{11}} & 0 \\ 0 & a_{c_{22}} & \boxed{b_{c_{21}}} & b_{c_{22}} \\ \hdashline c_{c_{11}} & 0 & d_{c_{11}} & 0 \\ 0 & c_{c_{22}} & \boxed{d_{c_{21}}} & d_{c_{22}} \end{array}\right]}^{P_M} \begin{bmatrix} x_{c1} \\ x_{c2} \\ y_1 \\ y_2 \end{bmatrix}. \tag{2.1}$$

The controller is of order 2 ($n_c = 2$), however, two sub-controllers of order 1 are present. We can observe that if the elements b_{c21} and d_{c21} are set be zero, we have decentralised sub-controllers, that is, interactions between their states, inputs, and outputs are decoupled. If elements b_{c21} and d_{c21} are non-zero, the sub-controllers are overlapping, that is, the input and sub-controller state interactions are decoupled, but one of the measured output is shared between the two sub-controllers. ◦

The sparsity pattern can be described by a binary matrix F_M of the same dimensions as P_M ($p_{Mi,j}$ being the (i,j)-th element of P_M), whose (i,j)-th element satisfies

$$f_{Mi,j} = \begin{cases} 0, & \text{if } p_{Mi,j} \text{ is an optimisation variable;} \\ 1, & \text{if } p_{Mi,j} \text{ is a fixed element.} \end{cases} \tag{2.2}$$

This allows us to redefine the parameter vector from (1.7) to include only the non-zero/non-fixed elements using the information in F_M,

$$\bar{p} = \underset{F_M}{\operatorname{vec}} P_M = \underset{F_M}{\operatorname{vec}} \left(\left[\begin{array}{c:c} A_c & B_c \\ \hdashline C_c & D_c \end{array}\right] \right), \tag{2.3}$$

where $\operatorname{vec}_{F_M} P_M$ is a vector containing the elements of P_M for which the corresponding element in F_M is equal to one, keeping the same order as in $\operatorname{vec} P_M$.

Notice that the (structured) control design problem for generic system (1.1) has been translated into sparsity patterns on the controller coefficient matrices.

That is, the controller parametrisation in (1.7) used for minimising the robust spectral abscissa function in (1.11) and the strong $\mathcal{H}_\infty$ norm function in (1.19) is replaced by the controller parametrisation in (2.3). The controller parameters (in $\bar{p}$) can also be optimised for the function $f_o(\bar{p})$,

$$f_o(\bar{p}) = \begin{cases} \infty, & \text{if } \; C(\bar{p}) \geq 0, \\ \alpha_o \; C(\bar{p}) + \; (1-\alpha_o) \; |||G(j\omega, \bar{p})|||_{\mathcal{H}_\infty}, & \text{if } \; C(\bar{p}) < 0. \end{cases} \tag{2.4}$$

Here $0 \leq \alpha_o \leq 1$ is the weight used for linear combination of the objective functions. The two objective functions in this combination are in general non-convex. They may be not-everywhere differentiable, even not-everywhere Lipschitz continuous, see (Gumussoy and Michiels, 2011; Michiels, 2011) where using the same approach (unstructured) fixed-order controllers are designed.

In our implementation, the HANSO (Hybrid Algorithm for Non-smooth Optimisation) code, see (Overton, 2009), is used for solving the optimisation tasks. The algorithm relies on a routine for the computation of the considered objective function as well as its gradient whenever the objective function is differentiable. The value of the objective function is obtained by computing rightmost eigenvalues of the DDAE for the spectral abscissa, and by a generalisation of the Boyd-Balakrishnan-Kabamba (Boyd et al., 1989) / Bruinsma-Steinbuch (Bruinsma and Steinbuch, 1990) algorithm for the $\mathcal{H}_\infty$ norm, relying on computing imaginary axis solutions of an associated Hamiltonian eigenvalue problem. It typically constitutes the dominant computational cost in every iteration. On the contrary, derivatives of the objective functions with respect to controller parameters are obtained at a negligible cost from left and right eigenvectors. By this property and by the fact that fixed-order controllers of lower order are desirable for application, reducing the number of variables beyond the imposed structure, e.g., by working with canonical forms, does not have a considerable impact on the overall computational cost. We refer to (Gumussoy and Michiels, 2011; Michiels, 2011) and the references therein for more information on the previously described algorithmic components.

A strongly exponentially stable closed-loop system is required to start the

optimisation of objective functions involving the strong $\mathcal{H}_\infty$ norm. If this is not the case, a preliminary stabilisation phase is performed based on optimising the robust spectral abscissa. Due to the non-convexity of the objective functions, there is no guarantee of convergence to the global minimum. In our software, this is addressed by using randomly generated initial values for the controller parameters, along with initial controllers specified by the user, and choosing the best solution from them.

Other controllers

One can use the concept of structural constraints to design many other types of controllers. A kind of distributed controller can be considered by including the off-diagonal elements of the A_c matrix in the vector $\bar{p}$. PID controllers are commonly used as feedback controllers in the industry. It is also possible to structurally constrain the dynamic controller to represent a PID controller and optimise its gains. Let us consider the PID controller mentioned in (Toscano, 2013),

$$K(s) = K_P + K_I \frac{1}{s} + K_D \frac{s}{1 + d_f s}, \tag{2.5}$$

for which a realisation is determined by the controller matrices,

$$\left[\begin{array}{c|c} A_c & B_c \\ \hline C_c & D_c \end{array}\right] = \left[\begin{array}{cc|c} 0 & 0 & K_I \\ 0 & -\frac{1}{d_f} & -\frac{1}{d_f^2} K_D \\ \hline 1 & 1 & K_P + \frac{1}{d_f} K_D \end{array}\right]. \tag{2.6}$$

Here d_f is the time constant of the filter applied to the derivative action. The physical reliability is safeguarded by ensuring the properness of the PID controller using this low-pass first order filter (Toscano, 2013). If we assume d_f to be a constant, we can translate the problem of designing a stabilising or robust PID controller into an optimisation problem for the proposed algorithm as given below.

$$F_M = \left[\begin{array}{cc:c} 0 & 0 & 1 \\ 0 & 0 & 1 \\ \hdashline 0 & 0 & 1 \end{array}\right] \rightarrow P_M = \left[\begin{array}{cc:c} 0 & 0 & b_{c_{11}} \\ 0 & -\frac{1}{d_f} & b_{c_{21}} \\ \hdashline 1 & 1 & d_{c_{11}} \end{array}\right] \rightarrow \bar{p} = \begin{bmatrix} b_{c_{11}} \\ b_{c_{21}} \\ d_{c_{11}} \end{bmatrix}$$

The new values for the gains of the PID controller can be obtained from the optimised dynamic controller using $K_I = b_{c_{11}}$, $K_D = -d_f^2 b_{c_{21}}$ and $K_P = d_{c_{11}} - \frac{1}{d_f} K_D$.

2.3 Exploiting network structure of systems

We particularise the approach (for generic systems) presented in Section 2.2 for the case of designing a decentralised (or overlapping) controller for a special class of systems. These systems have some network structure, consisting of identical subsystems to be controlled by identical local controllers, see Fig. 2.1b. We consider the case where a system of the form (1.1) is composed of subsystems of the form (1.20) and (1.21). We assume that each subsystem can be controlled using a fixed-order LTI feedback controller of the form

$$\begin{cases} \dot{x}_{ci}(t) = \hat{A}_c x_{ci}(t) + \hat{B}_c y_i(t), \\ u_i(t) = \hat{C}_c x_{ci}(t) + \hat{D}_c y_i(t), \ i = 1, ..., n. \end{cases} \tag{2.7}$$

Recall that the weighted adjacency matrix is denoted by

$$A_M = [a_{Mi,j}]_{i,j=1}^{n}.$$

Defining $x_i(t) = [x_{pi}^{\mathrm{T}}(t)\ u_i^{\mathrm{T}}(t)\ \gamma_{w_i}^{\mathrm{T}}\ x_{ci}^{\mathrm{T}}(t)\ y_i^{\mathrm{T}}(t)]^{\mathrm{T}}$, the closed-loop system state $x_i \in \mathbb{R}^{n_{cl}}$ which includes the plant and the controller can be written in the DDAE form as

$$\begin{cases} \hat{E}\dot{x}_i(t) & = \hat{A}_0 x_i(t) + \sum_{k=1}^{m} \hat{A}_k x_i(t - \tau_k) + \sum_{j=1}^{n} a_{Mi,j} \hat{B}\hat{C} x_j(t) + \hat{B}_2 w_i(t) \\ z_i(t) & = \hat{C}_2 x_i(t), \qquad\qquad i = 1, \ldots, n, \end{cases} \tag{2.8}$$

where

$$\hat{E} = \begin{bmatrix} \hat{E}_p & 0 & 0 & 0 & 0 \\ 0 & 0 & 0 & 0 & 0 \\ 0 & 0 & 0 & 0 & 0 \\ 0 & 0 & 0 & I & 0 \\ 0 & 0 & 0 & 0 & 0 \end{bmatrix}, \; \hat{A}_0 = \begin{bmatrix} \hat{A}_{p0} & \hat{B}_{p1} & \hat{B}_{p2} & 0 & 0 \\ \hat{C}_{p1} & 0 & 0 & 0 & -I \\ 0 & 0 & -I & 0 & 0 \\ 0 & 0 & 0 & \hat{A}_c & \hat{B}_c \\ 0 & -I & 0 & \hat{C}_c & \hat{D}_c \end{bmatrix}, \tag{2.9}$$

and

$$\hat{A}_k = \begin{bmatrix} \hat{A}_{pk} & 0 & 0 & 0 & 0 \\ 0 & 0 & 0 & 0 & 0 \\ 0 & 0 & 0 & 0 & 0 \\ 0 & 0 & 0 & 0 & 0 \\ 0 & 0 & 0 & 0 & 0 \end{bmatrix}, \; \hat{B} = \begin{bmatrix} \hat{B}_{p3} \\ 0 \\ 0 \\ 0 \\ 0 \end{bmatrix}, \; \hat{B}_2 = \begin{bmatrix} 0 \\ 0 \\ I \\ 0 \\ 0 \end{bmatrix},$$

$$\hat{C} = \begin{bmatrix} \hat{C}_{p3} & 0 & 0 & 0 & 0 \end{bmatrix}, \; \hat{C}_2 = \begin{bmatrix} \hat{C}_{p2} & 0 & 0 & 0 & 0 \end{bmatrix}.$$

The state-space representation for the overall structured system then takes the form

$$I \otimes \hat{E} \begin{bmatrix} \dot{x}_1(t) \\ \dot{x}_2(t) \\ \vdots \\ \dot{x}_n(t) \end{bmatrix} = I \otimes \hat{A}_0 \begin{bmatrix} x_1(t) \\ x_2(t) \\ \vdots \\ x_n(t) \end{bmatrix} + \sum_{k=1}^{m} I \otimes \hat{A}_k \begin{bmatrix} x_1(t-\tau_k) \\ x_2(t-\tau_k) \\ \vdots \\ x_n(t-\tau_k) \end{bmatrix}$$

$$+ A_M \otimes \hat{B}\hat{C} \begin{bmatrix} x_1(t) \\ x_2(t) \\ \vdots \\ x_n(t) \end{bmatrix} + I \otimes \hat{B}_2 \begin{bmatrix} w_1(t) \\ w_2(t) \\ \vdots \\ w_n(t) \end{bmatrix}, \quad \begin{bmatrix} z_1(t) \\ z_2(t) \\ \vdots \\ z_n(t) \end{bmatrix} = I \otimes \hat{C}_2 \begin{bmatrix} x_1(t) \\ x_2(t) \\ \vdots \\ x_n(t) \end{bmatrix}. \tag{2.10}$$

In the following subsections, we describe how the model in (2.10) can be decomposed for stability and robustness optimisation.

2.3.1 Decoupling for the stabilisation problem

Based on the (complex) Schur decomposition theorem (see (Meyer, 2000)), there always exists a unitary transformation matrix $T \in \mathbb{C}^{n\times n}$ and an upper-triangular matrix $Z \in \mathbb{C}^{n\times n}$ such that

$$TA_MT^{-1} = Z. \tag{2.11}$$

Note that spectrum of A_M appears on the diagonal of Z. Let us consider the whole system where $w(t) \in \mathbb{R}^{n\cdot\hat{n}_w}$ and $z(t) \in \mathbb{R}^{n\cdot\hat{n}_z}$ are the exogenous input and output respectively, and $x(t) \in \mathbb{R}^{n\cdot n_{cl}}$ and $\bar{x}(t) \in \mathbb{R}^{n\cdot n_{cl}}$ are the state before and after the transformation respectively. Also, $w(t) = [w_1^{\mathrm{T}}(t) \ \dots \ w_n^{\mathrm{T}}(t)]^{\mathrm{T}}$, $z(t) = [z_1^{\mathrm{T}}(t) \ \dots \ z_n^{\mathrm{T}}(t)]^{\mathrm{T}}$, $x(t) = [x_1^{\mathrm{T}}(t) \ \dots \ x_n^{\mathrm{T}}(t)]^{\mathrm{T}}$, and $\bar{x}(t) = [\bar{x}_1^{\mathrm{T}}(t) \ \dots \ \bar{x}_n^{\mathrm{T}}(t)]^{\mathrm{T}}$. If we apply the transformation using $\hat{T}$ (that is, $x(t) = \hat{T}^{-1}\bar{x}(t)$) to (2.10), where $\hat{T} = T \otimes I$, we obtain the equation

$$\begin{aligned}(I\otimes\hat{E})\dot{\bar{x}}(t) &= (I\otimes\hat{A}_0)\bar{x}(t) + \sum_{k=1}^{m}(I\otimes\hat{A}_k)\bar{x}(t-\tau_k) + (Z\otimes\hat{B}\hat{C})\bar{x}(t)\\ &+ \underbrace{\hat{T}(I\otimes\hat{B}_2)}_{(I\otimes\hat{B}_2)\hat{T}} w(t), \quad z(t) = \underbrace{(I\otimes\hat{C}_2)\hat{T}^{-1}}_{\hat{T}^{-1}(I\otimes\hat{C}_2)}\ \bar{x}(t).\end{aligned} \tag{2.12}$$

Note that this transformation does not affect $\hat{A}_0$, $\hat{A}_k$ or $\hat{E}$ because of the property

$$\hat{T}(I\otimes\hat{A}_0)\hat{T}^{-1} = (T\otimes I)(I\otimes\hat{A}_0)(T^{-1}\otimes I) = TT^{-1}\otimes\hat{A}_0.$$

Observing that for zero exogenous input, (2.12) has a cascaded structure, the following theorem directly follows.

Theorem 2.3.1 *Let the spectrum of A_M be denoted by $\{\lambda_{a1},\dots,\lambda_{an}\}$. System (2.12) with $w \equiv 0$ is exponentially stable if and only if the system*

$$\hat{E}\dot{\bar{x}}_i(t) = \left(\hat{A}_0 + \lambda_{ai}\hat{B}\hat{C}\right)\bar{x}_i(t) + \sum_{k=1}^{m}\hat{A}_k\bar{x}_i(t-\tau_k) \tag{2.13}$$

is exponentially stable $\forall\ i \in \{1, ..., n\}$. *Moreover we have*

$$C(\bar{p}) = \max_{1 \le i \le n} \tilde{C}(\bar{p}, \lambda_{ai}), \tag{2.14}$$

where $\tilde{C}(\bar{p}, \lambda_{ai})$ *is the robust spectral abscissa of (2.13).*

Proof. The assertions follow from the block-triangular structure of (2.12), with (2.13) appearing as a diagonal block, and from the corresponding structure of the associated eigenvalue problem. □

Now the the robust spectral abscissa function in the minimisation problem of (1.11) changes to (2.14) for systems of the form (2.10).

2.3.2 Decoupling for the $\mathcal{H}_\infty$ optimisation problem

Now we focus on the decomposition of the system norms, under an additional assumption, for $G(s)$ defined as the transfer function of (2.10) from w to z. We start by stating this assumption (recall that a matrix T is unitary if $T^*T = TT^* = I$).

Assumption 3 *There exists a unitary transformation matrix* T *such that* $TA_MT^{-1} = \Lambda_a$, *with* $\Lambda_a = \mathrm{diag}(\lambda_{a1}, \ldots, \lambda_{an})$.

The above assumption is satisfied for graphs with a symmetric or circulant adjacency matrix. We now arrive at the main theorem.

Theorem 2.3.2 *If Assumption 3 is satisfied, then we can express*

$$||G(j\omega, \bar{p})||_{\mathcal{H}_\infty} = \max_{i \in \{1,..,n\}} ||\tilde{G}(j\omega, \bar{p}; \lambda_{ai})||_{\mathcal{H}_\infty} \tag{2.15}$$

and

$$||G(j\omega, \bar{p})||_{\mathcal{H}_2} = \sqrt{\sum_{i=1}^{n} ||\tilde{G}(j\omega, \bar{p}; \lambda_{ai})||^2_{\mathcal{H}_2}}, \tag{2.16}$$

where $\tilde{G}(j\omega, \bar{p}; \lambda_{ai})$, $i = 1, \ldots, n$, *is the transfer function of system*

$$\begin{aligned} \hat{E}\dot{\bar{x}}_i(t) &= \left(\hat{A}_0 + \lambda_{ai}\hat{B}\hat{C}\right)\bar{x}_i(t) + \sum_{k=1}^{m} \hat{A}_k \bar{x}_i(t-\tau_k) + \hat{B}_2 \bar{w}_i(t), \\ \bar{z}_i(t) &= \hat{C}_2 \bar{x}_i(t). \end{aligned} \tag{2.17}$$

Proof. When choosing T in (2.11) according to Assumption 2, the transformation to (2.12) can be done with $Z = \Lambda_a$. Since Λ_a is a diagonal matrix, system (2.12) can be fully decoupled. However, input and output signals get mixed. We can express this decoupling as

$$G(s) = \hat{T}^{-1}\bar{G}(s)\hat{T}, \tag{2.18}$$

where $\hat{T} = T \otimes I$, with

$$\bar{G}(s) = \begin{bmatrix} \tilde{G}(s, \bar{p}; \lambda_{a1}) & \ldots & 0 \\ \vdots & \ddots & \vdots \\ 0 & \ldots & \tilde{G}(s, \bar{p}; \lambda_{an}) \end{bmatrix}. \tag{2.19}$$

Since $\hat{T}$ is a unitary matrix ($\hat{T}\hat{T}^* = \hat{T}^*\hat{T} = I$), induced by T being unitary from Assumption 3, we get

$$\left(\hat{T}^{-1}\bar{G}(s)\hat{T}\right)^* \left(\hat{T}^{-1}\bar{G}(s)\hat{T}\right) = \hat{T}^* \left(\bar{G}(s)^*\bar{G}(s)\right)\hat{T},$$

having the same spectrum as $\bar{G}(s)^*\bar{G}(s)$. In this way, we obtain

$$||G(s)||_{\mathcal{H}_\infty} = ||\bar{G}(s)||_{\mathcal{H}_\infty}, \quad ||G(s)||_{\mathcal{H}_2} = ||\bar{G}(s)||_{\mathcal{H}_2}.$$

The assertion regarding the $\mathcal{H}_\infty$ norm directly follows. For the $\mathcal{H}_2$ norm we get

$$\begin{aligned} ||\bar{G}(s)||_{\mathcal{H}_2} &= \sqrt{\frac{1}{2\pi}\int_{-\infty}^{+\infty} \text{trace}[\bar{G}(j\omega)^*\bar{G}(j\omega)]d\omega} \\ &= \sqrt{\sum_{i=1}^{n}\frac{1}{2\pi}\int_{-\infty}^{+\infty} \text{trace}[\tilde{G}(j\omega;\lambda_{ai})^*\tilde{G}(j\omega;\lambda_{ai})]d\omega} \end{aligned} \tag{2.20}$$

and the proof is complete. □

Now the strong $\mathcal{H}_\infty$ norm function in the minimisation problem of (1.19) changes to (2.15) for systems of the form (2.10) with a normal adjacency matrix. It is important to observe that equation (2.17) can be interpreted as the closed-loop system formed by (1.20) and (2.7), provided coupling (1.21) is replaced with $u_{ci}(t) = \lambda_{ai}y_{ci}(t)$. Hence, the decoupling (on which Theorem 2.3.2 is based) can be visualised as in Fig. 2.2.

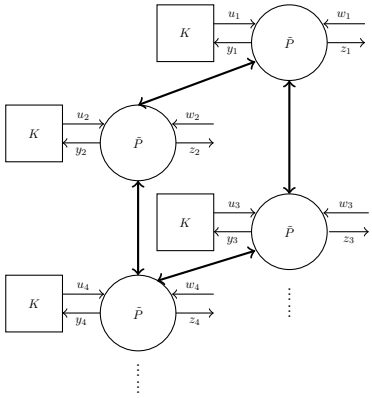

(a) Structured plant with identical subsystems and controllers.

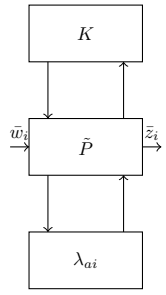

λ_{ai} are the eigenvalues of A_M, where $i \in \{1, 2, ..., n\}$.

(b) Decoupled system.

Figure 2.2: Decoupling of the structured plant of identical subsystems. The relation between their stability properties and their system norms of the transfer functions from w to z (and $\bar{w}$ to $\bar{z}$), are described by Theorems 2.3.1 and 2.3.2.

2.3.3 Discussion

The stabilisation and $\mathcal{H}_\infty$ optimisation problem of (2.10) can be turned into a *simultaneous* stabilisation and $\mathcal{H}_\infty$ optimisation problem of n plants of the form (2.13) and (2.17), respectively, to optimise the controller parameters contained in matrix $\hat{A}_0$, using Theorems 2.3.1-2.3.2. This is particularly useful for the adopted direct optimisation approach. Recall that the dominant computational cost of evaluating the robust spectral abscissa and the strong $\mathcal{H}_\infty$ norm amounts to computing the rightmost eigenvalues of a DDAE and the imaginary axis solutions of an associated Hamiltonian eigenvalue problem respectively. In both cases, the number of operations with the algorithms proposed in (Michiels, 2011) and the references therein scales with the cube of the dimension, leading to a reduction from $\mathcal{O}((n \cdot n_{cl})^3)$ to $\mathcal{O}(n \cdot (n_{cl})^3)$. Moreover, one can also interpret (2.17) as an uncertain system, where the uncertainty is contained in the eigenvalue parameter taking n different values. When handling this *uncertainty* using methods from robust control, similar to that done in (D'Andrea and Dullerud, 2003; Massioni and Verhaegen, 2010) for delay-free systems, there is potential to arrive at scalable design methods whose cost does not depend on the size of the network. This will be worked out in Section 2.4.

For the existence of the decoupling it is essential that the subsystems/nodes in $\mathcal{G}$ are identical with respect to system dynamics. We also assume that the coupling features are identical, including constant communication delays independent of the link (which are *absorbed* in the DDAE model for the subsystems, as we shall illustrate in Section 2.3.5). For the relation between system norms expressed in Theorem 2.3.2, two additional conditions are to be satisfied. First the transformation matrices used to diagonalise the adjacency matrix must be unitary. Note that this is satisfied whenever the adjacency matrix is symmetric, corresponding to symmetric bi-directional coupling, or circulant. The (complex) Schur decomposition and spectral decomposition of a matrix coincide when the matrix is a normal matrix. Second, one has to restrict to the induced norm from w to z in the $\mathcal{H}_\infty$ problem formulation, in which the exogenous inputs and regulated outputs of the individual nodes are equally weighted.

The exploitation of the network structure, inferred from Theorem 2.3.1 (spectral

abscissa) and first part of Theorem 2.3.2 ($\mathcal{H}_\infty$ norm) has been integrated in the publicly available software as an additional feature to `tds_hopt`. It relies on modifying the objective functions (1.9) and (1.18) accordingly.

2.3.4 Generalisations to distributed controllers

The approach discussed in the previous subsections might be misconceived to be restricted to the case of a fully decentralised control configuration. Due to the generality of DDAEs in modelling interconnected systems, it is possible to include namely classes of distributed and overlapping controllers in the framework sketched in the beginning of Section 2.3, see Figure 2.3. This is illustrated with the help of the following cases.

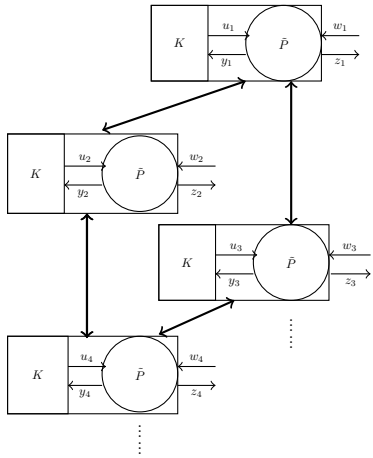

(a) Structured system with identical subsystems and distributed controller.

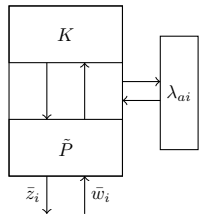

λ_{ai} are the eigenvalues of A_M, where $i \in \{1, 2, ..., n\}$.

(b) Decoupled system.

Figure 2.3: Decoupling of the structured system and distributed controller. The interactions between different subsystems and the interactions between different controllers are described by the same network.

Proposition 2.3.3 *The closed-loop system of plant (1.20)-(1.21) and a distributed controller of the form*

$$\begin{cases} \dot{x}_{ci}(t) = \hat{A}_c x_{ci}(t) + \hat{B}_{c1} y_i(t) + \sum_{j=1}^{n} a_{Mi,j} u_j(t), \\ u_i(t) = \hat{C}_{c1} x_{ci}(t) + \hat{D}_{c1} y_i(t) + \sum_{j=1}^{n} a_{Mi,j} u_j(t), \ i = 1, ..., n, \end{cases} \tag{2.21}$$

can be re-written as a closed-loop system consisting of a plant of the form (1.20)-(1.21) and a decentralised controller of the form (2.7).

Proof. Let us would modify system description (1.20)-(1.21) to

$$\begin{cases} \hat{E}_p \dot{x}_{pi}(t) &= \hat{A}_{p0} x_{pi}(t) + \sum_{k=1}^{m^A} \hat{A}_{pk} x_{pi}(t - h_k^A) + \hat{B}_{p1} u_i(t) + \hat{B}_{p2} w_i(t) \\ & \quad + [\hat{B}_{p3} \ 0] u_{ci}(t), \\ 0 &= -\xi_i(t) + u_i(t) \\ 0 &= -\eta_i(t) + [0 \ I] u_{ci}(t) \\ y_i(t) &= \begin{bmatrix} \hat{C}_{p1} x_{pi}(t) \\ \eta_i(t) \end{bmatrix}, \\ z_i(t) &= \hat{C}_{p2} x_{pi}(t), \\ y_{ci}(t) &= \begin{bmatrix} \hat{C}_{p3} x_{pi}(t) \\ \xi_i(t) \end{bmatrix}, \qquad i = 1, \ldots, n, \end{cases} \tag{2.22}$$

and

$$u_{ci}(t) = \sum_{j=1}^{n} a_{Mi,j} y_{cj}(t), \quad i = 1, \ldots, n. \tag{2.23}$$

where we consider the first three equations in (2.22) as the modified plant DDAE. Now the seemingly decentralised controller of the form (2.7) would correspond to an overlapping controller, whose input y_i consists not only of the original plant's output $C_{p1} x_{pi}$ but also of the weighted average of the outputs generated by neighbouring controllers. The latter can be seen from

$$\eta_i(t) = \sum_{j=1}^{n} a_{Mi,j} \xi_j(t) = \sum_{j=1}^{n} a_{Mi,j} u_j(t).$$

Now we can use Theorems 2.3.1-2.3.2 to design robust controller for this case.

Hence, the proof is complete. ○

Remark 1 *In Section 2.3.5, we will consider the control of a group of subsystems with diffusive coupling. In this application, the coupling between systems is only realised through the control. Such a control is of diffusive type resulting in overlapping controllers. We will show that the model for the closed loop system can still be turned into the form of (1.20) and (2.7).*

Finally, the decomposition approach trivially extends to the case where the controllers communicate their state to neighbouring controllers under the condition that the interactions between different subsystems and the interactions between different controllers are described by the same network,

$$\begin{cases} \dot{x}_{ci}(t) = \hat{A}_c x_{ci}(t) + \hat{B}_{c1} y_i(t) + \hat{B}_{c2} \left(\sum_{j=1}^{n} a_{Mi,j} \hat{C}_{c2} x_{cj}(t-\tau) \right), \\ u_i(t) = \hat{C}_{c1} x_{ci}(t) + \hat{D}_{c1} y_i(t) + \hat{D}_{c2} \left(\sum_{j=1}^{n} a_{Mi,j} \hat{C}_{c2} x_{cj}(t-\tau) \right), \end{cases}$$

$i = 1, ..., n$, with τ representing a transmission delay. However, after decoupling the system, the i-th controller would become

$$\begin{cases} \dot{\bar{x}}_{ci}(t) = \hat{A}_c \bar{x}_{ci}(t) + \lambda_{ai} \hat{B}_{c2} \hat{C}_{c2} \bar{x}_{ci}(t-\tau) + \hat{B}_{c1} \bar{y}_i(t), \\ \bar{u}_i(t) = \hat{C}_{c1} \bar{x}_{ci}(t) + \lambda_{ai} \hat{D}_{c2} \hat{C}_{c2} \bar{x}_{ci}(t-\tau) + \hat{D}_{c1} \bar{y}_i(t), \ i = 1, ..., n, \end{cases}$$

and, hence, it also depends on the eigenvalue parameter. This is consistent with (Massioni and Verhaegen, 2009) for the delay-free case.

2.3.5 Numerical examples

We use some numerical examples to illustrate the network exploitation methodology presented earlier. Note that all the simulations performed for this thesis used an Intel® Core™ i7-6820HQ CPU at 2.7 GHz with 8GB RAM.

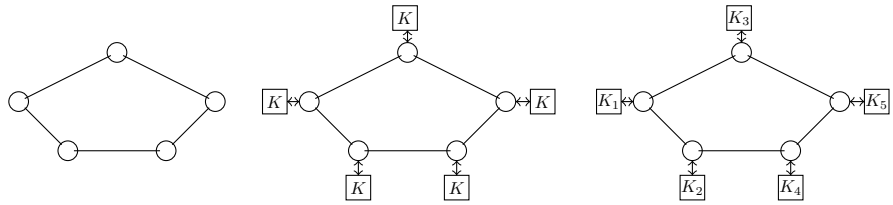

$C(\bar{p}=0)=0.8549$ $C(\bar{p})=-3.3672$ $C(\bar{p})=-4.0846$

(a) No feedback (b) $u_i = Ky_i$ (c) $u_i = K_i y_i$

Figure 2.4: Robust spectral abscissa computed for the example system and the closed-loop subsystems.

A system with input and coupling delays

Consider the following system with a network structure,

$$\begin{cases} \dot{x}_{pi}(t) = \begin{bmatrix} 0 & 0.5 \\ 0.5 & -3 \end{bmatrix} x_{pi}(t) + \begin{bmatrix} 0 \\ 5 \end{bmatrix} u_i(t-0.1) + I u_{ci}(t-0.3) + \begin{bmatrix} 1 \\ 1 \end{bmatrix} w(t), \\ y_i(t) = \begin{bmatrix} 1 & 1 \\ 0 & 1 \end{bmatrix} x_{pi}(t), \quad y_{ci}(t) = I x_{pi}(t), \quad u_{ci}(t) = \sum_{j=1}^{n} a_{Mi,j} x_{pj}(t), \\ z_i(t) = I x_{pi}(t), \ i = 1, ..., 5, \end{cases} \tag{2.24}$$

whose adjacency matrix can be written as

$$A_M = \begin{bmatrix} 0 & 0.5 & 0.5 & 0 & 0 \\ 0.5 & 0 & 0 & 0.5 & 0 \\ 0.5 & 0 & 0 & 0 & 0.5 \\ 0 & 0.5 & 0 & 0 & 0.5 \\ 0 & 0 & 0.5 & 0.5 & 0 \end{bmatrix}. \tag{2.25}$$

Without control the system is unstable, with robust spectral abscissa equal to 0.8549. The approach of Section 2.2 is used to design decentralised controllers of the form

$$u_i(t) = K_i y_i(t), \ i = 1, ..., 5, \tag{2.26}$$

using the following values (generated randomly) as starting points for optimisation,

$$\begin{aligned}\tilde{K}_1 &= \begin{bmatrix}-0.8045 & 0.6966\end{bmatrix},\ \tilde{K}_2 = \begin{bmatrix}0.8351 & -0.2437\end{bmatrix},\\ \tilde{K}_3 &= \begin{bmatrix}0.2157 & -1.1658\end{bmatrix},\ \tilde{K}_4 = \begin{bmatrix}-1.1480 & 0.1049\end{bmatrix},\\ \tilde{K}_5 &= \begin{bmatrix}0.7223 & 2.5855\end{bmatrix},\end{aligned} \tag{2.27}$$

leading to

$$\begin{aligned}K_1 &= \begin{bmatrix}-10.2555 & 9.2164\end{bmatrix},\ K_2 = \begin{bmatrix}-13.9911 & 12.3932\end{bmatrix},\\ K_3 &= \begin{bmatrix}-14.3001 & 12.7874\end{bmatrix},\ K_4 = \begin{bmatrix}-11.3138 & 9.9052\end{bmatrix},\\ K_5 &= \begin{bmatrix}-10.0127 & 9.1918\end{bmatrix},\end{aligned} \tag{2.28}$$

and a minimal robust spectral abscissa of -4.0846. Subsequently, using the methodology of Section 2.3, a static stabilising controller was designed by minimising the (robust) spectral abscissa, using the starting point (generated randomly) $\tilde{K} = [\ 0.3188\ \ -1.3077]$ for optimisation, leading to

$$u_i(t) = Ky_i(t) = \begin{bmatrix}-8.9481 & 7.7775\end{bmatrix} y_i(t), \tag{2.29}$$

and a minimal robust spectral abscissa of -3.3672. This value is greater than the value corresponding to the control law $u_i = K_i y_i$, because of the constraint that the gains are equal to each other. In Fig. 2.4, the robust spectral abscissa values for the subsystems and controllers are shown. Finally, the controller gains K and $K_i,\ i = 1, ..., 5$, were optimised for the (strong) $\mathcal{H}_\infty$ norm of the transfer function from w to z, to obtain $\breve{K}$ and $\breve{K}_i,\ i = 1, ..., 5$.

The results are shown in Table 2.1, which illustrates a trade-off between performance and robustness, expressed here in terms of the robust spectral abscissa and the $\mathcal{H}_\infty$ norms respectively. The average time taken for the objective function evaluation in the optimisation process is given in the column of "function evaluation time" in Table 2.1. As expected, we can also observe in Table 2.1 that the average time required for computing the objective functions have been reduced considerably by using the network structure exploitation approach (from $0.1079s$ to $0.0625s$ and from $13.676s$ to $1.7556s$ for spectral

Table 2.1: Results obtained for simple numerical example using the two approaches

Simple numerical example	Objective function	$\mathcal{H}_\infty$ norm	Spectral abscissa	Function evaluations (No.)	Function evaluation time (s)
No feedback	—	∞	0.8549	—	—
$u_i = Ky_i$	Robust spectral abscissa ($\alpha_o = 1$)	3.2246	-3.3672	326	0.0625↓
$u_i = \breve{K}y_i$	Strong $\mathcal{H}_\infty$ norm ($\alpha_o = 0$)	2.7661↓	-2.1936↑	38	1.7556↓
$u_i = K_i y_i$	Robust spectral abscissa ($\alpha_o = 1$)	2.8662	-4.0846	432	0.1079↑
$u_i = \breve{K}_i y_i$	Strong $\mathcal{H}_\infty$ norm ($\alpha_o = 0$)	2.7580↓	-2.6168↑	53	13.676↑

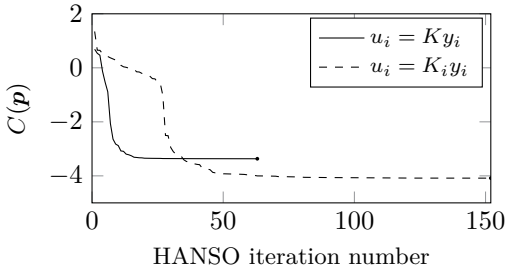

(a) Robust sectral abscissa optimisation.

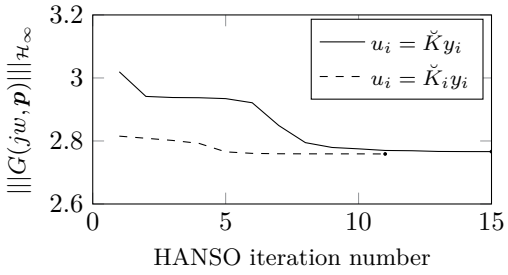

(b) Strong $\mathcal{H}_\infty$ norm optimisation.

Figure 2.5: Convergence profile of the optimisation process for (a) robust spectral abscissa ($\alpha_o = 1$) and (b) strong $\mathcal{H}_\infty$ norm ($\alpha_o = 0$) of the simple numerical example.

abscissa and $\mathcal{H}_\infty$ norm evaluations respectively).

Figure 2.5 shows the convergence of the optimisation problems through HANSO

iterations for the results given in Table 2.1. Due to the non-convexity of the problem, different starting points could lead to different results and therefore different convergence profiles (including the number of iterations or function evaluations). In the optimisation process, HANSO might perform multiple objective function evaluations within one iteration. For more details on the controllers and other results presented in this chapter, please refer to the complementary software package (Dileep and Michiels, 2018b).

A neutral type time-delay system

Let us consider a neutral type time-delay system

$$\begin{cases} \begin{bmatrix} 0 & 1 \\ 0.5 & 2 \end{bmatrix} \dot{x}_{pi}(t) + \begin{bmatrix} 0 & 0 \\ 0.2 & 1 \end{bmatrix} \dot{x}_{pi}(t-0.2) = \begin{bmatrix} 1 & -0.5 \\ 0 & 2 \end{bmatrix} x_{pi}(t) \\ \qquad\qquad + \begin{bmatrix} 1 \\ 0 \end{bmatrix} u_i(t-0.5) + I u_{ci}(t-0.3) + \begin{bmatrix} 1 \\ 1 \end{bmatrix} w(t), \\ y_i(t) = \begin{bmatrix} 1 & 1 \\ 0 & 1 \end{bmatrix} x_{pi}(t), \quad y_{ci}(t) = I x_{pi}(t), \quad u_{ci}(t) = \sum_{j=1}^{n} a_{Mi,j} x_{pj}(t), \\ z_i(t) = I x_{pi}(t), \ i = 1, ..., 5, \end{cases} \tag{2.30}$$

whose adjacency matrix is the same as in (2.25). Without control, this system is unstable with a robust spectral abscissa equal to 0.7927. However, using the approach of network structure exploitation presented in Section 2.3, we were able to find a stablising controller (optimising with $\alpha_o = 1$)

$$\hat{K} = \begin{bmatrix} -0.8420 & -3.2729 \end{bmatrix},$$

and subsequently a robust controller (optimising with $\alpha_o = 0$)

$$\bar{K} = \begin{bmatrix} -1.6118 & -2.5654 \end{bmatrix}.$$

The results corresponding to robust spectral abscissa and strong $\mathcal{H}_\infty$ norm are given in Table 2.2. In this example, the results have not been compared to the

Table 2.2: Results obtained for neutral type time-delay system

Neutral type system	Objective function	$\mathcal{H}_\infty$ norm	Spectral abscissa	Function evaluations (No.)	Function evaluation time (s)
No feedback	—	∞	0.7927	—	—
$u_i = \hat{K} y_i$	Robust spectral abscissa ($\alpha_o = 1$)	8.5494	-0.4870	96	0.80073
$u_i = \bar{K} y_i$	Strong $\mathcal{H}_\infty$ norm ($\alpha_o = 0$)	6.3943↓	-0.3719↑	48	4.3647

design approach using structural constraints in the controller. The resulting conclusions were not found to qualitatively differ from that presented in the previous example.

A consensus type problem

We use the following numerical example, motivated by the model from (Zheng et al., 2014), to treat consensus type problems.

$$\begin{aligned} \dot{\psi}_i(t) &= \underbrace{\begin{bmatrix} 0 & 1 & 0 \\ 0 & 0 & 1 \\ 0 & 0 & -\frac{1}{d_c} \end{bmatrix}}_{A_g} \psi_i(t) + \underbrace{\begin{bmatrix} 0 \\ 0 \\ 1 \end{bmatrix}}_{B_g} u_i(t - \breve{\tau}), \\ y_i(t) &= \underbrace{\begin{bmatrix} 0 & 1 & 0 \\ 0 & 0 & 1 \end{bmatrix}}_{C_g} \psi_i(t). \end{aligned} \tag{2.31}$$

We consider a network of n nodes, each node corresponding to a subsystem, and $R \geq 0$ virtual nodes, indexed by $i \in \{n+1, ..., n+R\}$. The dynamics of the virtual nodes, which are used to generate external reference trajectories

(e.g., a leader), can be written as

$$\begin{aligned} \dot{\psi}_i(t) &= A_g \psi_i(t), \\ y_i(t) &= C_g \psi_i(t) \quad \forall\ i = n+1, ..., n+R. \end{aligned} \tag{2.32}$$

We consider identical controllers for all subsystems and diffusive coupling between them. Let the function $t \in \mathbb{R} \to x_{ri}(t)$ be a reference trajectory for subsystem i such that

$$\begin{aligned} \dot{x}_{ri}(t) &= A_g x_{ri}(t), && i = 1, \ldots, n+R, \\ x_{ri}(t) &= \psi_i(t), && i = n+1, ..., n+R, \\ x_{ri}(t) - x_{rj}(t) &= \begin{bmatrix} d_{i,j} & 0 & 0 \end{bmatrix}^{\mathrm{T}}, && i, j \in \{1, ..., n+R\},\ t \geq 0, \end{aligned} \tag{2.33}$$

where $d_{i,j} \in \mathbb{R}^+$ is the constant prescribed reference between the subsystems i and j. If we consider the new state as $\bar{\psi}_i(t) = \psi_i(t) - x_{ri}(t)$ then we can reformulate (2.31) as

$$\begin{aligned} \dot{\bar{\psi}}_i(t) &= A_g \bar{\psi}_i(t) + B_g u_i(t - \breve{\tau}), \\ \bar{y}_i(t) &= C_g \bar{\psi}_i(t), \end{aligned} \tag{2.34}$$

since by definition $\psi_i - x_{ri} = 0,\ i = n+1, ..., n+R$, the control law[1] is

$$u_i(t) = K \underbrace{\left(\sum_{j=1}^{n} a_{Mi,j} \left(\bar{y}_j(t) - \bar{y}_i(t) \right) - \sum_{j=n+1}^{n+R} a_{Mi,j} \bar{y}_i(t) \right)}_{\sum_{j=1}^{n} a_{Mi,j} \bar{y}_j(t) - \bar{y}_i(t)}, \ i = 1, \ldots, n. \tag{2.35}$$

Unlike in the standard form of (1.20) and (2.7), system (2.34)-(2.35) features input delay as well as controllers acting (partly) on differences in outputs.

[1] In order to simplify notations and shorten the equations, we denote by $u(t) = Ky(t)$ the application of a feedback controller coupling $y(t)$ to $u(t)$, whose transfer function is given by $K(s)$.

However, using dummy variables (ν and ξ) we can rewrite (2.34)-(2.35) as

$$\begin{cases} \dot{\bar{\psi}}_i(t) & = A_g\bar{\psi}_i(t) + B_g\nu_i(t-\breve{\tau}) & + w(t) \\ 0 & = -\nu_i(t) & + u_i(t) \\ 0 & = -\xi_i(t) - C_g\bar{\psi}_i(t) & + u_{ci}(t) \\ \bar{y}_i(t) & = \xi_i(t) & \\ y_{ci}(t) & = C_g\bar{\psi}_i(t) & \\ z(t) & = \begin{bmatrix} 0 & 1 & 0 \end{bmatrix}\bar{\psi}_i(t) & \end{cases}, \tag{2.36}$$

which is of form (1.20) with $x_{pi} = \begin{bmatrix} \bar{\psi}_i^{\mathrm{T}}(t) & \nu_i^{\mathrm{T}}(t) & \xi_i^{\mathrm{T}}(t) \end{bmatrix}^{\mathrm{T}}$, while the coupling becomes

$$u_{ci}(t) = \sum_{j=1}^{n} a_{Mi,j}y_{cj}(t),\ i = 1, \ldots, n. \tag{2.37}$$

The feedback is described in the Laplace domain by

$$u_i(s) = K(s)\bar{y}_i(s),\ i = 1, \ldots, n, \tag{2.38}$$

where $K(s)$ is the transfer function of the dynamic controller. We allow virtual nodes, therefore, it is possible that $\sum_{j=1}^{n} a_{Mi,j} \leq 1$. Now we consider the system to have network topologies of ring and series type. They are presented as follows.

Ring topology: consensus problem

For a ring configuration there are no virtual nodes ($R = 0$), and recall that the adjacency matrix is described by

$$A_{M1} = \begin{bmatrix} 0 & \ldots & 0 & 1 \\ 1 & \ldots & 0 & 0 \\ \vdots & \ddots & \vdots & \vdots \\ 0 & \ldots & 1 & 0 \end{bmatrix} \tag{2.39}$$

for unidirectional coupling, and by

$$A_{M2} = \begin{bmatrix} 0 & 0.5 & 0 & \dots & 0 & 0.5 \\ 0.5 & 0 & 0.5 & \dots & 0 & 0 \\ 0 & 0.5 & 0 & \dots & 0 & 0 \\ \vdots & \vdots & \vdots & \ddots & \vdots & \vdots \\ 0 & 0 & 0 & \dots & 0 & 0.5 \\ 0.5 & 0 & 0 & \dots & 0.5 & 0 \end{bmatrix} \tag{2.40}$$

for bidirectional coupling. Without virtual nodes, the row-sum condition

$$\sum_{j=1}^{n} a_{Mi,j} = 1, \quad i = 1, \dots, n,$$

is satisfied, hence, the adjacency matrix always has an eigenvalue equal to one (Michiels and Nijmeijer, 2009). As shown in Appendix D, this implies that, independent of the control, the closed-loop system (2.36)-(2.38) always has a double eigenvalue at zero. This is because we are dealing with a consensus problem, where every solution with $x_{ri}(t) - x_{rj}(t) = \begin{bmatrix} d_{i,j} & 0 & 0 \end{bmatrix}^{\mathrm{T}}$, $i, j \in \{1, ..., n\}$, correspond to a stationary solution.

As a consequence of the above, the robust spectral abscissa for the closed-loop system is always greater than or equal to zero. However, to maximise the speed in which a consensus is reached we optimise instead

$$\begin{aligned} \breve{C}(\bar{p}; \bar{\tau}) &:= \lim_{\epsilon \to 0^+} \sup_{\bar{\tau}_\epsilon \in \mathcal{B}(\bar{\tau}, \epsilon)} \breve{c}(\bar{p}; \bar{\tau}_\epsilon), \\ \breve{c}(\bar{p}) &= \max_{\substack{1 \le i \le n \\ i \ne k}} \left\{ \sup_{\lambda \in \mathbb{C}} \{ \Re(\lambda) : \ \det \tilde{M}(\lambda; \lambda_{ai}) = 0 \} \right\}, \end{aligned} \tag{2.41}$$

where $\tilde{M}$ is the characteristic matrix of (2.13) and k is such that $\lambda_{ak} = 1$ (similar to (Rejeb et al., 2018)). When optimising the above modified spectral abscissa for plant (2.36)-(2.38) and (2.40), with $n = 5$ and controller order $n_c = 1$, we

obtain

$$\begin{cases} \dot{x}_{ci}(t) = \begin{bmatrix} -86.2588 \end{bmatrix} x_{ci}(t) + \begin{bmatrix} -249.5680 & -48.9190 \end{bmatrix} \bar{y}_i(t), \\ u_i(t) = \begin{bmatrix} -8.0038 \end{bmatrix} x_{ci}(t) + \begin{bmatrix} -23.8468 & -4.7045 \end{bmatrix} \bar{y}_i(t). \end{cases} \tag{2.42}$$

The corresponding rightmost eigenvalues are visualised in Figure 2.6. In general, defining any exogenous inputs and regulated outputs results in the strong $\mathcal{H}_\infty$ norm for the closed-loop system to be equal to infinity, due to the fact that the system does not settle back to the original stationary solution after a perturbation.

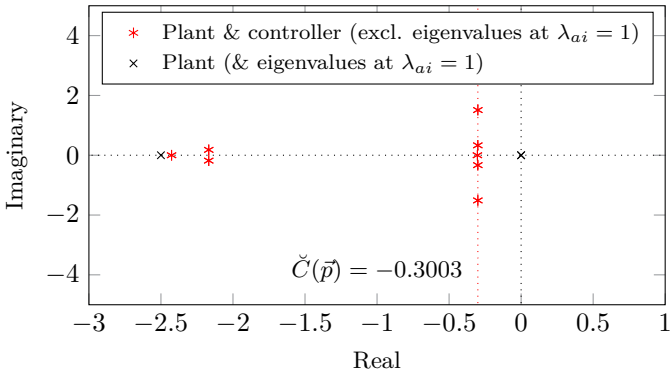

Figure 2.6: Optimised spectrum plotted for the consensus problem of five subsystems in a ring topology with bidirectional communication links.

Series topology: mixed consensus/reference tracking problem

Let us now consider the system to be in series topology. In case of unidirectional coupling, a special treatment should be given to the first subsystem, which we can solve by adding a virtual node ($R \neq 0$) that serves as a generator of the reference trajectory for this subsystem. In this way we arrive at elements $a_{Mi,j}$ contained in

$$A_{M3} = \begin{bmatrix} 0 & \dots & 0 & 0 \\ 1 & \dots & 0 & 0 \\ \vdots & \ddots & \vdots & \vdots \\ 0 & \dots & 1 & 0 \end{bmatrix}. \tag{2.43}$$

All eigenvalues of A_{M3} are equal to zero, implying that the decomposition approach leads to identical subsystems of form (2.17). The interpretation is as follows: for each subsystem we have to solve the same control problem of tracking the outputs generated by preceding subsystem. For bidirectional coupling, a special treatment should also be given to the last subsystem, in order to preclude any asymmetry, and the adjacency matrix takes the form

$$A_{M4} = \begin{bmatrix} 0 & 0.5 & 0 & \dots & 0 & 0 \\ 0.5 & 0 & 0.5 & \dots & 0 & 0 \\ 0 & 0.5 & 0 & \dots & 0 & 0 \\ \vdots & \vdots & \vdots & \ddots & \vdots & \vdots \\ 0 & 0 & 0 & \dots & 0 & 0.5 \\ 0 & 0 & 0 & \dots & 0.5 & 0 \end{bmatrix}, \tag{2.44}$$

where there exist virtual nodes ($R \neq 0$) communicating with the first and last nodes. We consider $n(= 4)$ subsystems and we first design controller $K(s)$

Table 2.3: Strong $\mathcal{H}_\infty$ norm optimisation.

Example	Feedback control	Robust spectral abscissa	Strong $\mathcal{H}_\infty$ norm
A group of four subsystems	$u_i = K(s)\bar{y}_i$	-0.2103	20.5379
	$u_i = \breve{K}(s)\bar{y}_i$	$-0.1648\uparrow$	$8.2504\downarrow$

in (2.35) as a dynamic LTI controller of order $n_c = 3$ minimising the (robust) spectral abscissa, resulting in a spectral abscissa of -0.2103. Subsequently, we use this controller as starting point to optimise the (strong) $\mathcal{H}_\infty$ norm of the transfer function from w to z for the system in (2.36) and we obtain the robust controller $\breve{K}(s)$. The robust spectral abscissa and strong $\mathcal{H}_\infty$ norm values obtained are shown in Table 2.3. The maximum singular value plots of the transfer function from w to z for the structured closed-loop systems ($u_i = K(s)\bar{y}_i$ and $u_i = \breve{K}(s)\bar{y}_i$) are shown in Figure 2.7.

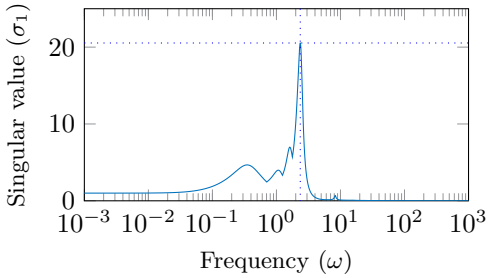

(a) $u_i = K(s)\bar{y}_i$.

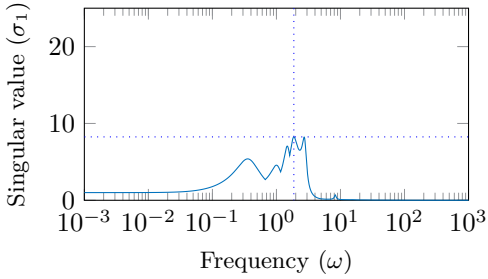

(b) $u_i = \breve{K}(s)\bar{y}_i$.

Figure 2.7: The maximum singular value plot of the transfer function from w to z for the structured closed-loop systems before and after the strong $\mathcal{H}_\infty$ norm optimisation of the controller parameters.

2.4 Extension to a scalable algorithm

From Theorem 2.3.1, the design of stabilising decentralised controllers can be recast as the simultaneous stabilisation problem of finding controller parameters such that (2.17), with $\bar{w}_i \equiv 0$, is exponentially stable $\forall\ i = 1, \ldots, n$. For some typologies, the eigenvalues corresponding to their network adjacency matrices (λ_{ai}) for any number of nodes (n) are confined to a real interval, i.e $\lambda_{ai} \in \Omega := [p, q]$ where $p \in \mathbb{R}$, $q \in \mathbb{R}$ and $p < q$. Since the only difference between the systems' equations in (2.17) lies in parameters λ_{ai}, a sufficient condition for stability is given by the *robust stability* of the *uncertain* system

$$\hat{E}\dot{\eta}(t) = \left(\hat{A}_0 + \lambda_a \hat{B}\hat{C}\right)\eta(t) + \sum_{k=1}^{m} \hat{A}_k \eta(t - \tau_k), \tag{2.45}$$

subject to interval uncertainty $\lambda_a \in [p, q]$, for which necessary and sufficient conditions can be obtained within the real structured pseudospectral framework developed in (Borgioli and Michiels, 2018). The characteristic matrix of (2.45) can be written as

$$\breve{M}(\lambda) = \lambda\hat{E} - \left(\hat{A}_0 + \hat{B}\lambda_{av}\hat{C} + \hat{B}\delta\hat{A}_0\hat{C}\right) - \sum_{k=1}^{m} \hat{A}_k \mathrm{e}^{-\lambda\tau_k}, \tag{2.46}$$

with $\lambda_{av} = \frac{p+q}{2}$ and the uncertainty $|\delta\hat{A}_0| \leq \frac{|q-p|}{2}$. We note that this is a special type of the problem mentioned in (Borgioli and Michiels, 2018).

Considering all real valued perturbations such that

$$|\delta\hat{A}_0| \leq \epsilon := \frac{|q-p|}{2},$$

we can define the real structured pseudospectrum of (2.46) as

$$\Lambda_\epsilon := \bigcup_{|\delta\hat{A}_0|\leq\epsilon} \left\{\lambda \in \mathbb{C} : \det\breve{M}(\lambda) = 0\right\}.$$

The pseudospectral abscissa (α_ϵ) is given by

$$\alpha_\epsilon := \sup\{\Re(\lambda) : \lambda \in \Lambda_\epsilon\}. \tag{2.47}$$

Hence, a *necessary and sufficient* condition for exponential stability of (2.45) $\forall\ \lambda_a \in [p, q]$ is given by $\alpha_\epsilon < 0$. An algorithm to compute the pseudospectral abscissa is provided in (Borgioli and Michiels, 2018). It is based on generating a sequence of ϵ-bounded perturbations, such that the spectral abscissa is monotonically increasing, and the corresponding eigenvalue converges to the globally right-most point of the pseudospectrum.

2.4.1 Controller design approach

Recall that the stabilisation problem of (2.10) was turned into a *simultaneous* stabilisation optimisation problem of n subsystems of the form (2.13) to optimise the controller parameters contained in matrix $\hat{A}_0$, using Theorem 2.3.1. However,

the stability property of the closed-loop system of the plant and the (resulting) controller is dependent on the number of subsystems. Now we reformulate the stabilisation problem of (2.10) as a robust stabilisation problem of uncertain (sub-)system (2.45) for scalability with the number of subsystems (n). That is, we design a controller of the form (2.7) that stabilises a system of the form (1.20) independent of the number of subsystems (n). In order to find such a robustly stabilising controller and minimise the worst-case asymptotic decay rate of solutions, we can minimise the pseudospectral abscissa by tuning controller parameters, i.e., we solve the optimisation problem

$$\min_{\bar{p}} \alpha_\epsilon. \tag{2.48}$$

Recall that vector $\bar{p}$ contains all the tunable controller parameters, which are contained in the closed-loop system matrix $\hat{A}_0$ (see (2.3) and (2.9)). As the objective function is non-convex and not-everywhere differentiable we use a dedicated optimisation algorithm for this task, HANSO (see (Overton, 2009)).

In Section 2.4.2, we will show an example for which $\lambda_{ai} \in \mathbb{R} \ \forall \ i = 1, ..., n$, however there are other network topologies for which the adjacency matrix has non-real eigenvalues (e.g., a ring topology with unidirectional coupling). This would translate to a problem with complex valued perturbations ($\hat{B}\lambda_a\hat{C}$) to system matrix $\hat{A}_0$. The algorithm in (Borgioli and Michiels, 2018) can be extended to treat such problems.

The pseudospectral abscissa optimisation approach for designing decentralised controller has many advantages. First, the size (n) of A_M increases with the number of subsystems in the structured system, leading to more eigenvalues (λ_{ai}). Therefore, the computational complexity of optimising the spectral abscissa of the overall system depends on the number of subsystems ($\mathcal{O}(n \cdot (n_{cl})^3)$) (and even $\mathcal{O}((n \cdot n_{cl})^3)$ if the decomposition is not employed). However, the computational complexity of the pseudospectral abscissa optimisation does not depend on the number of subsystems. Second, a controller designed to stabilise "n" subsystems might not be stabilising for a different value of "n", as will be demonstrated using a numerical example in the next subsection.

2.4.2 Numerical example

Let us consider a simple numerical example for which a stabilising controller has to be designed such that it can control a group of identical subsystems arranged in a network topology (with adjacency matrix A_M whose eigenvalues satisfy $\lambda_{ai} \in [-1, 1]\ \forall\ i \in \{1, ..., n\}$). The sub-systems can be described by

$$\begin{cases} \dot{x}_{pi}(t) = & \begin{bmatrix} 1 & 3 \\ 2 & -0.5 \end{bmatrix} x_{pi}(t) + \begin{bmatrix} 0 \\ 1 \end{bmatrix} u_i(t - 0.1) \\ & + \begin{bmatrix} 4 & 0 \\ 0 & 0 \end{bmatrix} u_{ci}(t - 0.2), \\ y_i(t) = & \begin{bmatrix} 1 & 1 \\ 0 & 1 \end{bmatrix} x_{pi}(t), \\ y_{ci}(t) = & I x_{pi}(t), \quad u_{ci}(t) = \sum_{j=1}^{n} a_{Mi,j} x_{pj}, \end{cases} \tag{2.49}$$

$\forall\ i = 1, ..., n$. In the following subsections, we will consider systems (2.49), arranged in two network topologies.

Series network topology

Let us consider a series network topology with bidirectional coupling, for which matrix A_M is of the form (same as (2.44))

$$A_M = \begin{bmatrix} 0 & 0.5 & 0 & \dots & 0 & 0 \\ 0.5 & 0 & 0.5 & \dots & 0 & 0 \\ 0 & 0.5 & 0 & \dots & 0 & 0 \\ \vdots & \vdots & \vdots & \ddots & \vdots & \vdots \\ 0 & 0 & 0 & \dots & 0 & 0.5 \\ 0 & 0 & 0 & \dots & 0.5 & 0 \end{bmatrix}_{n \times n}, \tag{2.50}$$

whose eigenvalues consist of

$$\lambda_{ai} = \cos(i \frac{\pi}{n+1}) :\ \ i = 1, ..., n. \tag{2.51}$$

For $n = 3$, the adjacency matrix has a spectrum given by $\hat{\boldsymbol{\lambda}}_{\boldsymbol{a}} = \{-0.7071, 0, 0.7071\}$. Choosing the controller order equal to one and minimising the spectral abscissa $c(\bar{p})$ of the coupled system lead us to the controller K_{s1} given by

$$\begin{cases} \dot{x}_{ci}(t) &= -9.5309 x_{ci}(t) + [-15.3689 \ -3.5134] y_i(t), \\ u_i(t) &= -2.9752 x_{ci}(t) + [-19.3607 \ 5.8863] y_i(t), \end{cases} \tag{2.52}$$

for $1 \leq i \leq 3$.

The optimisation of the pseudospectral abscissa of (2.46), constraining λ_{ai} to the interval $[-1, 1]$, leads us to controller K_α given by

$$\begin{cases} \dot{x}_{ci}(t) &= -4.3275 x_{ci}(t) + [-4.3547 \ 6.2463] y_i(t), \\ u_i(t) &= 6.9677 x_{ci}(t) + [-13.8842 \ 0.8332] y_i(t), \end{cases} \tag{2.53}$$

for $1 \leq i \leq n$, which is in fact stabilising for any $n \in [1, \infty]$.

In Figures 2.8-2.9 we compare the performance of both controllers. The

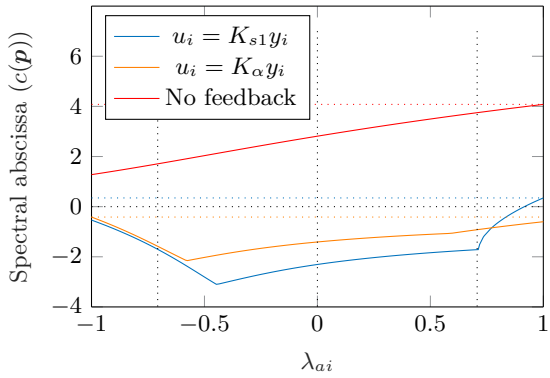

Figure 2.8: The spectral abscissa of (2.49) with (according to the decomposition) $u_{ci}(t) = \lambda_{ai} y_{ci}(t)$, for varying $\lambda_{ai} \in [-1, 1]$. We consider i) local controller K_{s1} ($\alpha_\epsilon = 0.3478$) designed by minimising $c(\bar{p})$ for $n = 3$ (i.e., for $\hat{\boldsymbol{\lambda}}_{\boldsymbol{a}} = \{-0.7071, 0, 0.7071\}$), ii) local controller K_α ($\alpha_\epsilon = -0.4151$) designed by minimising the pseudospectral abscissa of (2.45) for $\lambda_a \in [-1, 1]$, and iii) the absence of feedback control ($\alpha_\epsilon = 4.0793$).

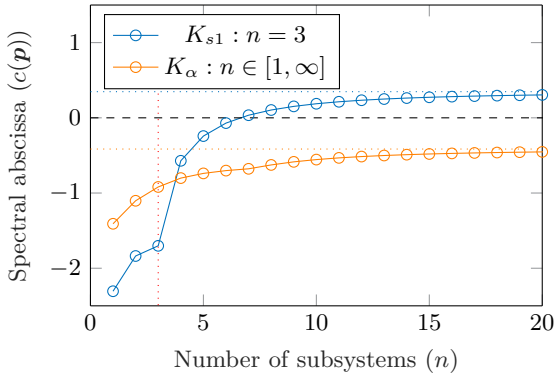

Figure 2.9: The local controller K_{s1} obtained by optimising the spectral abscissa of three ($n = 3$) subsystems in a bidirectionally coupled series network, with the spectrum of the adjacency matrix given by $\hat{\boldsymbol{\lambda}}_{\boldsymbol{a}} = \{-0.7071, 0, 0.7071\}$, results in a unstable network system for more than seven subsystems. Therefore, for improved scalability we could design a controller K_α through pseudospectral abscissa optimisation, $\forall\ \lambda_{ai} \in [-1, 1]$ leading to a stable network system for any number of subsystems $n \in [1, \infty]$.

pseudospectral abscissa (when $\lambda_{ai} \in [-1, 1]$) for the system reduced from $\alpha_\epsilon = 4.0793$ for the case of no feedback control to $\alpha_\epsilon = -0.4151$ when controlled using K_α (see Figure 2.8). Therefore, the structured closed loop system is stable as long as the adjacency matrix of the network structure A_M has all its eigenvalues in the interval $[-1, 1]$. This means that the closed loop system is guaranteed to be stable (with spectral abscissa ≤ -0.4151) for any number of nodes in the series, ring, star and fully connected network topologies with bidirectional coupling. Since, under mild conditions on the coupling weights, the eigenvalues of their adjacency matrices are contained in the interval $[-1, 1]$ (see Appendix A for more details).

Although controller K_{s1} achieves lower spectral abscissa for $\hat{\boldsymbol{\lambda}}_{\boldsymbol{a}}$, it results in a positive pseudospectral abscissa. We show the evaluation time for computing spectral abscissa (using the network structure exploitation algorithm for various n) and pseudo-spectral abscissa functions in Table 2.4.

Table 2.4: Evaluation times for computing spectral abscissa (using the network structure exploitation approach) and pseudo-spectral abscissa functions for the closed-loop system of (2.49) and $\bar{K}_\alpha$.

n	Spectral abscissa	Pseudo-spectral abscissa
1	0.1705s	
2	0.2129s	
3	0.2559s	
4	0.2755s	
5	0.3163s	
10	0.3974s	0.4642s
20	0.5570s	
30	0.7449s	
100	1.8449s	
200	3.3440s	
300	4.9742s	

Ring network topology

Let us consider the sub-systems in (2.49) to be arranged in a ring topology with bidirectional coupling. Recall from (A.5) and (A.6) in Chapter 1 that we have a circulant A_M matrix of the form

$$A_M = \begin{bmatrix} 0 & 0.5 & 0 & \dots & 0 & 0.5 \\ 0.5 & 0 & 0.5 & \dots & 0 & 0 \\ 0 & 0.5 & 0 & \dots & 0 & 0 \\ \vdots & \vdots & \vdots & \ddots & \vdots & \vdots \\ 0 & 0 & 0 & \dots & 0 & 0.5 \\ 0.5 & 0 & 0 & \dots & 0.5 & 0 \end{bmatrix}_{n\times n},$$

with the spectrum given in (Michiels and Nijmeijer, 2009) as

$$\lambda_{ai} = \cos(\frac{2\pi}{n}(i-1)) : \ i = 1, ..., z \text{ and } n \in \mathbb{Z}^+ \setminus \{1\},$$

where $z = \frac{n+2}{2}$ or $\frac{n+1}{2}$ for even or odd values of n respectively. All the eigenvalues given by (A.6) have a multiplicity of two, except for '± 1' which have multiplicity one.

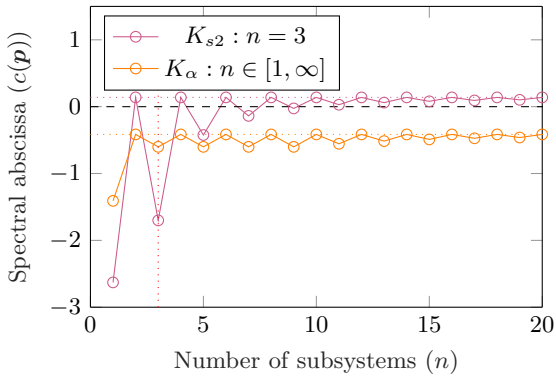

Figure 2.10: The local controller K_{s2} obtained by optimising the spectral abscissa for three ($n = 3$) subsystems in a bidirectionally coupled ring network, with the spectrum of the adjacency matrix given by $\tilde{\boldsymbol{\lambda}}_{\boldsymbol{a}} = \{-0.5, -0.5, 1\}$, results in an unstable network system for two or four subsystems. On the contrary, the local controller K_α obtained by minimising the pseudospectral abscissa stabilises the system for any number of subsystems n.

Optimising the spectral abscissa of the closed-loop system for $n = 3$ (for which the adjacency matrix has a spectrum $\tilde{\boldsymbol{\lambda}}_{\boldsymbol{a}} = \{-0.5, -0.5, 1\}$) results in the controller K_{s2} given by

$$\begin{cases} \dot{x}_{ci}(t) &= -10.1209 x_{ci}(t) + [3.0604 \ 12.1140] y_i(t), \\ u_i(t) &= 3.5645 x_{ci}(t) + [-19.3998 \ 6.0459] y_i(t), \end{cases} \tag{2.54}$$

for $1 \leq i \leq 3$ ($n = 3$). Note that we can control the subsystems in this network also using the controller K_α in (2.53), as the eigenvalues of the network adjacency matrix satisfy $\lambda_{ai} \in [-1, 1] \ \forall \ i \in \{1, \ldots, n\}$, $\forall \ n \in [1, \infty]$. We observe in Figure 2.10 that the stability of this network is affected adversely by small change in n for the closed-loop system with the controller K_{s2}. This is due to the presence of the eigenvalue '-1' in the spectrum of A_M for even numbers of subsystems (n).

2.5 Conclusions

The problem of the decentralised/overlapping controller design for systems with time-delays has been addressed in this chapter. A technique for generic LTI systems modelled by DDAEs is presented, based on imposing sparsity constraints in the controller parameterisation, and a structure exploiting approach is proposed for networks of identical systems and local controllers. By means of a numerical example, the applicability to consensus type problems is demonstrated, while also illustrating the flexibility of the modelling framework and control technique.

Additionally, a scalable methodology to design dynamic (LTI) fixed-order controllers for large-scale interconnected systems was presented. We conclude that using a direct optimisation approach and a decomposition, it might be possible to design a stabilising decentralised controller independent of the number of nodes. Here, the network related parameters are interpreted as a bounded uncertainty and handled by considering the corresponding pseudospectral abscissa function as the objective function. As already mentioned in Section 2.3.4, the decomposition approach can be extended to classes of distributed or overlapping controllers, including the case of interacting controllers communicating their state with neighbours.

The proposed direct optimization approach is a non-conservative technique for controller design in the frequency domain, grounded in necessary and sufficient stability conditions. The approach is flexible with respect to the structure that can be imposed on the controller. Issues related non-convexity and non-smoothness of the optimisation problem in general (especially for $\mathcal{H}_\infty$ norm) are still present as in the centralised setting. The non-smoothness is handled by using the special algorithm HANSO. With respect to the non-convexity, the algorithm can converge to local optima which are not global. The latter is mitigated by considering sufficiently large number of randomly generated (or user specified) starting points for the optimisation problem.

Finally, note that all the algorithms presented in this chapter have been implemented in a publicly available software (Dileep and Michiels, 2018b).

Chapter 3

Decentralised controllers in a network of sampled-data systems

3.1 Introduction

For many applications, stability and performance levels may be guaranteed for their (respective) continuous-time system models. However, when implemented, continuous time information is not available (Hristu-Varsakelis and Levine, 2005), the sensors and actuators may not be operating synchronously, and the sampling may be aperiodic. Systems with aperiodic sampling can be interpreted as Time-Delay Systems (TDSs), hybrid systems, discrete-time systems with varying parameters, feedback interconnections of systems, etc. (Bragagnolo et al., 2016; Fiacchini and Morarescu, 2016; Hetel et al., 2017; Kruszewski et al., 2012; Prieur et al., 2018). In this chapter, the case of Linear Time Invariant (LTI) systems with time-delays (at state, controlled-input, and measured-output) of retarded type is addressed from a feedback interconnection point of view. In the centralised control setting, techniques have been proposed

for stability analysis of LTI systems in (Fridman, 2014; Fujioka, 2007; Kao and Lincoln, 2004; Kao and Rantzer, 2007; Mirkin, 2007) and the references therein. Furthermore, the stability analysis of LTI systems with distributed sensors and aperiodic sampling was dealt in (Fiter et al., 2018) and was extended to include static decentralised controllers and time-varying delays (arising from controllers, sensors, and actuators) in (Thomas et al., 2018). Some researchers have also contributed to the field of (centralised) controller design for the case of periodic sampling such as (Fujioka et al., 2005; Mirkin et al., 1999). In this chapter, we focus on both stability conditions and design approaches for sampled-data fixed-order decentralised controllers for LTI systems with time-delays. These controllers may be subjected to control imperfections such as aperiodic sampling, jitter, varying time-delays, and asynchrony. This is largely an open problem in the literature.

The main contributions of this chapter are three-fold. First, stability conditions are presented for generic LTI systems with constant time-delays (at input, output, and state) stabilised by fixed-order decentralised controllers taking into account control imperfections (induced by the implementation of the controller in a sampled-data system with feedback delays). The approach is based on rewriting the closed-loop system of the Multiple Input Multiple Output (MIMO) plant and sampled-data fixed-order controller as a feedback interconnection of a nominal (continuous-time) Delay Differential Algebraic Equation (DDAE) and an uncertainty block. Then, an input-output $\mathcal{L}_2$ stability criterion is proposed. All the control imperfections are *absorbed* at the uncertainty (operator) block in this feedback interconnection.

Second, the frequency domain-based direct optimisation approach of (Gumussoy and Michiels, 2011; Michiels, 2011) is used to optimise the controller parameters for robustness against control imperfections by minimising the $\mathcal{H}_\infty$ norm of an appropriately defined transfer function. Additionally, it is shown that the conservatism of the optimised robustness criterion can be reduced by exploiting the structure of the uncertainty block using *scaling* parameters. The methodology used to design these parameters is grounded in the frequency domain-based direct optimisation approach, where objective functions specifying performance criteria are optimised as a function of the controller parameters.

The spectral abscissa (stability) and $\mathcal{H}_\infty$ norm (robustness) are, in general, non-smooth non-convex functions of fixed-order controller parameters (Gumussoy and Michiels, 2011; Michiels, 2011). The work of (Gumussoy and Michiels, 2011; Michiels, 2011) generalises the one underlying the HIFOO package (see Burke et al. (2006)) and the MATLAB function `hinfstruct` (see Apkarian and Noll (2006)) from finite dimensional systems to that considering time-delay systems. The adopted frequency domain-based optimisation approach for controller parameters complements the approach for infinite dimensional systems considered in (Apkarian and Noll, 2018). The adopted approach is very flexible in exploiting the structure of the controller. Structures such as decentralised, distributed, overlapping, lower-order, and PID[1] controllers can be handled.

As a third contribution and main result of this chapter, a scalable controller design approach is proposed for large-scale systems composed of quasi-identical subsystems connected through some delayed network. In this chapter, identical subsystems that have non-identical uncertainties or control imperfections are considered as quasi-identical subsystems. The control design problem is solved for a lower dimensional system using network structure exploitation (using the approach of Chapter 2) while guaranteeing stability of the large network. Even though we consider the subsystems to be identical in the problem formulation, it will be shown that the control imperfections (or other uncertainties) need not be identical.

The remainder of the chapter is organised as follows. Section 3.2 introduces the MIMO time-delay plants which are to be stabilised by sampled-data decentralised controllers. Section 3.3 recasts the problem of maximizing robustness against the control imperfections to a standard $\mathcal{H}_\infty$ norm optimisation problem. Section 3.4 presents the direct optimisation approach in the frequency domain to optimise robustness (in terms of $\mathcal{H}_\infty$ norm) of the controllers against control imperfections. This $\mathcal{H}_\infty$ norm characterises the maximum allowable uncertainty. Section 3.4.2 recalls the concept of network structure exploitation (from Chapter 2) and how it may be utilised to improve computational efficiency in designing decentralised

[1] See the recent survey of (Samad, 2019), wherein PID controllers still have a strong industrial impact.

controllers that are robust (against control imperfections). A numerical example is presented in Section 3.5. Finally, some concluding remarks are given in Section 3.6. The results of this chapter have been presented in (Dileep et al., 2020).

3.2 MIMO plant and decentralised controllers

In applications, controllers are often implemented as algorithms programmed on embedded processors which might work at different frequencies. The controllers could be distributed over different communication channels which may function aperiodically. In this chapter, we first consider a generic Multiple Input Multiple Output (MIMO) continuous-time plant with $n \in \mathbb{N}$ inputs and outputs, to be controlled by n decentralised dynamic controllers. The dynamics of the Linear Time Invariant (LTI) MIMO plants with constant time-delays considered in this chapter are described by

$$\begin{cases} \dot{\psi}_p(t) & = A_{\psi_p,0}\ \psi_p(t) + \sum_{j=1}^{m} A_{\psi_p,j}\psi_p(t-\tau_{\psi,j}) + \sum_{i=1}^{n} B_{\psi_p,i}\ u_i(t-\tau_{u,i}), \\ y_i(t) & = C_{\psi_p,i}\ \psi_p(t-\tau_{y,i}),\ i = 1, ..., n, \end{cases} \tag{3.1}$$

for almost all $t \geq 0$, where $\dot{\psi}_p$ is the right-hand derivative of the state vector ψ_p, $u_i \in \mathbb{R}^{n_{ui}}$ is the ith controlled-input, $y_i \in \mathbb{R}^{n_{yi}}$ is the ith measured-output, $\psi_p \in \mathbb{R}^{n_p}$ is the plant state vector, $\tau_j, \tau_{y,i}, \tau_{u,i} > 0$ are constant delays, and $A_{\psi_p,0},\ A_{\psi_p,j},\ C_{\psi_p,i},\ B_{\psi_p,i}$ are real valued constant matrices, $i = 1, ..., n,\ j = 1, ..., m$.

In Chapter 2 and (Michiels, 2011), it has been shown that plants of the form (3.1) can be rewritten in the general DDAE form using an augmented state vector $x_p = [\psi_p^{\mathrm{T}}\ \gamma_{\psi,y}^{\mathrm{T}}\ \gamma_{\psi,u}^{\mathrm{T}}]^{\mathrm{T}}$ as

$$\begin{cases} E_p\dot{x}_p(t) & = A_{p0}\ x_p(t) + \sum_{j=1}^{m_n} A_{pj}x_p(t-\tau_j) \\ & \quad + \sum_{i=1}^{n} B_{pi}\ u_i(t), \\ y_i(t) & = C_{pi}\ x_p(t),\ i = 1, ..., n, \end{cases} \tag{3.2}$$

where $\gamma_{\psi,y}$ and $\gamma_{\psi,y}$ are dummy vectors used for representing output vector $y = [y_1^{\mathrm{T}}, ..., y_n^{\mathrm{T}}]^{\mathrm{T}}$ and input vector $u = [u_1^{\mathrm{T}}, ..., u_n^{\mathrm{T}}]^{\mathrm{T}}$ respectively, and E_p may be singular. Notice that all the time-delays are now associated with the augmented state vector, that is, $\{\tau_1, ..., \tau_{m_n}\} = \{\tau_{\psi,1}, ..., \tau_{\psi,m}\} \cup \{\tau_{y,1}, ..., \tau_{y,n}\} \cup \{\tau_{u,1}, ..., \tau_{u,n}\}$. Sections 3.2.1-3.2.2 will introduce the problem of stabilising plants of the form (3.2) through sampled-data control and a related input-output $\mathcal{L}_2$ stability criterion.

Furthermore, a special case of plant (3.2) is also considered in this chapter. The special case corresponds to a MIMO plant composed of "n" identical subsystems coupled through a network. Similar to Section 1.6, we consider a network described by a directed graph $\mathcal{G} = \{\mathcal{V}, \mathcal{E}, A_M\}$ with a set of nodes $\mathcal{V} = \{1, 2, ..., n\}$ and a set of edges $\mathcal{E} \subset \mathcal{V} \times \mathcal{V}$. The edge $(i, j) \in \mathcal{E}$ connects from node $j \in \mathcal{V}$ to node $i \in \mathcal{V}$. A_M is the adjacency matrix of the corresponding network structure, with $a_{Mi,j}$ being the entry at row i and column j. The adjacency matrix is a square matrix with zero diagonal elements and its off-diagonal element $(a_{Mi,j})$ is considered to be the weight of the corresponding edge (i, j). We assume that the associated time-delays and the information exchange between these subsystems are identical. Then, we can re-write (3.2), which correspond to the (nodal) dynamics, as

$$\begin{cases} \hat{E}_p\ \dot{x}_{pi}(t) & = \hat{A}_{p0} x_{pi}(t) + \sum_{j=1, j\neq i}^{n} a_{Mi,j} \hat{F}_p x_{pj}(t) \\ & \quad + \sum_{k=1}^{m_n} \hat{A}_{pk}\ x_{pi}(t - \tau_k) + \hat{B}_p\ u_i(t), \\ y_i(t) & = \hat{C}_p\ x_{pi}(t), \qquad i = 1, ..., n. \end{cases} \tag{3.3}$$

The above system model is also in the most general DDAE form since $\bar{E}_p$ is allowed to be singular. Hence, this system can also be used to represent subsystems which are delay coupled with the help of an augmented state vector. The design of robust (identical) decentralised controllers for such systems can be made computationally efficient using the network structure exploitation approach developed in Chapter 2.

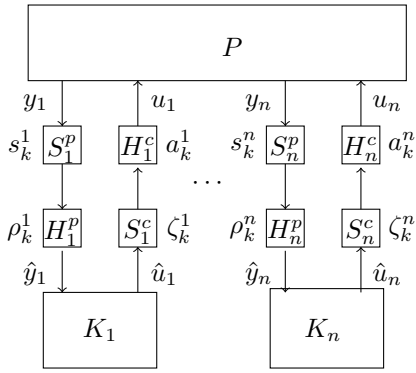

Figure 3.1: Closed-loop system of the decentralised controllers (K_i) and the MIMO plant (P) with constant time-delays and control imperfections.

3.2.1 Sampled-data decentralised control

Consider the sampled-data decentralised control configuration shown in Figure 3.1. The sampling and actuation sequences for the control are introduced as follows. The ith measured output (y_i) is sampled according to a sampling sequence $\{s_k^i\}_{k\in\mathbb{Z}_0^+}$, represented using a set of instants, where $s_0^i \in (0, \bar{h}_i]$,

$$s_{k+1}^i = s_k^i + h_k^i, \tag{3.4}$$

and $h_k^i \in (0, \bar{h}_i]$, $k \in \mathbb{Z}_0^+$, $i = 1, ..., n$. The sampling intervals (h_k^i) consider imperfections in sampling such as jitters and data packet dropouts. The ith controlled-input is sampled according to a sequence $\{\zeta_k^i\}_{k\in\mathbb{Z}_0^+}$ where $\zeta_0^i \in (0, \bar{\kappa}_i]$,

$$\zeta_{k+1}^i = \zeta_k^i + \kappa_k^i, \tag{3.5}$$

and $\kappa_k^i \in (0, \bar{\kappa}_i]$, $k \in \mathbb{Z}_0^+$, $i = 1, ..., n$. The sequence of instants at which the ith controller receives the sampled output is denoted by $\{\rho_k^i\}_{k\in\mathbb{Z}_0^+}$, where

$$\rho_k^i = s_k^i + \vartheta_k^i, \tag{3.6}$$

and $\vartheta_k^i \in [0, \bar{\vartheta}_i]$, $k \in \mathbb{Z}_0^+$, $i = 1, ..., n$. The asynchrony between sensors and controllers are denoted by ϑ_k^i, $k \in \mathbb{Z}_0^+$, $i = 1, ..., n$. Asynchrony may occur due

to sensor delays. The controlled-input is implemented at the plant according to actuation instants $\{a_k^i\}_{k\in\mathbb{Z}_0^+}$, where

$$a_k^i = \zeta_k^i + \varkappa_k^i, \tag{3.7}$$

and $\varkappa_k^i \in [0, \overline{\varkappa}_i],\ k \in \mathbb{Z}_0^+,\ i = 1, ..., n$. Here, $\varkappa_k^i$ denote the asynchrony between controllers and actuators (which includes the computation delays in the controllers). The following assumption is considered throughout this chapter for the sampling and receiving instants of the closed-loop system with control imperfections.

Assumption 4 *We assume that there exist positive real valued bounds* $\overline{h}_i, \overline{\eta}_i, \overline{\vartheta}_i, \overline{\varkappa}_i,$ *and* $\overline{\kappa}_i$ *such that the* k^{th} *closed-loop control sequence satisfies*

$$0 < s_k^i \leq \rho_k^i \leq \zeta_k^i \leq a_k^i,\ \forall\ k \in \mathbb{Z}_0^+,\ i = 1, ..., n. \tag{3.8}$$

The above assumption ensures that the output sampled at the instant s_k^i from the sensor is used for the computation of controlled-input at the instant ζ_k^i which is implemented at the instant a_k^i. That is, the actuation data and control data are ordered with respect to the moments of time when sensor data is transmitted. This ensures that the control input based on $y_i(s_k^i)$ can be applied at time-interval $[a_k^i, a_{k+1}^i),\ k \in \mathbb{Z}_0^+$. Notice that the contrary case $\rho_k^i > \zeta_k^i$ corresponds to an irrational case where the kth sequence input to the controller is received before the kth sequence controlled input is computed. Also, the cases $\rho_k^i > a_k^i$ or $\zeta_k^i > a_k^i$ correspond to the cases where the kth sequence control data is processed before the kth sequence actuation data is applied. The asynchrony between sensors and actuators can be described using $\{\eta_k^i\}_{k\in\mathbb{Z}_0^+}$, where

$$\eta_k^i = a_k^i - s_k^i, \tag{3.9}$$

and $\eta_k^i \in [0, \overline{\eta}_i],\ k \in \mathbb{Z}_0^+,\ i = 1, ..., n$. Based on the sufficient condition of Assumption 4, the sampled-output received at the controller is

$$\hat{y}_i(t) = \begin{cases} y_i(0), & \forall\ t \in [0, \rho_0^i), \\ y_i(s_k^i), & \forall\ t \in [\rho_k^i, \rho_{k+1}^i), \end{cases} \tag{3.10}$$

$\forall\ k \in \mathbb{Z}_0^+,\ i = 1, ..., n$. We consider the dynamics of the ith fixed-order controller to be

$$\begin{aligned} \dot{x}_{ci}(t) &= A_{ci}\ x_{ci}(t) + B_{ci}\ \hat{y}_i(t), \\ \hat{u}_i(t) &= C_{ci}x_{ci}(t) + D_{ci}\hat{y}_i(t), \end{aligned} \tag{3.11}$$

for almost all $t \geq 0$, where the controller state is denoted by $x_{ci}(t) \in \mathbb{R}^{n_{ci}}$, the controller coefficient matrices A_{ci}, B_{ci}, C_{ci}, and D_{ci} are constant and real valued, and the controlled-input implemented at the plant is

$$u_i(t) = \begin{cases} \hat{u}_i(0), & \forall\ t \in [0, a_0^i), \\ \hat{u}_i(\zeta_k^i), & \forall\ t \in [a_k^i, a_{k+1}^i), \end{cases} \tag{3.12}$$

$\forall\ k \in \mathbb{Z}_0^+,\ i = 1, ..., n$. We recall from Assumption 4 that $x_{ci}(\zeta_k)$ and $y_i(s_k)$ are the ith controller state information and the measured-output from i^{th} plant, respectively, used for computing $\hat{u}_i(\zeta_k^i)$. Then, we have

$$\begin{aligned} \hat{u}_i(0) &= C_{ci}x_{ci}(0) + D_{ci}\hat{y}_i(0) = C_{ci}x_{ci}(0) + D_{ci}y_i(0), \\ \hat{u}_i(\zeta_k^i) &= C_{ci}x_{ci}(\zeta_k^i) + D_{ci}\hat{y}_i(\zeta_k^i) \\ &= C_{ci}x_{ci}(\zeta_k^i) + D_{ci}y_i(s_k^i), \quad k \in \mathbb{Z}_0^+,\ i = 1, ..., n. \end{aligned} \tag{3.13}$$

3.2.2 A feedback interconnection interpretation

In this subsection, we rewrite the closed-loop system of (3.2) and (3.11) as a feedback interconnection of a nominal system and an uncertainty block. This interpretation allows us to use a simple input-output $\mathcal{L}_2$ stability criterion, extending the work of (Fiter et al., 2018; Thomas et al., 2018), for the design of dynamic controllers for DDAEs. For this purpose, we represent the piecewise-constant controlled-input and measured-output in continuous-time using time-varying errors, that is,

$$\begin{cases} \dot{x}_{ci}(t) &= A_{ci}\ x_{ci}(t) + B_{ci}(y_i(t) + e_1^i(t)), \\ u_i(t) &= (C_{ci}x_{ci}(t) + e_2^i(t)) + D_{ci}(y_i(t) + e_3^i(t)), \end{cases} \tag{3.14}$$

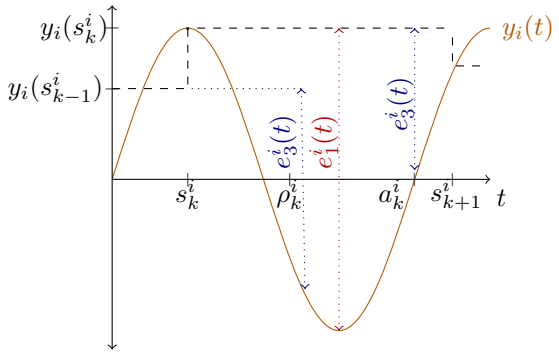

Figure 3.2: A signal $y_i(t)$ used to illustrate that the errors e_1^i and e_3^i due to sampling need not be same.

$\forall\ t \geq 0,\ i = 1, ..., n$, where the error signals are

$$e_1^i(t) = \begin{cases} y_i(0) - y_i(t), & \forall\ t \in [0, \rho_0^i) \\ y_i(s_k^i) - y_i(t), & \forall\ t \in [\rho_k^i, \rho_{k+1}^i) \end{cases}, \tag{3.15}$$

$$e_2^i(t) = \begin{cases} C_{c,i}x_{ci}(0) - C_{ci}x_{ci}(t), & \forall\ t \in [0, a_0^i) \\ C_{c,i}x_{ci}(\zeta_k^i) - C_{ci}x_{ci}(t), & \forall\ t \in [a_k^i, a_{k+1}^i) \end{cases}, \tag{3.16}$$

$$e_3^i(t) = \begin{cases} y_i(0) - y_i(t), & \forall\ t \in [0, a_0^i) \\ y_i(s_k^i) - y_i(t), & \forall\ t \in [a_k^i, a_{k+1}^i) \end{cases}, \tag{3.17}$$

$\forall\ k \in \mathbb{Z}_0^+,\ i = 1, ..., n$. Here, $e_1^i(t)$ arises due to the sampled output implemented at the controller, $e_2^i(t)$ arises due to the sampled controller-state implemented at the input, and $e_3^i(t)$ arises due to the sampled output implemented at the input. Note that e_1^i and e_3^i need not be same due to the transport delay, this is evident in Figure 3.2. Now we define the uncertainty operator. For this purpose, consider $z_i = [z_{i,1}^{\mathrm{T}}\ z_{i,2}^{\mathrm{T}}]^{\mathrm{T}},\ z_i \in \mathcal{L}_{2e}[0, \infty)$, $w_i = [e_1^i\ e_3^i\ e_2^i]^{\mathrm{T}},\ w_i \in \mathcal{L}_{2e}[0, \infty)$, and the (bounded) integral operators Δ_1^i, Δ_2^i and Δ_3^i on $\mathcal{L}_{2e}[0, \infty)$, $i = 1, ..., n$, such

that

$$e_1^i(t) = (\Delta_1^i z_{i,1})(t)$$
$$:= \begin{cases} -\int_0^t z_{i,1}(\theta)\mathrm{d}\theta, & \forall\ t \in [0, \rho_0^i) \\ -\int_{s_k^i}^t z_{i,1}(\theta)\mathrm{d}\theta, & \forall\ t \in [\rho_k^i, \rho_{k+1}^i) \end{cases}, \tag{3.18}$$

$$e_2^i(t) = (\Delta_2^i z_{i,2})(t)$$
$$:= \begin{cases} -\int_0^t z_{i,2}(\theta)\mathrm{d}\theta, & \forall\ t \in [0, a_0^i) \\ -\int_{\zeta_k^i}^t z_{i,2}(\theta)\mathrm{d}\theta, & \forall\ t \in [a_k^i, a_{k+1}^i) \end{cases}, \tag{3.19}$$

$$e_3^i(t) = (\Delta_3^i z_{i,1})(t)$$
$$:= \begin{cases} -\int_0^t z_{i,1}(\theta)\mathrm{d}\theta, & \forall\ t \in [0, a_0^i) \\ -\int_{s_k^i}^t z_{i,1}(\theta)\mathrm{d}\theta, & \forall\ t \in [a_k^i, a_{k+1}^i) \end{cases}, \tag{3.20}$$

$\forall\ k \in \mathbb{Z}_0^+,\ i = 1, ..., n$. Let $\tilde{\Delta}_i$ be an (uncertainty) operator on $\mathcal{L}_{2e}[0, \infty)$ defined by

$$w_i(t) = (\tilde{\Delta}_i z_i)(t) := \begin{bmatrix} (\Delta_1^i z_{i,1})(t) \\ (\Delta_3^i z_{i,1})(t) \\ (\Delta_2^i z_{i,2})(t) \end{bmatrix},\ i = 1, ..., n, \tag{3.21}$$

where $w_i(t)$ is an exogenous input to the nominal system and $z_i(t)$ is an exogenous output from the nominal system.

We introduce the following proposition to recast the closed-loop system of (3.2) and (3.11) as a feedback interconnection of a continuous-time nominal system and an uncertainty block.

Proposition 3.2.1 *Closed-loop system (3.2) and (3.11) can be rewritten as a feedback interconnection of a nominal system in the DDAE form, using the augmented state vector x,*

$$\begin{cases} E\dot{x}(t) & = A_0 x(t) + \sum_{j=1}^{m_n} A_j x(t - \tau_j) + Bw(t), \\ z(t) & = Cx(t), \end{cases} \tag{3.22}$$

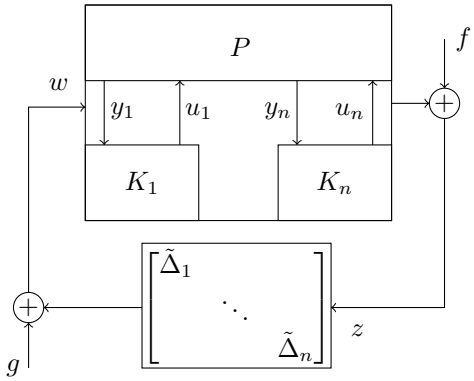

Figure 3.3: The control imperfections in Figure 3.1 are *absorbed* in the operators $\tilde{\Delta}_i,\ i = 1, ..., n.$

and an uncertainty operator on $\mathcal{L}_{2e}[0, \infty)$ *defined by*

$$w(t) = (\tilde{\Delta}z)(t) := \begin{bmatrix} (\tilde{\Delta}_1 z_1)(t) \\ \vdots \\ (\tilde{\Delta}_n z_n)(t) \end{bmatrix}, \tag{3.23}$$

where $w = [w_1^T \ \dots \ w_n^T]^T$, $z = [z_1^T \ \dots \ z_n^T]^T$ *(see Figure 3.3), and the coefficient matrices in (3.22) are*

$$A_0 = \begin{bmatrix} A_{p0} & B_p & 0 & 0 & 0 & 0 \\ 0 & -I & B_{w1} & 0 & C_c & D_c \\ 0 & 0 & -I & 0 & 0 & 0 \\ 0 & 0 & 0 & I & 0 & 0 \\ 0 & 0 & B_{w2} & 0 & A_c & B_c \\ C_p & 0 & 0 & 0 & 0 & -I \end{bmatrix},$$

$$A_i = \begin{bmatrix} A_{pi} & 0 & 0 & 0 & 0 & 0 \\ 0 & 0 & 0 & 0 & 0 & 0 \\ 0 & 0 & 0 & 0 & 0 & 0 \\ 0 & 0 & 0 & 0 & 0 & 0 \\ 0 & 0 & 0 & 0 & 0 & 0 \\ 0 & 0 & 0 & 0 & 0 & 0 \end{bmatrix},$$

$$E = \begin{bmatrix} E_p & 0 & 0 & 0 & 0 & 0 \\ 0 & 0 & 0 & 0 & 0 & 0 \\ 0 & 0 & 0 & 0 & 0 & 0 \\ C_{z1} & 0 & 0 & 0 & C_{z2} & 0 \\ 0 & 0 & 0 & 0 & I & 0 \\ 0 & 0 & 0 & 0 & 0 & 0 \end{bmatrix},$$

$$C = \begin{bmatrix} 0 & 0 & 0 & I & 0 & 0 \end{bmatrix},$$

$$B = \begin{bmatrix} 0 & 0 & I & 0 & 0 & 0 \end{bmatrix}^T,$$

$$B_p = \begin{bmatrix} B_{p1} & \dots & B_{pn} \end{bmatrix},\ C_p = \begin{bmatrix} C_{p1} \\ \vdots \\ C_{pn} \end{bmatrix},$$

$$C_c = \begin{bmatrix} C_{c1} & & 0 \\ & \ddots & \\ 0 & & C_{cn} \end{bmatrix},\ D_c = \begin{bmatrix} D_{c1} & & 0 \\ & \ddots & \\ 0 & & D_{cn} \end{bmatrix},$$

$$A_c = \begin{bmatrix} A_{c1} & & 0 \\ & \ddots & \\ 0 & & A_{cn} \end{bmatrix},\ B_c = \begin{bmatrix} B_{c1} & & 0 \\ & \ddots & \\ 0 & & B_{cn} \end{bmatrix},$$

$$B_{w1} = \begin{bmatrix} 0\ I\ D_{c1} & & 0 \\ & \ddots & \\ 0 & & 0\ I\ D_{cn} \end{bmatrix},$$

$$B_{w2} = \begin{bmatrix} B_{c1}\ 0\ 0 & & 0 \\ & \ddots & \\ 0 & & B_{cn}\ 0\ 0 \end{bmatrix},$$

$$C_{z1} = \begin{bmatrix} C_{p1} \\ 0 \\ \vdots \\ C_{pn} \\ 0 \end{bmatrix},\ C_{z2} = \begin{bmatrix} 0 & & 0 \\ C_{c1} & & \\ & \ddots & \\ 0 & & 0 \\ & & C_{cn} \end{bmatrix}.$$

Proof. Since the controlled-inputs are piecewise constant and there is no feed-through, the outputs $y_i, i = 1, ..., n$, are piecewise continuously differentiable. That is, for any $t_2 > t_1 \geq 0$, we can expess $y_i(t_2) - y_i(t_1) = \int_{t_1}^{t_2} \dot{y}_i(\theta)\mathrm{d}\theta\ \forall\ i = 1, ..., n$. Similarly, the functions $C_{ci}x_{ci}, i = 1, ..., n$, are also piecewise continuously differentiable, then we can express $C_{ci}x_{ci}(t_2) - C_{ci}x_{ci}(t_1) = \int_{t_1}^{t_2} C_{ci}\dot{x}_{ci}(\theta)\mathrm{d}\theta,\ i = 1, ..., n$. Therefore, the errors can be rewritten as

$$e_1^i(t) = \begin{cases} -\int_0^t \dot{y}_i(\theta)\mathrm{d}\theta, & \forall\ t \in [0, \rho_0^i) \\ -\int_{s_k^i}^t \dot{y}_i(\theta)\mathrm{d}\theta, & \forall\ t \in [\rho_k^i, \rho_{k+1}^i) \end{cases},$$

$$e_2^i(t) = \begin{cases} -\int_0^t C_{ci}\dot{x}_{ci}(\theta)\mathrm{d}\theta, & \forall\ t \in [0, a_0^i) \\ -\int_{\zeta_k^i}^t C_{ci}\dot{x}_{ci}(\theta)\mathrm{d}\theta, & \forall\ t \in [a_k^i, a_{k+1}^i) \end{cases}, \tag{3.24}$$

$$e_3^i(t) = \begin{cases} -\int_0^t \dot{y}_i(\theta)\mathrm{d}\theta, & \forall\ t \in [0, a_0^i) \\ -\int_{s_k^i}^t \dot{y}_i(\theta)\mathrm{d}\theta, & \forall\ t \in [a_k^i, a_{k+1}^i) \end{cases},$$

$\forall\, k \in \mathbb{Z}_0^+,\ i = 1, ..., n$. Then closed-loop system (3.2) and (3.14) can be rewritten in the feedback interconnection form of

$$\begin{cases} E_p \dot{x}_p(t) & = A_{p0}\ x_p(t) + \sum_{j=1}^{m_n} A_{pj} x_p(t-\tau_j) + \sum_{i=1}^{n} B_{pi}\ u_i(t), \\ y_i(t) & = C_{pi}\ x_p(t), \\ \dot{x}_{ci}(t) & = A_{ci} x_{ci}(t) + B_{ci} y_i(t) + \begin{bmatrix} B_{ci} & 0 & 0 \end{bmatrix} w_i(t), \\ u_i(t) & = C_{ci} x_{ci}(t) + D_{ci} y_i(t) + \begin{bmatrix} 0 & I & D_{ci} \end{bmatrix} w_i(t), \\ z_i(t) & = \begin{bmatrix} \dot{y}_i(t) \\ C_{ci} \dot{x}_{ci}(t) \end{bmatrix},\ i = 1, ..., n, \end{cases} \tag{3.25}$$

and

$$w_i(t) = (\tilde{\Delta}_i z_i)(t),\ i = 1, ..., n. \tag{3.26}$$

The plant in (3.22) is another simplified DDAE form of (3.25) where $z_{i,1}(t) = \dot{y}_i(t),\ z_{i,2}(t) = C_{ci}\dot{x}_{ci}(t),\ i = 1, ..., n$, hence proved. ∘

Remark 2 *Plant (3.22) is obtained using the augmented state vector* $x = [x_p^T u^T \gamma_w^T \gamma_z^T x_c^T y^T]^T$, *where* γ_w *and* γ_z *are dummy vectors for* w *and* z, *respectively,* $x_c = [x_{c1}^T\ \ldots\ x_{cn}^T]^T$, $u = [u_1^T\ \ldots\ u_n^T]^T$, *and* $y = [y_1^T\ \ldots\ y_n^T]^T$.

Remark 3 *Plant (3.2) has no exogenous inputs or outputs. However, it is possible to consider other exogenous inputs (which will arise in the first line of (3.25)) or outputs in its dynamics in addition to the control imperfections. Such a system can also be recast into the form of (3.22) with minor changes in the coefficient matrices, input vector, and output vector.*

Notice that by rewriting the system in the DDAE form (3.22), we have enforced all the controller parameters to be contained within A_0.

3.3 Stability criterion: generic case

Using the problem described in the previous section as our motivation, we study the feedback interconnection of a plant $\mathbf{G}$ and an uncertainty block $\tilde{\Delta}$

$$\begin{cases} z &= \mathbf{G}w + f \\ w &= \tilde{\Delta}z + g, \end{cases} \tag{3.27}$$

where $f, g \in \mathcal{L}_{2e}[0, \infty)$. The operator $\mathbf{G}$ on $\mathcal{L}_{2e}[0, \infty)$ describes the input-output map of the nominal system (3.22) (with zero initial conditions). In the frequency domain, it is described by the transfer function matrix

$$G(s) := C(sE - A_0 - \sum_{j=1}^{m_n} A_j \mathrm{e}^{-s\tau_j})^{-1}B. \tag{3.28}$$

The operator $\tilde{\Delta}$ is already defined in (3.23). The feedback interconnection (3.27) can represent the decentralised control system given by (3.2) and (3.14), affected by perturbations at the state, represented by f and g, and with zero initial condition. A direct consequence of the small gain theorem (Fridman, 2014; Khalil, 2002; Zames, 1966) recalled in Appendix B is that the mapping

$$\begin{bmatrix} f \\ g \end{bmatrix} \longrightarrow \begin{bmatrix} w \\ z \end{bmatrix}, \tag{3.29}$$

resulting from the feedback interconnection of (3.27) has a finite $\mathcal{L}_2$ gain if $||\mathbf{G}||_{\mathcal{L}_2} \cdot ||\tilde{\Delta}||_{\mathcal{L}_2} < 1$. We consider a feedback interconnection to be input-output $\mathcal{L}_2$ stable when its mapping has a finite $\mathcal{L}_2$ gain. Since $\mathbf{G}$ is linear and time-invariant, the induced-$\mathcal{L}_2$ norm $||\mathbf{G}||_{\mathcal{L}_2} = ||G||_{\mathcal{H}_\infty}$. Based on Assumption 4, we introduce the following lemma.

Lemma 3.3.1 *The integral operators Δ_1^i, Δ_2^i, and Δ_3^i satisfy*

$$||\Delta_j^i||_{\mathcal{L}_2} \leq \gamma_j^i, \;\; j = 1, 2, 3, \;\; i = 1, ..., n, \tag{3.30}$$

where

$$\begin{aligned}\gamma_1^i &= \bar{h}_i + \bar{\vartheta}_i,\\ \gamma_2^i &= \bar{\kappa}_i + \bar{\varkappa}_i,\\ \gamma_3^i &= \bar{h}_i + \bar{\eta}_i,\ \ i = 1, ..., n.\end{aligned} \tag{3.31}$$

Proof. The proof is given in Appendix E. □

To determine a condition for input-output stability of the feedback interconnection of (3.27), the following lemma is presented.

Lemma 3.3.2 *The $\mathcal{L}_2$ gain of the operator $\tilde{\Delta}_i$ can be bounded as follows,*

$$||\tilde{\Delta}_i||_{\mathcal{L}_2} \leq \bar{\gamma}_i, \tag{3.32}$$

where

$$\bar{\gamma}_i := \max\{\sqrt{(\gamma_1^i)^2 + (\gamma_3^i)^2}, \gamma_2^i\},\ \ i = 1, ..., n. \tag{3.33}$$

Proof. The proof follows from Lemma 3.3.1 and by considering the worst case $\mathcal{L}_2$ gain. □

Combining the above results, a sufficient condition for input-output stability of the feedback interconnection of (3.27) is presented in the following theorem.

Theorem 3.3.3 *Assume that the nominal system described using the transfer function matrix defined in (3.28) is exponentially stable. Then, the feedback interconnection (3.27) (as in Figure 3.3) is guaranteed to be input-output $\mathcal{L}_2$ stable if it satisfies the condition,*

$$\max_{i \in \{1,...,n\}} \bar{\gamma}_i < \left(||G(j\omega)||_{\mathcal{H}_\infty}\right)^{-1},$$

where the transfer function matrix $G(j\omega)$ from w to z is defined in (3.28) and $\bar{\gamma}_i,\ i = 1, ..., n$, are defined in terms of the sampling interval and asynchrony bounds in (3.31) and (3.33).

Proof. The proof follows directly by virtue of the small gain theorem and Lemma 3.3.2. ∘

Next, we introduce a less conservative robust stability condition by exploiting the structure of the operator $\tilde{\Delta}$. To do so, we rely on scaling the feedback connection according to the structure of the block diagonal operator $\tilde{\Delta}$ (see (Michiels et al., 2009a; Shamma, 1994) and the references therein for more details). We define (diagonal) scaling matrices X and $\tilde{X}$, such that

$$X := \begin{bmatrix} \breve{\delta}_1 & \dots & 0 \\ \vdots & \ddots & \vdots \\ 0 & \dots & \breve{\delta}_n \end{bmatrix}, \; \tilde{X} := \begin{bmatrix} \hat{\delta}_1 & \dots & 0 \\ \vdots & \ddots & \vdots \\ 0 & \dots & \hat{\delta}_n \end{bmatrix}, \tag{3.34}$$
$$\breve{\delta}_i = \begin{bmatrix} \delta_{i,1} & 0 \\ 0 & \delta_{i,2} \end{bmatrix}, \; \hat{\delta}_i = \begin{bmatrix} \delta_{i,1} I_{2\times 2} & 0 \\ 0 & \delta_{i,2} \end{bmatrix}, \; i = 1, ..., n,$$

and $\delta_{i,j} \in \mathbb{R} \setminus \{0\}$, $i = 1, ..., n$, $j = 1, 2$, are scalar parameters. Notice that X and $\tilde{X}$ have a structure related to $\tilde{\Delta}$, and $\tilde{X} \neq X$ because the dimensions of input and output vectors are different. For simplicity of the presentation, we combine all the scalar parameters in a vector, $\bar{\delta} = [\delta_{1,1} \; \delta_{1,2} \; \dots \; \delta_{n,1} \; \delta_{n,2}]^{\mathrm{T}}$. For the block-diagonal operator considered, we have, by definition, $X^{-1}\tilde{\Delta}\tilde{X} = \tilde{\Delta}$. Due to the feedback interconnection of (3.25)-(3.26), we know that introducing the scaling matrices does not affect its stability property. We are now ready to improve the criterion in Theorem 3.3.3 using the following proposition.

Proposition 3.3.4 *Assume that the nominal system described using the transfer function matrix in (3.28) is exponentially stable. Then, a sufficient condition for the feedback interconnection of (3.27) to be input-output $\mathcal{L}_2$ stable is*

$$\max_{i\in\{1,\dots,n\}} \bar{\gamma}_i < \left(\inf_{\bar{\delta}} ||X(\bar{\delta})G(j\omega)\tilde{X}^{-1}(\bar{\delta})||_{\mathcal{H}_\infty} \right)^{-1}. \tag{3.35}$$

For simplicity of the presentation, we define a new (transfer) function $\hat{G}(j\omega, \bar{\delta}) := XG\tilde{X}^{-1}(j\omega, \bar{\delta})$.

Remark 4 *The values for scaling parameters ($\bar{\delta}$) in (3.35) are determined by*

solving a non-convex optimisation problem. This problem will be shown later in Secton 3.4.1.

3.4 Controller design

We build on the approach of (Gumussoy and Michiels, 2011; Michiels, 2011) to directly optimise the robustness against control imperfections (by minimising $||G||_{\mathcal{H}_\infty}$) of the nominal time-delay system (3.22) as a function of the parameter vector $\bar{p}$. Notice that an exponentially stable nominal system (DDAE with continuous-time control) is required to initialise the optimisation of objective functions involving the $\mathcal{H}_\infty$ norm. If this is not the case, a preliminary stabilisation phase is conducted based on optimising the spectral abscissa. The vector $\bar{p}$ contains the tunable parameters of the decentralised controllers

$$\bar{p}^{\mathrm{T}} = [\bar{p}_1^{\mathrm{T}} \ \dots \ \bar{p}_n^{\mathrm{T}}], \text{ where } \bar{p}_i = \mathrm{vec}\left(\begin{bmatrix} A_{ci} & B_{ci} \\ C_{ci} & D_{ci} \end{bmatrix}\right), \tag{3.36}$$

$i = 1, ..., n$. For the special case of static controller (as considered by Thomas et al. (2018)), only elements of D_{ci} exist. In the following subsections, we describe the objective functions for which the controller parameters may be optimised.

3.4.1 Generic case

Recall that the spectral abscissa of the nominal system (3.22) with $w \equiv 0$ is defined as follows,

$$c(\bar{p}) = \sup_{\lambda \in \mathbb{C}} \{\Re(\lambda) : \det M(\lambda, \bar{p}) = 0\}, \tag{3.37}$$

where the characteristic matrix

$$M(\lambda, \bar{p}) := \lambda E - A_0(\bar{p}) - \sum_{i=1}^{m_n} A_i \mathrm{e}^{-\lambda \tau_i}.$$

Note that the dependence of functions on $\bar{p}$ is only made explicit in the notation when necessary. The exponential stability of the null solution of the system in (3.22) is determined by the condition $c(\bar{p}) < 0$ (see (Michiels, 2011)). We know that the null solution of the system in (3.22) is exponentially stable iff $c(\bar{p}) < 0$. With respect to the optimisation problem, the objective function is tuned with respect to the controller parameters ($\bar{p}$). To obtain a exponentially stable system that maximises the exponential decay rate of the solutions, the controller parameters (in $\bar{p}$) are optimised for the minimum of spectral abscissa, that is, they are obtained by

$$\min_{\bar{p}} c(\bar{p}). \tag{3.38}$$

The transfer function matrix from w to z of the nominal system represented by (3.22) is given by

$$G(s, \bar{p}) = C\Big(sE - A_0(\bar{p}) - \sum_{i=1}^{m_n} A_i \mathrm{e}^{-s\tau_i}\Big)^{-1} B. \tag{3.39}$$

Given that system (3.22) is exponentially stable, that is $c(\bar{p}) < 0$, the $\mathcal{H}_\infty$ norm of the transfer function matrix given in (3.39) can be expressed as

$$||G(j\omega, \bar{p})||_{\mathcal{H}_\infty} = \sup_{\omega \in \mathbb{R}} \sigma_1(G(j\omega, \bar{p})). \tag{3.40}$$

To improve robustness against control imperfections written in terms of the $\mathcal{H}_\infty$ norm of (3.40), controller parameters (in $\bar{p}$) may be optimised by minimising the function

$$\min_{\bar{p}} ||G(j\omega, \bar{p})||_{\mathcal{H}_\infty}. \tag{3.41}$$

Hence, the maximum allowable upper-bound for the sampling intervals and asynchrony for which the closed-loop system is stable is improved by solving the non-convex optimisation problem in (3.41). This can be implemented numerically using the algorithm in (Gumussoy and Michiels, 2011). For minimsing both the objective functions, we use gradient-based optimisation algorithm HANSO (Overton, 2009) which can handle non-smooth optimisation problems.

For a less conservative result, it also possible to consider Proposition 3.3.4 and simultaneously tune parameters in both $\bar{\delta}$ and $\bar{p}$ to minimise

$$\min_{\bar{\delta},\ \bar{p}} ||\hat{G}(j\omega, \bar{p}, \bar{\delta})||_{\mathcal{H}_\infty}. \tag{3.42}$$

Alternatively, it is possible to consider a two layer (min-min) optimisation problem, wherein the outer layer tunes $\bar{p}$ and inner layer tunes $\bar{\delta}$ for minimising the function

$$\min_{\bar{p}} \left(\min_{\bar{\delta}} ||\hat{G}(j\omega, \bar{p}, \bar{\delta})||_{\mathcal{H}_\infty} \right). \tag{3.43}$$

Although optimisation problems (3.42) and (3.43) have the same solution, the numerical implementation may lead to different results. Since these optimisation problems are in general non-convex, the local minima found may not correspond to each other. We use the gradient-based optimisation algorithm HANSO to solve the optimisation problems of (3.42) and (3.43). We compute gradients for the optimisation problems using the approach in (Gumussoy and Michiels, 2011).

3.4.2 Network structure exploitation

In this section, the special case of structured MIMO plant as in (3.3) is considered. Assume that the identical subsystems are to be controlled using identical fixed-order controllers, that is, $A_{ci} = \hat{A}_c$, $B_{ci} = \hat{B}_c$, $C_{ci} = \hat{C}_c$, and $D_{ci} = \hat{D}_c \ \forall\ i = 1, ..., n$ in (3.25), see Figure 3.4. Let us consider an augmented (sub-)system state vector $x_i^{\mathrm{T}} = [x_{pi}^{\mathrm{T}}\ u_i^{\mathrm{T}}\ \gamma_{wi}^{\mathrm{T}}\ \gamma_{zi}^{\mathrm{T}}\ x_{ci}^{\mathrm{T}}\ y_i^{\mathrm{T}}] \ \forall\ i = 1, ..., n$, where γ_{zi} and γ_{wi} are dummy vectors used to represent z_i and w_i respectively. Then, we can rewrite closed-loop system (3.3) and identical fixed-order controllers using the state vector $x^{\mathrm{T}} = [x_1^{\mathrm{T}}\ \ldots\ x_n^{\mathrm{T}}]$ as

$$\begin{cases} I \otimes \hat{E}_{cl}\dot{x}(t) & = (I \otimes \hat{A}_{cl,0} + A_M \otimes \hat{F}_{cl})x(t) + \sum_{k=1}^{m_n} I \otimes \hat{A}_{cl,k}\ x(t - \tau_k) \\ & \quad + I \otimes \hat{B}_{cl} w(t), \\ z(t) & = I \otimes \hat{C}_{cl} x(t), \end{cases} \tag{3.44}$$

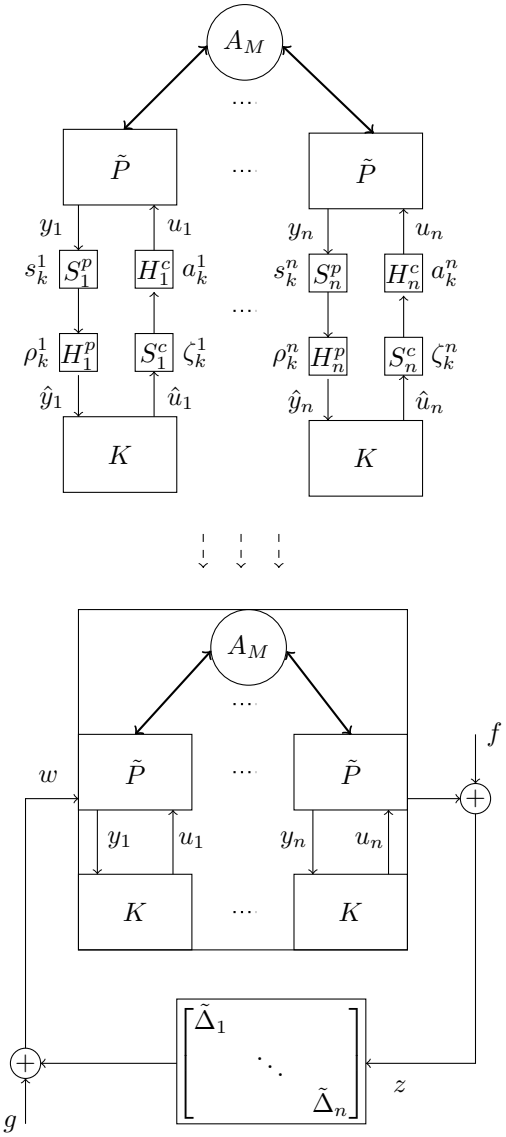

Figure 3.4: The structured MIMO plant considered in this chapter. Identical subsystems $\tilde{P}$ (with constant time-delays at input, output, and state) connected through some network (described by the adjacency matrix A_M) are to be stabilised by identical local (fixed-order) controllers with non-identical control imperfections.

and at the level of uncertainty operator, there is no change from (3.23). The coefficient matrices in (3.44) are

$$\hat{A}_{cl,0} = \begin{bmatrix} \hat{A}_{p0} & \hat{B}_p & 0 & 0 & 0 & 0 \\ 0 & -I & \begin{bmatrix} 0 & I & \hat{D}_c \end{bmatrix} & 0 & \hat{C}_c & \hat{D}_c \\ 0 & 0 & -I & 0 & 0 & 0 \\ 0 & 0 & 0 & I & 0 & 0 \\ 0 & 0 & \begin{bmatrix} \hat{B}_c & 0 & 0 \end{bmatrix} & 0 & \hat{A}_c & \hat{B}_c \\ \hat{C}_p & 0 & 0 & 0 & 0 & -I \end{bmatrix},$$

$$\hat{A}_{cl,k} = \begin{bmatrix} \hat{A}_{pi} & 0 & 0 & 0 & 0 & 0 \\ 0 & 0 & 0 & 0 & 0 & 0 \\ 0 & 0 & 0 & 0 & 0 & 0 \\ 0 & 0 & 0 & 0 & 0 & 0 \\ 0 & 0 & 0 & 0 & 0 & 0 \\ 0 & 0 & 0 & 0 & 0 & 0 \end{bmatrix},$$

$$\hat{E}_{cl} = \begin{bmatrix} \hat{E}_p & 0 & 0 & 0 & 0 & 0 \\ 0 & 0 & 0 & 0 & 0 & 0 \\ 0 & 0 & 0 & 0 & 0 & 0 \\ \begin{bmatrix} \hat{C}_p \\ 0 \end{bmatrix} & 0 & 0 & 0 & \begin{bmatrix} 0 \\ \hat{C}_c \end{bmatrix} & 0 \\ 0 & 0 & 0 & 0 & I & 0 \\ 0 & 0 & 0 & 0 & 0 & 0 \end{bmatrix},$$

$$\hat{F}_{cl} = \begin{bmatrix} \hat{F}_p & 0 & 0 & 0 & 0 & 0 \\ 0 & 0 & 0 & 0 & 0 & 0 \\ 0 & 0 & 0 & 0 & 0 & 0 \\ 0 & 0 & 0 & 0 & 0 & 0 \\ 0 & 0 & 0 & 0 & 0 & 0 \\ 0 & 0 & 0 & 0 & 0 & 0 \end{bmatrix}, \quad \hat{B}_{cl} = \begin{bmatrix} 0 \\ 0 \\ I \\ 0 \\ 0 \\ 0 \end{bmatrix},$$

$$\hat{C}_{cl} = \begin{bmatrix} 0 & 0 & 0 & I & 0 & 0 \end{bmatrix}.$$

According to the complex Schur decomposition theorem (Meyer, 2000), there always exists an unitary matrix T such that

$$A_M = TZT^*, \tag{3.45}$$

where Z is an upper triangular matrix. Then, by performing a similarity transformation using $\bar{x} = (T \otimes I)x$ and using the property that some matrices commute (like $(T \otimes I)(I \otimes \hat{B}_{cl}) = (I \otimes \hat{B}_{cl})(T \otimes I)$) we obtain

$$z(t) = (T^* \otimes I)(I \otimes \hat{C}_{cl})\bar{x}(t). \tag{3.46}$$

It is clear from above that omitting the transformation by $(T \otimes I)$ at input side and $(T^* \otimes I)$ at output side in (3.46) does not affect the $\mathcal{H}_\infty$ norm since T is unitary. In this chapter, the control imperfections are considered only at the communication between controllers and plants. We recall the main result (Theorems 2.3.1-2.3.2) of Chapter 2, which is stated as the following theorem (see Chapter 2 for proof).

Theorem 3.4.1 *Let $\{\lambda_{a1}, \ldots, \lambda_{an}\}$ denote the spectrum of A_M. Also, we consider the group of subsystems*

$$\begin{aligned} \hat{E}_{cl}\dot{\bar{x}}_i(t) &= \left(\hat{A}_{cl,0} + \lambda_{ai}\hat{F}_{cl}\right)\bar{x}_i(t) + \sum_{k=1}^{m_n} \hat{A}_{cl,k}\bar{x}_i(t-\tau_k) + \hat{B}_{cl}\bar{w}_i(t), \\ \bar{z}_i(t) &= \hat{C}_{cl}\bar{x}_i(t), \qquad\qquad i = 1, \ldots, n. \end{aligned} \tag{3.47}$$

Then the following results hold:

1. *System (3.44) with $w \equiv 0$ is exponentially stable if and only if system (3.47) with $\bar{w}_i \equiv 0 \ \forall \ i = 1, ..., n$ is exponentially stable. Moreover the spectral abscissa $c(\bar{p})$ of (3.44) satisfies*

$$c(\bar{p}) = \max_{i \in \{1,..,n\}} \tilde{c}(\bar{p}, \lambda_{ai}), \tag{3.48}$$

where

$$\tilde{c}(\bar{p}, \lambda_{ai}) = \sup_{\lambda \in \mathbb{C}} \{\Re(\lambda) : \det \bar{M}(\lambda, \lambda_{ai}, \bar{p}) = 0\}, \tag{3.49}$$

and the characteristic matrix

$$\hat{M}(\lambda, \lambda_{ai}, \bar{p}) := \lambda \hat{E}_{cl} - \hat{A}_{cl,0}(\bar{p}) - \lambda_{ai} \hat{F}_{cl} - \sum_{k=1}^{m_n} \hat{A}_{cl,k} \mathrm{e}^{-\lambda \tau_k}. \tag{3.50}$$

2. *If A_M is a normal matrix, then*

$$||G(jw, \bar{p})||_{\mathcal{H}_\infty} = \max_{i \in \{1,..,n\}} ||\tilde{G}(jw, \lambda_{ai}, \bar{p})||_{\mathcal{H}_\infty}, \tag{3.51}$$

where $\tilde{G}(jw, \lambda_{ai}, \bar{p})$ is the transfer function matrices of system (3.47) from $\bar{w}_i$ to $\bar{z}_i$.

Then, we have the following corollary from the theorem stated above.

Corollary 3.4.2 *Assume that A_M is a normal matrix. Then, a sufficient condition for the feedback interconnection of (3.27), for the case where system (3.22) is structured as in (3.44), to be input-output $\mathcal{L}_2$ stable becomes*

$$\max_{i \in \{1,\ldots,n\}} \bar{\gamma}_i < \left(\max_{i \in \{1,\ldots,n\}} ||\tilde{G}(jw, \lambda_{ai}, \bar{p})||_{\mathcal{H}_\infty} \right)^{-1}, \tag{3.52}$$

where

$$\tilde{G}(s, \lambda_{ai}, \bar{p}) = \hat{C}_{cl} \Big(\hat{M}(s, \lambda_{ai}, \bar{p}) \Big)^{-1} \hat{B}_{cl}.$$

Proof. The proof follows from Theorem 3.3.3 and the latter part of Theorem 3.4.1. ∘

In order to efficiently design identical decentralised controllers of the form (3.14) that are robust against control imperfections, we replace the minimisation objective (3.38) with

$$\min_{\bar{p}} \max_{i \in \{1,..,n\}} \tilde{c}(\bar{p}, \lambda_{ai}), \tag{3.53}$$

for faster exponential decay rate of the solutions and (3.41) with

$$\min_{\bar{p}} \max_{i\in\{1,..,n\}} ||\tilde{G}(jw, \lambda_{ai}, \bar{p})||_{\mathcal{H}_\infty}, \tag{3.54}$$

for improving robustness against control imperfections. The network structure exploitation is performed by transforming the coupling between subsystems to some kind of *self-coupling* through λ_{ai}. Recall that the transformation matrices used to diagonalise the adjacency matrix must be unitary, which is satisfied when the adjacency matrix is symmetric, corresponding to bi-directional coupling, or a circulant matrix.

Notice that using the approach of network structure exploitation implies that we can no longer reduce conservatism using the scaling approach presented at the end of Section 3.3, since the scaling would not correspond to a unitary transformation.

3.5 Numerical example

In this section, we perform simulation-based studies on a numerical example made up of n identical third order subsystems subject to different control and input perturbations. This example provides a simple illustration for the systems in Section 3.4.2. The simulations are performed using the MATLAB software tool described in (Dileep and Michiels, 2018c), which relies on extending the results in (Gumussoy and Michiels, 2011; Michiels, 2011) towards scalable algorithms for the design of sampled-data decentralised controllers. We specify

the plant (3.3) as

$$\begin{cases} \dot{x}_{pi}(t) &= \begin{bmatrix} -10 & 0 & 0 \\ 1 & 0 & 0 \\ 0 & 1 & 0 \end{bmatrix} x_{pi}(t) + \sum_{j=1}^{n} a_{Mi,j} \begin{bmatrix} 1 & 0 & 0 \\ 0 & 1 & 0 \\ 0 & 0 & 0 \end{bmatrix} x_{pj}(t-0.2) \\ &\quad + \begin{bmatrix} 10 \\ 0 \\ 0 \end{bmatrix} u_i(t) + \Omega_i(t), \\ y_i(t) &= \begin{bmatrix} 0 & 1 & 0 \\ 0 & 0 & 1 \end{bmatrix} x_{pi}(t-0.1), \ i = 1, ..., n, \end{cases} \tag{3.55}$$

where the normal adjacency matrix A_M has the elements

$$a_{Mi,j} = \begin{cases} 0.5, & \text{if } |i-j| = 1, \\ 0, & \text{otherwise}, \end{cases} \tag{3.56}$$

$\forall\ i, j = 1, ..., n$. In (3.55), there is an additional exogenous input vector $\Omega_i(t)$ whose role will be discussed later on. The above plant is to be controlled by identical dynamic controllers of the form (3.11). The third and fourth equations of the corresponding system (3.25) then take the form

$$\begin{cases} \dot{x}_{ci} = \bar{A}_c x_{ci} + \bar{B}_c y_i + \begin{bmatrix} \bar{B}_c & 0 & 0 \end{bmatrix} w_i(t), \\ u_i = \bar{C}_c x_{ci} + \bar{D}_c y_i + \begin{bmatrix} 0 & I & \bar{D}_c \end{bmatrix} w_i(t), \ i = 1, ..., n. \end{cases} \tag{3.57}$$

The exogenous outputs are

$$z_i(t) = \begin{bmatrix} C_g \dot{x}_{pi}(t) \\ \bar{C}_c \dot{x}_{ci}(t) \end{bmatrix}, \ \Upsilon_i(t) = x_{pi}(t), \qquad i = 1, ..., , n. \tag{3.58}$$

Notice that closed-loop system (3.55)-(3.58) is an example of the form (3.44) and hence we can exploit the network structure. However, we also consider new exogenous inputs ($\Omega_i(t)$) to the subsystems in (3.55) and new exogenous outputs ($\Upsilon_i(t)$) in (3.58). These terms allow us to consider some additional disturbances to the subsystems, besides the control imperfections. For example,

these terms could provide an insight on the allowable parametric uncertainties on the plant's state-coefficient matrix. However, it can be easily shown that all the results presented in the previous sections still carry over to this situation.

First, we consider system (3.55)-(3.58) to be a small network with three subsystems ($n = 3$). To illustrate the instability that may be due to the control imperfections in Figure 3.5, we use a second order controller K_b, whose coefficient matrices are

$$\begin{aligned}
\bar{A}_c &= 10^3 \cdot \begin{bmatrix} -2.4639 & -0.9459 \\ 2.796 & -2.2546 \end{bmatrix}, \\
\bar{B}_c &= 10^3 \cdot \begin{bmatrix} 0.0660 & -0.4056 \\ -0.2102 & 0.1232 \end{bmatrix}, \\
\bar{C}_c &= 10^3 \cdot \begin{bmatrix} 7.8543 & 1.0195 \end{bmatrix}, \\
\bar{D}_c &= 10^3 \cdot \begin{bmatrix} -0.2953 & 1.0865 \end{bmatrix},
\end{aligned} \tag{3.59}$$

for each of the three subsystems in (3.55). The spectral abscissa of closed-loop system (3.55) and K_b is -2.050, when $n = 3,\ w_i \equiv 0,\ \Omega_i \equiv 0,\ i = 1, 2, 3$. For the purpose of illustration, controller K_b was selected in such a way that the $\mathcal{H}_\infty$ norm of the transfer function matrix resulting from the corresponding closed-loop system was high.

We obtain a new controller K_{sd} by minimising the $\mathcal{H}_\infty$ norm of the transfer function matrix of system (3.55)-(3.58), when $n = 3$, from

$$\hat{w} = [w_1^{\mathrm{T}}\ w_2^{\mathrm{T}}\ w_3^{\mathrm{T}}\ \Omega_1^{\mathrm{T}}\ \Omega_2^{\mathrm{T}}\ \Omega_3^{\mathrm{T}}]^{\mathrm{T}},$$

to

$$\hat{z} = [z_1^{\mathrm{T}}\ z_2^{\mathrm{T}}\ z_3^{\mathrm{T}}\ \Upsilon_1^{\mathrm{T}}\ \Upsilon_2^{\mathrm{T}}\ \Upsilon_3^{\mathrm{T}}]^{\mathrm{T}},$$

to 9.93 using the network structure exploiting algorithm. That is, a feedback interconnection of (3.55)-(3.58) and any bounded uncertainty operator with an induced-$\mathcal{L}_2$ norm less than $\frac{1}{9.93}$ is input-output $\mathcal{L}_2$ stable. For example, in addition to the control imperfections, closed-loop system (3.55)-(3.58), when

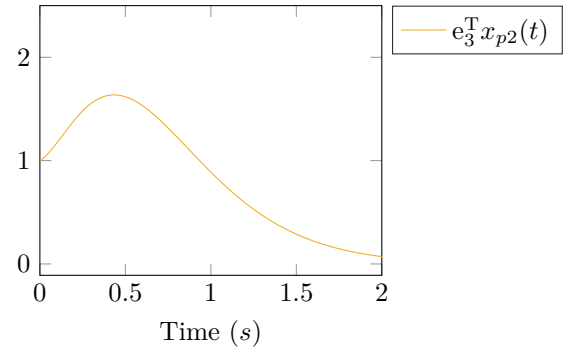

(a) Continuous-time system stabilised by the second order controller K_b with no control imperfections. The spectral abscissa of the closed-loop system is -2.050.

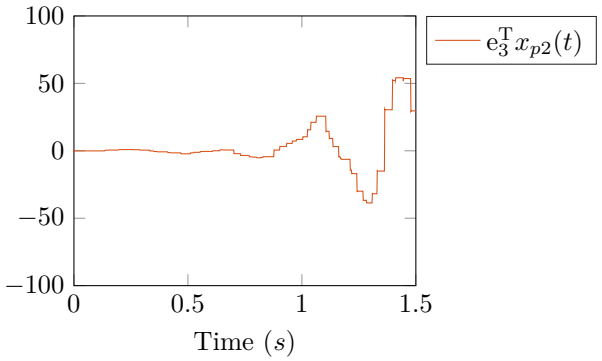

(b) The closed-loop system is unstable with control imperfections.

Figure 3.5: Simulation of closed-loop system (3.55) and K_b, when $n = 3$, for the initial value $x_{pi}(0) = 1, x_{ci}(0) = 1 \; \forall \; i = 1, 2, 3$. For clarity of presentation, we use only $e_3^T x_{p2}$, where e_3 is the 3rd column vector of the identity matrix.

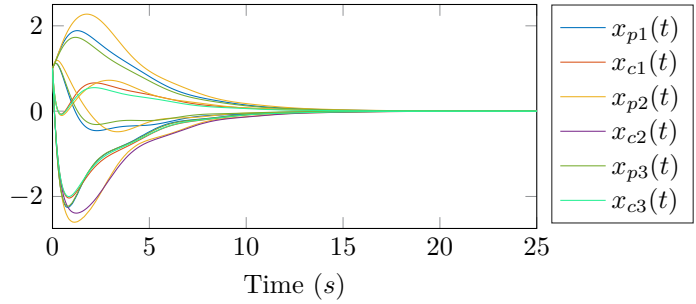

Figure 3.6: Closed-loop system of plant (3.55) and K_{sd} in (3.60) with control imperfections, when $n = 3$, is stable even though it is slower than K_b. The spectral abscissa of plant (3.55) and K_{sd} in (3.60) when $\hat{w} \equiv 0$ is -0.3569. The upper-bounds for sampling intervals and asynchrony used in this simulation were defined to satisfy (3.52) (to verify the result presented in the previous section) and were identical to that used for the simulation of Figure 3.5b.

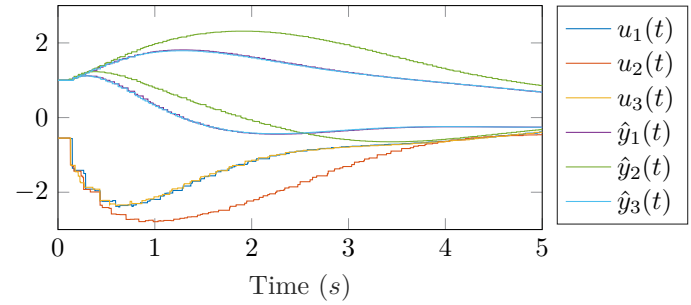

Figure 3.7: The input signals (received at plant) and output signals (received at controllers) corresponding to the plant and K_{sd} in(3.60) with control imperfections (using the settings same as Figure 3.6).

$n = 3$, is also input-output $\mathcal{L}_2$ stable for any (non-identical) perturbation on the subsystem's state (x_{pi}) coefficient matrices which has an induced-$\mathcal{L}_2$ norm less than $\frac{1}{9.93}$. We observe that the $\mathcal{H}_\infty$ norm corresponding to (only) control imperfections, when $n = 3$, from $w = [w_1^{\mathrm{T}}\ w_2^{\mathrm{T}}\ w_3^{\mathrm{T}}]^{\mathrm{T}}$ to $z = [z_1^{\mathrm{T}}\ z_2^{\mathrm{T}}\ z_3^{\mathrm{T}}]^{\mathrm{T}}$ while we assume $\Omega_i \equiv 0,\ i = 1, 2, 3$, in (3.55)-(3.58) is equal to 5.81. The $\mathcal{H}_\infty$ synthesis controller K_{sd} has the coefficient matrices

$$\begin{aligned} \bar{A}_c &= \begin{bmatrix} -6.8101 & -0.0109 \\ -0.3745 & -4.5357 \end{bmatrix},\ \bar{B}_c = \begin{bmatrix} -2.9243 & 1.8633 \\ -4.0221 & -4.0900 \end{bmatrix}, \\ \bar{C}_c &= \begin{bmatrix} 0.0524 & 0.5468 \end{bmatrix},\qquad \bar{D}_c = \begin{bmatrix} -0.6876 & -0.4615 \end{bmatrix}. \end{aligned} \tag{3.60}$$

The simulation results for the initial conditions of $x_{pi}(t_0) = \bar{1},\ x_{ci}(t_0) = \bar{1},\ i = 1, 2, 3,\ t_0 \leq 0$ are presented in Figures 3.6-3.7, where $\bar{1}$ is used to represent a matrix or vector of appropriate dimension having all elements equal to 1. Note that the control imperfections (or the upper-bounds for the sampling intervals and asynchrony) were ensured to be the same ($\frac{1}{5.8}$) for obtaining results using K_b in Figure 3.5 and using K_{sd} in Figures 3.6-3.7 (see (Dileep and Michiels, 2018c) for details on the software and numerical data used for the example).

Additionally, we note that the conservatism in these results was not negligible in simulations. Therefore, we aim at reducing the conservatism using the approach of Section 3.4.1. For this purpose, the scaling parameters ($\delta_{i,j},\ i = 1, 2, 3,\ j = 1, 2$ in (3.34)) are optimised using "1" (no scaling) as their initial value while not exploiting the network structure. Among other experiments, the *scaled* $\mathcal{H}_\infty$ norm as in (3.43), when $n = 3$, from w to z was minimised (by tuning only $\bar{\delta}$) from 5.81 to 4.86 for the plant (3.55) and controller K_{sd} in (3.60).

Now consider that system (3.55)-(3.58) has a large number of subsystems ($n \gg 3$), while retaining the same topology, then the general approach proposed in Section 3.4.1 becomes computationally cumbersome. The eigenvalues (λ_{ai}) of A_M in (3.56) can be expressed as

$$\lambda_{ai} = \cos(i\frac{\pi}{n+1}),\ i = 1, ..., n, \tag{3.61}$$

that is, $\lambda_{ai} \in [-1, 1]\ \forall\ i = 1, ..., n$. Therefore, an increase in the number

Table 3.1: The $\mathcal{H}_\infty$ norms computed for closed-loop system (3.55)-(3.58), when $n > 3$, from $\hat{w}(= [w_1^{\mathrm{T}} \ \dots \ w_n^{\mathrm{T}} \ \Omega_1^{\mathrm{T}} \ \dots \ \Omega_n^{\mathrm{T}}]^{\mathrm{T}})$ to $\hat{z}(= [z_1^{\mathrm{T}} \ \dots \ z_n^{\mathrm{T}} \ \Upsilon_1^{\mathrm{T}} \ \dots \ \Upsilon_n^{\mathrm{T}}]^{\mathrm{T}})$ with $\bar{K}_{sd}$ in (3.62) using the network structure exploitation approach.

n	$\mathcal{H}_\infty$ norm
10	11.8721
50	12.8393
100	12.8770
300	12.8885
500	12.8895

of subsystems (n) results in a denser distribution of the eigenvalues (λ_{ai}) in the interval $[-1, 1]$. This allows us to extend the scalable algorithm for the design of stabilising controllers described in Section 2.4. More precisely, λ_{ai} is interpreted as an uncertain parameter confined to the interval $[-1,\ 1]$ and the worst case value of the $\mathcal{H}_\infty$ norm is optimised over this interval (solving a min-max optimisation problem) to obtain a controller $\bar{K}_{sd}$ whose coefficient matrices are

$$\bar{A}_c = \begin{bmatrix} -7.4310 & 0.9451 \\ -1.7851 & -6.9873 \end{bmatrix}, \ \bar{B}_c = \begin{bmatrix} -3.5450 & 1.8700 \\ -2.2913 & -4.4404 \end{bmatrix}, \\ \bar{C}_c = \begin{bmatrix} -2.8900 & 1.5787 \end{bmatrix}, \qquad \bar{D}_c = \begin{bmatrix} -3.3538 & -0.0728 \end{bmatrix}. \tag{3.62}$$

$\bar{K}_{sd}$ guarantees an upper bound on the $\mathcal{H}_\infty$ norm (from $\hat{w}$ to $\hat{z}$) of 12.89, which is *independent* of the number of subsystems n in (3.55)-(3.58) and asymptotically exact as $n \to \infty$ (see Table 3.1). Simulation-based studies were also performed for closed-loop system (3.55)-(3.58), when $n = 500$, with $\bar{K}_{sd}$ in (3.62). Also, the sampling instants and delays were defined to satisfy the criterion in (3.52). The simulation results for the initial condition of $x_{pi}(t_0) = \bar{1}, x_{ci}(t_0) = \bar{1},\ i = 1, ..., 500,\ t_0 \leq 0$, are presented in Figures 3.8-3.9. For simplicity of representation, simulation results of only three subsystems ($i = 1, 250, 500$) are shown in Figures 3.8-3.9.

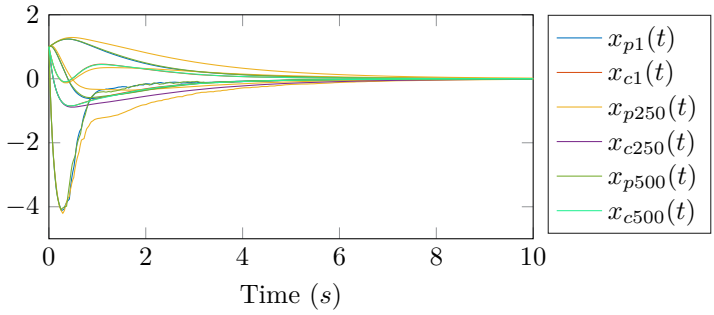

Figure 3.8: Closed-loop system of plant (3.55) and $\bar{K}_{sd}$ with control imperfections, when $n = 500$, is stable. The upper-bounds for sampling intervals and asynchrony used in this simulation were defined to satisfy (3.52) (to verify the result presented in the previous section).

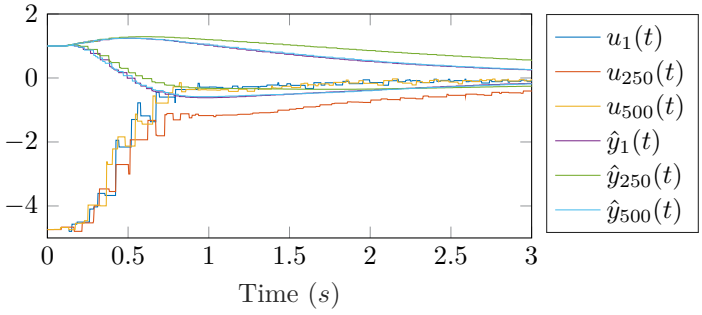

Figure 3.9: The input signals (received at plant) and output signals (received at controllers) corresponding to the plant and $\bar{K}_{sd}$ with control imperfections (using the settings same as Figure 3.8), when $n = 500$.

3.6 Conclusions

In this chapter, we presented an approach to design stabilising decentralised controllers for generic MIMO plants which are robust against control imperfections (due to sampled-data controllers) and other input disturbances. The system (with the sampled-data decentralised controllers) was rewritten as a feedback interconnection of a continuous-time closed-loop system and a bounded (integral) operator. The closed-loop systems are modelled using DDAEs, which are flexible in modelling interconnected systems. Sparsity constraints are enforced in the parameterisation process within the optimisation to ensure that decentralised controllers are obtained. Additionally, we proposed a method to reduce some conservativeness in the result, which exploits the structure of the operator. Furthermore, the computational efficiency of the controller design algorithm is significantly improved in the case of a structured MIMO plant, wherein the plant is composed of quasi-identical subsystems, at the price that the local controllers need to be identical and the scaling approach to reduce the conservatism is not applicable any more.

Throughout the chapter we assumed that the controllers were dynamic LTI controllers, whose parameters are determined by solving optimisation problems. The methodology trivially extends to other classes of controllers, such as (decentralised) PID controllers, as shown in Section 2.2.

Finally, note that all the algorithms presented in this chapter have been implemented in a publicly available software (Dileep and Michiels, 2018c).

Chapter 4

Application to cooperative adaptive cruise control

4.1 Introduction

Problems related to traffic jams, growing constraints in highway capacities, and improving efficiency in road transport systems have caught the attention of researchers worldwide. Cooperative Adaptive Cruise Control (CACC) techniques are attractive as an automated vehicle following system based on inter-vehicular exchange of data through wireless communication, in addition to radar or lidar (Ferguson et al., 2017; Ploeg et al., 2014b; Qin et al., 2017). As a matter of fact, CACC is known to reduce the time gaps between vehicles significantly (Ploeg et al., 2014b). For the case of CACC, it is impractical to employ centralised controllers (see (Ferguson et al., 2017; Gao et al., 2018; Guanetti et al., 2018; Li et al., 2018; Ploeg et al., 2014a; Qin et al., 2017) and the references therein). One of the main objectives to be considered when designing controllers for CACC is the prevention of amplification of disturbances in the upstream direction of vehicles. This problem is generally represented using the notion of string

stability[1]. There are several definitions available for string stability in the literature, focusing on various aspects of cascaded systems (see (Oncu et al., 2014; Wang and Nijmeijer, 2015; Wang et al., 2017)).

Many researchers assume homogeneity of vehicles in large platoons (networks). Homogeneity in the platoon is assumed at a higher layer in (Ploeg et al., 2014b) by considering the possibility of cancelling out heterogeneity using lower layer controllers. However, this might not be suitable for some scenarios which include multi-brand vehicular platoons with heterogeneity in time-delays. In (Gao et al., 2016), sufficient conditions for designing string stable distributed controllers for a heterogeneous platoon (solved using small gain theorem and LMI) were presented. In (Wang and Nijmeijer, 2015), a pole-zero cancellation method was proposed to cancel heterogeneity in engine time constants through post-compensation of the wireless feed-forward signal. In (Wang et al., 2017), the string stability of heterogeneous vehicular platoons in an adaptive cruise control configuration with non-connected automated vehicles has been considered. We refer to (Gao et al., 2018; Guanetti et al., 2018; Li et al., 2018,1; Sabau et al., 2017) and the references therein for recent advancements in the corresponding field. In general, control design methods proposed in literature were not easily applicable to platoons with heterogeneous time-delay parameters.

In this chapter, we study the possibility to optimise, with reduced complexity, the stability and robustness/performance of (identical) local controllers for the large scale LTI heterogeneous vehicular platoons in an one vehicle look-ahead topology with numerous (constant) time-delays. The heterogeneous time-delays could be present in these systems due to actuation, sensors or communication (see (Ploeg et al., 2015)). We consider sufficient conditions for (strict) string stability, based on the $\mathcal{L}_2$ gain, as in (Ploeg et al., 2014a). The method proposed in (Ploeg et al., 2014b) has been modified to incorporate the problem of heterogeneity and time-delays. The one vehicle look-ahead topology is considered to design identical controllers for heterogeneous (parameter) vehicles, by optimising them for sufficient conditions of string stability in terms of (maximum) $\mathcal{L}_2$ gain. It is important to note that by considering the (energy-based) $\mathcal{L}_2$ string stability conditions for heterogeneous vehicular platoon, there is no insight on the $\mathcal{L}_\infty$

[1]The string stability condition considered in this chapter will be defined in Section 4.4.3.

string stability (which is related to the possible overshoot for signal in the time domain). Since we consider the frequency domain approach, we have necessary and sufficient stability conditions for the LTI system with time-delays. Additionally, it might be possible to add an upper layer of control to one vehicle look-ahead CACC, so as to include the possibility of information transfer from the last vehicle to the first vehicle (see (Fusco et al., 2016; Zegers et al., 2017)). Similar to previous chapters, we adopt non-conservative frequency domain-based approaches proposed in (Gumussoy and Michiels, 2011; Michiels, 2011) to design structured and fixed-order controllers for the application of automated vehicular platoons that uses CACC.

The remainder of this chapter is organised as follows. Section 4.2 presents the linearised vehicle plant model considered and the outputs available to the controller. Section 4.3 describes the Delay Differential Algebraic Equation (DDAE) used to model the heterogeneous vehicular platoon with time-delays. Section 4.4 reviews the direct optimisation-based approach available for designing robust fixed-order (identical) controllers for CACC. Section 4.5 validates the proposed approach using MATLAB software. Finally, Section 4.6 contains the concluding remarks. The results of this chapter have been presented in (Dileep et al., 2019).

4.2 Vehicle model

Table 4.1: Heterogeneity in the CACC network.

Notation	Parameter of the vehicle i
h_i	Head-way time constant
d_{ci}	Drive-line time constant
τ_{ai}	Actuation delay
τ_{bi}	Communication delay
τ_{ci}	Sensor delay

In this section, we present the vehicle models used for the CACC problem considered in this chapter. The LTI vehicle model has been taken from (Ploeg et al., 2014b), however, we consider existing (constant) time-delays and some

heterogeneous elements in the dynamics of the vehicles. The heterogeneity considered in this chapter is confined to the parameters in Table 4.1.
We assume all the parameters in Table 4.1 to be positive and real-valued. We consider the ith vehicle model as

$$\begin{pmatrix} \dot{s}_i(t) \\ \dot{v}_i(t) \\ \dot{f}_i(t) \end{pmatrix} = \begin{pmatrix} v_i(t) \\ f_i(t) \\ -\frac{1}{d_{ci}} f_i(t) + \frac{1}{d_{ci}} u_i(t - \tau_{ai}) \end{pmatrix}, \tag{4.1}$$

$\forall\ i = 1, ..., n$ where n is the total number of vehicles in the platoon, s_i is the position, v_i is the velocity, and f_i is the acceleration of vehicle i. Given a reference trajectory, $s_{ref,0}(t) = v_{ref,0} \cdot t$, we stabilise and control the system around the stationary solution (when $u_i = 0$)

$$s_i(t) = s_{ref,i}(t) = v_{ref,0} \cdot t - \sum_{k=1}^{i} (h_k v_{ref,0} + L_k + r_k),$$

$i = 1, ..., n$, where L_i is the length, r_i is the standstill distance, and h_i is the head-way time constant of vehicle i. That is, we consider each vehicle to be associated with a reference trajectory with real-valued constant velocity $v_{k,0}$. Note that the reference distance for vehicle i from the vehicle ahead has a velocity component. We can describe the relative motion of the ith vehicle as

$$\begin{aligned} &\psi_{si}(t) = s_i(t) - s_{ref,i}(t),\ \psi_{vi}(t) = v_i(t) - \dot{s}_{ref,i}(t), \\ &\psi_{fi}(t) = f_i(t) - \ddot{s}_{ref,i}(t) = f_i(t), \quad \forall\ i = 1, ..., n. \end{aligned} \tag{4.2}$$

For the virtual vehicle 0, we consider $v_0 = v_{ref,0},\ s_0 = s_{ref,0}$, then $\psi_{s0} = 0,\ \psi_{v0} = 0$. The equations in (4.1) change to

$$\begin{pmatrix} \dot{\psi}_{si}(t) \\ \dot{\psi}_{vi}(t) \\ \dot{\psi}_{fi}(t) \end{pmatrix} = \begin{pmatrix} \psi_{vi}(t) \\ \psi_{fi}(t) \\ -\frac{1}{d_{ci}} \psi_{fi}(t) + \frac{1}{d_{ci}} u_i(t - \tau_{ai}) \end{pmatrix}, \tag{4.3}$$

and the corresponding transfer function from u_i to ψ_{si} can be written as

$$G_i(s) = \frac{\mathrm{e}^{-\tau_{ai}s}}{(d_{ci}s+1)s^2}. \tag{4.4}$$

We assume that the controller of vehicle i has access to the position error $(e_{pi}(t))$, the velocity error $(\dot{e}_{pi}(t))$, and the input signal transmitted from the vehicle ahead through wireless communication $(u_{i-1}(t))$, that is $y_i(t) = [e_{pi}(t-\tau_{ci})\ \dot{e}_{pi}(t-\tau_{ci})\ u_{i-1}(t-\tau_{b(i-1)})]^{\mathrm{T}}$. The position error is given by

$$\begin{aligned} e_{pi}(t) &= s_{i-1}(t) - s_i(t) - h_i v_i(t) - L_i - r_i \\ &= \psi_{s(i-1)}(t) - \psi_{si}(t) - h_i\psi_{vi}(t), \end{aligned} \tag{4.5}$$

and the velocity error is given by

$$\begin{aligned} \dot{e}_{pi}(t) &= v_{i-1}(t) - v_i(t) - h_i f_i(t) \\ &= \psi_{vi-1}(t) - \psi_{vi}(t) - h_i\psi_{fi}(t), \end{aligned} \tag{4.6}$$

for all vehicles $i = 1, ..., n$ (by definition, $\psi_{s0} = 0,\ \psi_{v0} = 0$).

4.3 One vehicle look-ahead platoon with CACC

The dynamics of the one vehicle look-ahead platoon without control is given (using the state $x_{pi}(t) = [e_{pi}(t)\ \psi_{vi}(t)\ \psi_{fi}(t)\ \gamma_{ui}(t)\ \gamma_{yi}^{\mathrm{T}}(t)]^{\mathrm{T}}$) by

$$\begin{aligned} &E_p\dot{x}_{pi} = A_{pi0}x_{pi}(t) + A_{pi1}x_{pi}(t-\tau_{ai}) \\ &+ A_{pi2}x_{pi}(t-\tau_{ci}) + B_{pi1}u_i(t) + F_{pi0}x_{p(i-1)}(t) \\ &+ F_{pi1}x_{p(i-1)}(t-\tau_{b(i-1)}) + F_{pi2}x_{p(i-1)}(t-\tau_{ci}), \\ &y_i(t) = C_{pi0}x_{pi}(t), \qquad\qquad i = 1, ..., n, \quad x_{p0} \equiv 0, \end{aligned} \tag{4.7}$$

where e_{pi} is the position error, v_i is the relative velocity, and a_i is the acceleration of plant/vehicle i, whereas γ_{ui} and γ_{yi} are dummy variables for controlled input

u_i and output to controller y_i respectively. Note that for simplicity of the presentation we consider $i = 1, ..., n$ in (4.7) and for the case where $i = 1$, we define $x_{p,(i-1)} = x_{p,0} \equiv 0$. We use I and 0 to denote the identity matrix and the matrix with zero entries of appropriate dimensions, respectively, and $[\,\cdot\,]_{(j,k)}$ denotes the element at the jth row and k^{th} column of a matrix. In the matrices below

$$A_{pi0} = \begin{bmatrix} 0 & -1 & -h_i & 0 & 0 \\ 0 & 0 & 1 & 0 & 0 \\ 0 & 0 & -\frac{1}{d_{ci}} & 0 & 0 \\ 0 & 0 & 0 & -1 & 0 \\ 0 & 0 & 0 & 0 & -I \end{bmatrix}, \; B_{pi1} = \begin{bmatrix} 0 \\ 0 \\ 0 \\ 1 \\ 0 \end{bmatrix},$$

$$[F_{pi0}]_{(j,k)} = \begin{cases} 1, & \text{if } (j,k) = (1,2) \\ 0, & \text{otherwise,} \end{cases}$$

$$[A_{pi1}]_{(j,k)} = \begin{cases} \frac{1}{d_{ci}}, & \text{if } (j,k) = (3,4) \\ 0, & \text{otherwise,} \end{cases}$$

$$C_{pi0} = \begin{bmatrix} 0 & 0 & 0 & 0 & I \end{bmatrix},$$

$$A_{pi2} = \begin{bmatrix} & 0 & & 0 & \dots & 0 \\ & \vdots & & \vdots & \ddots & \vdots \\ & 0 & & 0 & \dots & 0 \\ \begin{bmatrix} 1 & 0 & 0 \\ 0 & -1 & -h_i \\ 0 & 0 & 0 \end{bmatrix} & & & 0 & \dots & 0 \end{bmatrix},$$

$$[F_{pi1}]_{(j,k)} = \begin{cases} 1, & \text{if } (j,k) = (7,4) \\ 0, & \text{otherwise,} \end{cases}$$

$$[F_{pi2}]_{(j,k)} = \begin{cases} 1, & \text{if } (j,k) = (6,2) \\ 0, & \text{otherwise,} \end{cases}$$

$$E_p = \begin{bmatrix} 1 & 0 & 0 & 0 & 0 \\ 0 & 1 & 0 & 0 & 0 \\ 0 & 0 & 1 & 0 & 0 \\ 0 & 0 & 0 & 0 & 0 \\ 0 & 0 & 0 & 0 & 0 \end{bmatrix},$$

$A_{pi,j}$ is given for $i = 1, ..., n$, $F_{pi,j}$ is given for $i = 2, ..., n$, and $F_{p1j} = 0$ $(i = 1)$, where $j = 0, 1, 2$. We also consider each subsystem to be controlled by a fixed-order LTI feedback controller (order n_c) of the form

$$\begin{cases} \dot{x}_{ci}(t) & = A_c x_{ci}(t) + B_c y_i(t), \\ u_i(t) & = C_c x_{ci}(t) + D_c y_i(t), \ i = 1, ..., n. \end{cases} \tag{4.8}$$

A static controller ($n_c = 0$) would have only the D_c component corresponding to $[k_p \ k_d \ k_{ff}]$ as in (Ploeg et al., 2014b) (with $k_{ff} = 1$). We consider the scenario of the heterogeneous vehicles being controlled using identical local controllers $u_i(s) = K(s)y_i(s) \ \forall \ i = 1, ..., n$. We define the following state vector for the closed-loop system

$$x_i(t) = [x_{pi}^{\mathrm{T}}(t) \ u_i^{\mathrm{T}}(t) \ x_{ci}^{\mathrm{T}}(t) \ y_i^{\mathrm{T}}(t)]^{\mathrm{T}},$$

which includes plants, controllers, and network interconnections. We re-write the system equations using the new state $x_i \in \mathbb{R}^{n_{cl}}$, in the form of DDAE (see Chapter 2 and (Gumussoy and Michiels, 2011) for more details on DDAE)

$$\begin{cases} E\dot{x}_i(t) & = A_{i0}x_i(t) + A_{i1}x_i(t - \tau_{ai}) + A_{i2}x_i(t - \tau_{ci}) \\ & \quad + F_{i0}x_{i-1}(t) + F_{i1}x_{i-1}(t - \tau_{b(i-1)}) \\ & \quad + F_{i2}x_{i-1}(t - \tau_{ci}) \quad \forall \ i = 1, \ldots, n, \ x_0 = 0, \end{cases} \tag{4.9}$$

where the matrices are

$$E = \begin{bmatrix} E_p & 0 & 0 & 0 \\ 0 & 0 & 0 & 0 \\ 0 & 0 & I & 0 \\ 0 & 0 & 0 & 0 \end{bmatrix}, A_{i0} = \begin{bmatrix} A_{pi0} & B_{pi1} & 0 & 0 \\ C_{pi0} & 0 & 0 & -I \\ 0 & 0 & A_c & B_c \\ 0 & -I & C_c & D_c \end{bmatrix},$$

$$A_{i1} = \text{blkdiag}\{A_{pi1}, 0, 0, 0\}, F_{i0} = \text{blkdiag}\{F_{pi0}, 0, 0, 0\},$$

$$A_{i2} = \text{blkdiag}\{A_{pi2}, 0, 0, 0\}, F_{i1} = \text{blkdiag}\{F_{pi1}, 0, 0, 0\},$$

$$F_{i2} = \text{blkdiag}\{F_{pi2}, 0, 0, 0\},$$

$i = 1, ..., n$, where the abbreviation blkdiag$\{\cdot\}$ implies the block diagonal matrix. Notice in the above equation that the controller parameters are contained in matrix A_{i0}, as indicated with the dashed box. Recall that in the direct optimisation approach from Section 2, stability and performance measures expressed in terms of the spectral abscissa and $\mathcal{H}_\infty$ norms are optimised as a function of the elements of controller matrices A_c, B_c, C_c and D_c. For this application, we contain all the controller parameters in a vector

$$\bar{p} = \text{vec}\left[\begin{array}{c:c} A_c & B_c \\ \hdashline C_c & D_c \end{array}\right]. \tag{4.10}$$

Whenever appropriate, we stress the dependence of A_{i0} on these parameters with the notation $A_{i0}(\bar{p})$.

4.4 Stability and performance objectives

We optimise the controller parameters in $\bar{p}$ for stability objectives in terms of spectral abscissa and pseudo-spectral abscissa using algorithms which have been already mentioned in Chapter 2. Additionally, we tune controller parameters for robustness objectives in terms of induced-$\mathcal{L}_2$ norms, using a graphical frequency-gridding approach[2]. In this section, we present an approach to exploit the one vehicle look-ahead topology of the platoon for the (efficient) design of controllers. The objective functions considered in this chapter are as follows.

4.4.1 Platoon stability: spectral abscissa

The linear models of vehicles and the platoon used in this chapter are not stable. The vehicle models in (4.3), when $u_i \equiv 0$, have a double eigenvalue at

[2]We use bode plot and `patternsearch`: a built-in optimisation algorithm within MATLAB.

zero. This has a physical interpretation. Since the remaining eigenvalue is in the open left half plane ($-\frac{1}{d_{ci}}$), the reached solution with respect to the speed and the offset of the position component depend on the initial condition and disturbances. Therefore, as a first step we stabilise the platoon by computing local controllers that minimise the spectral abscissa. The spectral abscissa ($c(\bar{p})$) of the closed-loop system in (4.9) can be expressed as follows

$$c(\bar{p}) = \sup_{\lambda \in \mathbb{C}} \{\Re(\lambda) : \det M(\lambda, \bar{p}) = 0\},$$

where,

$$M(\lambda, \bar{p}) = \begin{bmatrix} M_1 & 0 & 0 & \dots & 0 \\ \hat{F}_{2,1} & M_2 & 0 & \dots & 0 \\ 0 & \hat{F}_{3,2} & M_3 & \dots & 0 \\ \vdots & \vdots & \ddots & \ddots & \vdots \\ 0 & 0 & \dots & \hat{F}_{n,(n-1)} & M_n \end{bmatrix}, \tag{4.11}$$

where

$$M_i(\lambda, \bar{p}) = \lambda E - A_{i0}(\bar{p}) - A_{i1}\mathrm{e}^{-\lambda \tau_{ai}} - A_{i2}\mathrm{e}^{-\lambda \tau_{ci}}, \tag{4.12}$$

$\forall\ i = 1, ..., n$ and

$$\hat{F}_{i,(i-1)}(\lambda) = -F_{i,0} - F_{i,1}\mathrm{e}^{-\lambda \tau_{b(i-1)}} - F_{i,2}\mathrm{e}^{-\lambda \tau_{ci}}, \tag{4.13}$$

$\forall\ i = 2, ..., n$. Recall that we use the notation $\Re(\lambda)$ to indicate the real part of the complex number λ (eigenvalue), also, M_i corresponds to the characteristic matrix of individual vehicles and $\hat{F}_{i(i-1)}$ appears due to the interaction between vehicles.

Since the differences between $M_i\ \forall\ i = 1, ..., n$ lie in some parameters within the state coefficient matrices (see (4.12)), we can rewrite it as

$$M_\delta(\lambda, \bar{p}, \hat{p}_i) = \lambda E - \bar{A}_0(\bar{p}, \hat{p}_i) - \bar{A}_1(\lambda, \hat{p}_i) - \bar{A}_2(\lambda, \hat{p}_i), \tag{4.14}$$

$\forall\ i = 1, ..., n$, where $\hat{p}_i = [d_{ci}\ \ h_i\ \ \tau_{ai}\ \ \tau_{bi}\ \ \tau_{ci}]^{\mathrm{T}}$ is the plant parameter vector corresponding to vehicle i, $\bar{A}_0(\bar{p}, \hat{p}_i) = A_{i0}(\bar{p})$, $\bar{A}_1(\lambda, \hat{p}_i) = A_{i1}\mathrm{e}^{-\lambda \tau_{ai}}$, and

$\bar{A}_2(\lambda, \hat{p}_i) = A_{i2} \mathrm{e}^{-\lambda \tau_{ci}}$.

Theorem 4.4.1 *For the systems given in (4.9), the spectral abscissa in (4.11) is equivalent to*

$$c(\bar{p}) = \max \left\{ \sup_{\lambda \in \mathbb{C}} \{ \Re(\lambda) : \det(M_\delta(\lambda, \bar{p}, \hat{p}_i)) = 0 \} : \ i = 1, ..., n \right\}. \tag{4.15}$$

Proof. The assertions for Theorem 4.4.1 directly follow from the block-triangular structure of (4.11), then (4.15) arises from the diagonal blocks, and from the structure of the associated eigenvalue problem. □

The *exponential* stability of the whole CACC network in look-ahead topologies does not depend on the interaction/coupling of vehicles due to the lower block diagonal structure of the eigenvalue problem which is evident from (4.12). We minimise the spectral abscissa of the platoon in (4.9) for a faster exponential decay rate of solutions (towards the stationary reference solution),

$$\min_{\bar{p}} c(\bar{p}).$$

However, the computational complexity of this stabilisation approach (using network structure exploitation) still depends on the number of vehicles.

4.4.2 Motivation for string stability

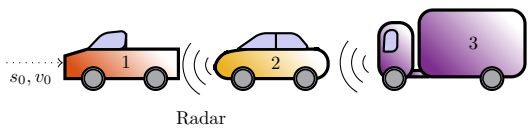

Figure 4.1: Heterogeneous platoon of three vehicles in a classical ACC one vehicle look-ahead topology.

We illustrate the importance of guaranteeing *performance* levels for heterogeneous platoons using a classical Adaptive Cruise Control (ACC) configuration (see Figure 4.1). We simulated the heterogeneous vehicular platoon using third

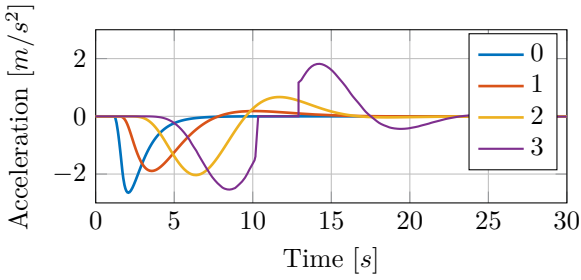

Figure 4.2: Deceleration response, accelerations of heterogeneous (parameter) vehicles in an ACC platoon which is exponentially stable but the energy of the signals is amplified through the string of vehicles.

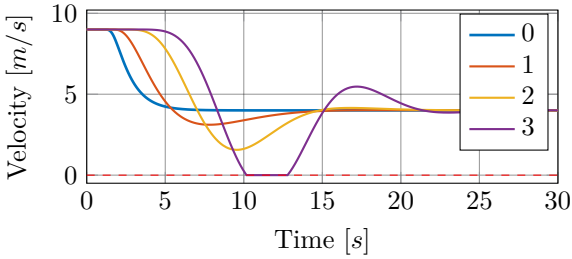

Figure 4.3: Deceleration response, velocities of heterogeneous (parameter) vehicles in an ACC platoon which is exponentially stable. The amplification of energy in the acceleration signals through the string results in the braking of the third vehicle.

order LTI models with delays (using (4.1)-(4.6)) in the ACC configuration stabilised by a random PD controller which uses delayed information on the position and velocity errors. We now introduce a disturbance (deceleration input) in the reference vehicle. As we can see in Figures 4.2 and 4.3, a small deceleration signal in the reference vehicle (0), results in undesirable responses through the string. In Figure 4.3, it can be seen that the deceleration reference signal could result in negative velocity during simulation. However, in reality, it would be saturated (at zero). One way to interpret this effect would be that the lack of performance standards could result in undesirable stops (velocity $= 0\ m/s^2$) or traffic jams. Even though the undesirable effects on traffic flow are simulated in this subsection using a platoon of three vehicles, due to the

nature of the problem and based on intuition, we can say that the performance worsens as the number of vehicles increase in the string. Hence, in addition to exponential stability, it would be useful to guarantee *performance* levels of automated vehicles for smooth traffic flows. An approach was proposed to mitigate this problem in (Ploeg et al., 2014b) using energy based induced-$\mathcal{L}_2$ norm of cascaded subsystems. We build on the approach of (Ploeg et al., 2014b) to redefine the *performance* problem as a "strict string stability problem" for heterogeneous platoons in terms of the induced-$\mathcal{L}_2$ norm. We call the (exponentially stable) platoon to be *strict* string stable for any finite disturbance (in terms of $\mathcal{L}_2$ norm) at input u_1 and time $t_1 \geq 0$ if

$$||z_i(t)||_{\mathcal{L}_2} \leq ||z_{i-1}(t)||_{\mathcal{L}_2}, \ \forall \ i = 2, ..., n,$$

where z_i can be ψ_{ai} or ψ_{vi}. The above condition is *strict* due to the fact that we require all the individual vehicles to reduce the energy of the disturbance through the string of vehicles in the platoon.

4.4.3 Platoon string stability

In this subsection, we focus on formulating a condition for the strict string stability of the vehicular platoon. We assume throughout this chapter that we observe signals (inputs, accelerations, and velocities) for some exogenous disturbance ($w_c(s)$) at the input of the first vehicle such that $u_1(s) = w_c(s) + K(s)y_1(s)$. We define the transfer function of the closed-loop system (4.9) from $w_c(s)$ to the input observed at vehicle i as

$$P_i(s) := \frac{u_i(s)}{w_c(s)} \ \forall \ i = 1, ..., n.$$

The induced-$\mathcal{L}_2$ norm of the transfer function can be written as

$$||P_i||_{\mathcal{H}_\infty} = \sup_{w \neq 0} \frac{||u_i||_{\mathcal{L}_2}}{||w_c||_{\mathcal{L}_2}} \ \forall \ i = 1, ..., n,$$

where the $\mathcal{L}_2$ norm is defined on the interval $t \in [0, \infty)$

$$||u_i(t)||_{\mathcal{L}_2} = \sqrt{\int_0^\infty (u_i(t))^2 dt},$$

hence,

$$||u_i||_{\mathcal{L}_2} \leq ||P_i||_{\mathcal{H}_\infty} ||w_c||_{\mathcal{L}_2} \ \forall \ i = 1, ..., n.$$

The string stability sensitivity function corresponding to the controlled input is

$$\Gamma(s) := \frac{\frac{u_i(s)}{w_c(s)}}{\frac{u_{i-1}(s)}{w_c(s)}} = P_i(s)(P_{i-1}(s))^{-1}. \tag{4.16}$$

If we derive the above string stability function assuming heterogeneity in the parameters of vehicles in the platoon, we would obtain

$$\Gamma(s, \bar{p}, \hat{p}_i, \hat{p}_{i-1}) = \frac{(K^{\text{ff}} \text{e}^{-\tau_{b(i-1)} s} + G_{i-1} K^{\text{fb}} \text{e}^{-\tau_{ci} s})}{(1 + K^{\text{fb}}(h_i s + 1) G_i \text{e}^{-\tau_{ci} s})}, \tag{4.17}$$

$\forall \ i = 2, ..., n$, where G_i contains the plant dynamics as in (4.4),

$$\begin{aligned} K(s) &= C_c(sI - A_c)^{-1} B_c + D_c \\ &= \begin{bmatrix} K^{\text{fb1}}(s) & K^{\text{fb2}}(s) & K^{\text{ff}}(s) \end{bmatrix} \end{aligned} \tag{4.18}$$

is the stabilising controller ($u_i(s) = K(s) y_i(s), \ u_i \in \mathbb{R}, \ y_i \in \mathbb{R}^3$). For simplicity of the presentation, we use $K^{\text{fb}}(s) = K^{\text{fb1}}(s) + sK^{\text{fb2}}(s)$ to denote the feedback part of the controller corresponding to the signal e_{pi}. The function Γ in (4.17) contains the plant and the controller parameters of vehicle i, and some plant parameters of vehicle $i - 1$. Recall that we denote the controller parameters and the plant parameters of vehicle i using $\bar{p}$ and $\hat{p}_i$ respectively. The CACC configuration that arises from (4.9) for heterogeneous (parameter) vehicles is given in Figure 4.4.

Note that (4.17) is considered in (Ploeg et al., 2014b) for strict string stability. This is sufficient for their case, as the string stability sensitivity function corresponding to the controlled input and the acceleration are the same for

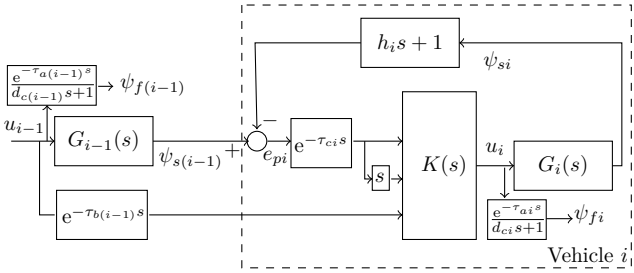

Figure 4.4: The one vehicle look-ahead configuration of CACC.

homogeneous vehicular platoons. However, this is not valid for the case of heterogeneous vehicular platoons. Therefore, we rewrite the string stability sensitivity function in terms of acceleration (observing the accelerations for the exogenous input w_c). The new string stability sensitivity function (corresponding to acceleration) becomes

$$\begin{aligned}\Psi(s,\bar{p},\hat{p}_i,\hat{p}_{i-1}) &= \frac{\frac{\psi_{fi}(s)}{w_c(s)}}{\frac{\psi_{f(i-1)}(s)}{w_c(s)}} = \frac{\frac{e^{-\tau_{ai}s}}{d_{ci}s+1}\cdot\frac{u_i(s)}{w_c(s)}}{\frac{e^{-\tau_{a(i-1)}s}}{d_{c(i-1)}s+1}\cdot\frac{u_{i-1}(s)}{w_c(s)}} \\ &= \frac{(K^{\mathrm{ff}}e^{-\tau_{b(i-1)}s}+G_{i-1}K^{\mathrm{fb}}e^{-\tau_{ci}s})(d_{c(i-1)}s+1)e^{-\tau_{ai}s}}{(1+K^{\mathrm{fb}}(h_is+1)G_ie^{-\tau_{ci}s})(d_{ci}s+1)e^{-\tau_{a(i-1)}s}},\end{aligned} \tag{4.19}$$

$\forall\ i = 2,...,n$. Note that Ψ is the string stability sensitivity function corresponding to both acceleration and velocity ($\psi_{fi}(s) = s\cdot\psi_{vi}(s)$). Based on the assumptions mentioned above, for $\mathcal{L}_2$ *strict* string stability of heterogeneous vehicular platoons, we define the following (similar to (Ploeg et al., 2014b)).

Definition 4.4.2 *We consider the interconnected system (4.9) to be $\mathcal{L}_2$ strict string stable if $c(\bar{p}) < 0$ and*

$$\sup_{\omega\in\mathbb{R}} |\Psi(j\omega,\bar{p},\hat{p}_i,\hat{p}_{i-1})| \leq 1\ \forall\ i = 2,...,n.$$

Finally, we optimise (using frequency-gridding approach) the function

$$\min_{\bar{p}} \max_{i\in\{2,\dots,n\}} \left(\sup_{\omega\in\mathbb{R}} |\Psi(j\omega, \bar{p}, \hat{p}_i, \hat{p}_{i-1})| \right),$$

subject to the constraint $c(\bar{p}) < 0$, in order to obtain a stabilising controller that achieves strict $\mathcal{L}_2$ string stability.

4.4.4 Platoon stability: pseudospectral abscissa

In this section, we solve the stabilisation problem of platoons in look-ahead topologies, using a method whose computational complexity is independent of the platoon size. We can formulate it as a problem of a parameterised system, and compute the pseudospectral abscissa for some structured real-valued perturbations. Since the differences between the vehicles in (4.12) lie in some parameters within the state coefficient matrices (see (4.14)), a sufficient condition for stability is given by the *robust stability* of the corresponding *uncertain* system. Let us define the pseudospectrum of the perturbed system,

$$\Lambda := \bigcup_{\hat{p}_\delta\in\mathcal{R}} \{\lambda \in \mathbb{C} : \det(M_\delta(\lambda, \bar{p}, \hat{p}_\delta)) = 0\}, \tag{4.20}$$

where the vector $\hat{p}_\delta$ (corresponding to a vehicle) is the uncertainty vector belonging to a closed region $\mathcal{R} \in \mathbb{R}^5$. We assume that each element of the uncertain parameter vector $\hat{p}_\delta$ is independent of other elements and lies in a closed real interval. That is, $\hat{p}_{\delta,i} \in [\hat{a}_i, \hat{b}_i]$, where $\hat{p}_{\delta,i}$ is the i-th element of $\hat{p}_\delta$ and $0 < \hat{a}_i < \hat{b}_i,\ i = 1, ..., n$.

Note that $\bar{M}_\delta$ in (4.20) can include all the characteristic matrices $M_i\ \forall\ i = 1, ..., n$ as in (4.12) by defining the heterogeneity in vehicle parameters to be contained within $\mathcal{R}$. For robust stability optimisation, we introduce the pseudospectral abscissa

$$\alpha := \sup\{\Re(\lambda) : \lambda \in \Lambda\}. \tag{4.21}$$

Since the matrices in (4.14) are affine in the uncertain parameters, the pseudospectral abscissa can be computed using the structure exploiting

algorithm for real-valued perturbations in (Borgioli and Michiels, 2018). The objective would be to minimise the pseudospectral abscissa

$$\min_{\bar{p}} \alpha,$$

to obtain a stable system for all perturbations belonging to the region $\mathcal{R}$ with $\alpha < 0$.

4.4.5 Investigating a robust string stabilising controller

The platoon string stability problem in the previous subsection can be extended to find a controller optimising an "uncertain" string stability function Ψ to increase scalability to multiple vehicles (when heterogeneity in vehicle parameters can be confined to real intervals). Let us consider the function Ψ to be *uncertain* with perturbations at all the vehicle/plant parameters (including time-delays). We define the vectors $\hat{p}_\delta$ (corresponding to the parameters of a vehicle) and $\breve{p}_\delta$ (corresponding to the parameters of the vehicle ahead) as the uncertainty vectors belonging to a closed region $\mathcal{R} \in \mathbb{R}^5$. Similar to Section 4.4.4, we assume that each element of the uncertain parameter vectors ($\hat{p}_\delta$ and $\breve{p}_\delta$) is independent of other elements and lies in a closed real interval. That is, $\hat{p}_{\delta,i} \in [\hat{a}_i, \hat{b}_i]$ and $\breve{p}_{\delta,i} \in [\breve{a}_i, \breve{b}_i]$, where $\breve{p}_{\delta,i}$ is the i-th element of $\breve{p}_\delta$, $0 < \breve{a}_i < \breve{b}_i$, and $0 < \hat{a}_i < \hat{b}_i,\ i = 1, ..., n$.

We define the objective function corresponding to the robust induced-$\mathcal{L}_2$ norm (the worst case $\mathcal{L}_2$ gain for all the perturbations) as

$$\chi_\infty := \begin{cases} \max_{\hat{p}_\delta, \breve{p}_\delta \in \mathcal{R}} \left\{ \sup_{\omega \in \mathbb{R}} |\Psi(j\omega, \bar{p}, \hat{p}_\delta, \breve{p}_\delta)| \right\}, & \alpha < 0, \\ \infty, & \alpha \geq 0. \end{cases} \tag{4.22}$$

By intuitively minimising the worst case scenarios using the approach in Section 4.4.3, the robust induced-$\mathcal{L}_2$ norm may be brought to a desirable value ($\chi_\infty \leq 1$). This provides robust performance for all the bounded perturbations/uncertainties in terms of the maximum induced-$\mathcal{L}_2$ norm. In this chapter, we determined χ_∞ by maximising induced-$\mathcal{L}_2$ norm for all the possible

combinations of the elements from the uncertain parameter vectors ($\hat{p}_\delta$ and $\breve{p}_\delta$) which lie in closed intervals in the real coordinate space.

4.5 Simulation-based studies

Let us consider a case of a heterogeneous platoon with three vehicles ($n = 3$), whose parameters are given in Table 4.2. We consider only three vehicles in the platoon for simplicity of the presentation. Our aim is to guarantee (exponential)

Table 4.2: The vehicle parameters used for simulations.

i	d_{ci}	h_i	τ_{ai}	τ_{bi}	τ_{ci}
1	0.07	0.7	0.18	0.018	0.18
2	0.1	0.8	0.2	0.02	0.2
3	0.01	0.6	0.15	0.015	0.15

stability and (string stability) performance for the platoon[3]. The string stability sensitivity function considered is

$$\Psi(s,\bar{p},\hat{p}_l,\hat{p}_k) = \frac{(K^{\mathrm{ff}}\mathrm{e}^{-\tau_{bk}s} + G_k K^{\mathrm{fb}}\mathrm{e}^{-\tau_{cl}s})(d_{ck}s+1)\mathrm{e}^{-\tau_{al}s}}{(1+K^{\mathrm{fb}}(h_l s+1)G_l\mathrm{e}^{-\tau_{cl}s})(d_{cl}s+1)\mathrm{e}^{-\tau_{ak}s}}, \tag{4.23}$$

$k = 1,2,3$, $l = 1,2,3$, where vehicle l is following vehicle k. The nine possible combinations of vehicles result in nine (strict) string stability functions corresponding to each pair.

Considering that the vehicles (with parameters in Table 4.2) are to be controlled by identical controllers, we minimise the objective function (while $c(\bar{p}) < 0$)

$$\min_{\bar{p}} \max_{k,l\in\{1,2,3\}} \left(\sup_{\omega\in\mathbb{R}} |\Psi(j\omega,\bar{p},\hat{p}_l,\hat{p}_k)| \right), \tag{4.24}$$

[3]The software tool and the vehicular platoon example are available in (Dileep and Michiels, 2018a)

to obtain the string stabilising controller (K)

$$\begin{cases} \dot{x}_{ci}(t) &= \begin{bmatrix} -1.4999 & 1.5909 \\ 0.5346 & -3.8166 \end{bmatrix} x_{ci}(t) \\ &\quad + \begin{bmatrix} 1.9677 & -1.2820 & -1.7317 \\ -0.4932 & 1.1862 & 0.7864 \end{bmatrix} y_i(t) \\ u_i(t) &= \begin{bmatrix} -1.0527 & 0.3931 \end{bmatrix} x_{ci}(t) \\ &\quad + \begin{bmatrix} 1.7204 & 0.0702 & 0.0178 \end{bmatrix} y_i(t), \\ &\qquad \forall\ i = 1, 2, 3. \end{cases} \tag{4.25}$$

In (4.24), we considered the worst case over all possible configurations of the

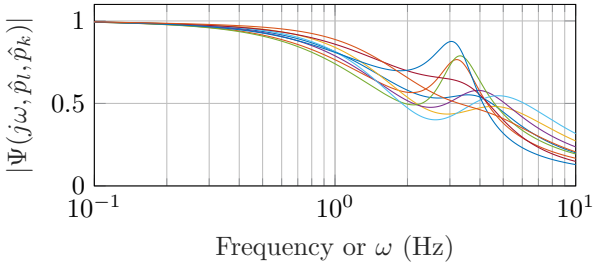

Figure 4.5: Frequency response of the function Ψ for all the nine possible combinations of the three heterogeneous vehicles in the platoon.

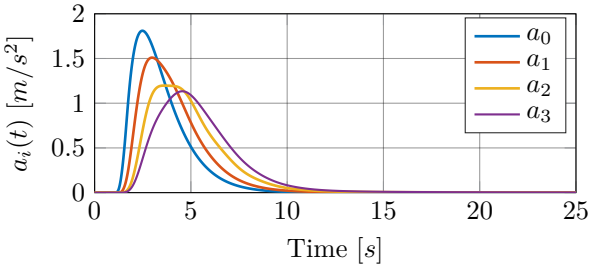

Figure 4.6: Acceleration response for the reference signal $v_{ref,0}$ (platoon of the three vehicles controlled using the controller K).

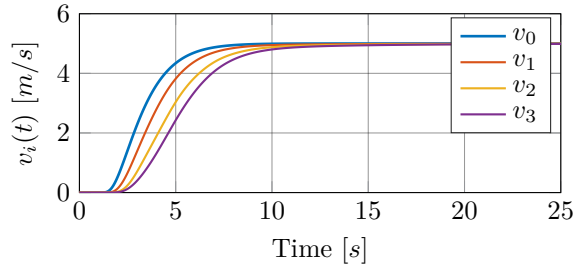

Figure 4.7: Velocity response for the reference signal $v_{ref,0}$ (platoon of the three vehicles controlled using the controller K).

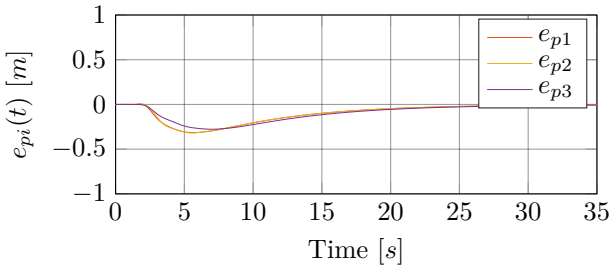

Figure 4.8: Position errors for the reference signal $v_{ref,0}$ (platoon of the three vehicles controlled using the controller K).

platoon. Note that a change in the configuration of the platoon does not affect its exponential stability (or spectral abscissa). A preliminary minimisation of $c(\bar{p})$ was performed to ensure that the starting values for $\bar{p}$ in (4.24) had $c(\bar{p}) < 0$ (exponential stability). The frequency responses are plotted in Figure 4.5 for the function $\Psi(s, \bar{p}, \hat{p}_l, \hat{p}_k)$ with K given in (4.25) $\forall\ k = 1, 2, 3,\ l = 1, 2, 3$. The time responses of accelerations and velocities for a reference signal ($v_0 = v_{ref,0},\ a_0 = \dot{v}_{ref,0}$) are shown in Figures 4.6-4.7 for a combination of the three vehicles from Table 4.2 (in the platoon) simulated using MATLAB. Similarly, the time responses of position errors for vehicles in the same arrangement are given in Figure 4.8.

Notice that the above mentioned approach is not scalable with the number of vehicles, since its computational complexity is dependent on the number

of vehicles (n^2 string stability functions). To improve the scalability of the controller design algorithm with the number of vehicles, we may use the objective functions mentioned in Sections 4.4.4 and 4.4.5. Let us consider a platoon with the number of vehicles $n \gg 3$. Now we assume that the elements of the parameter vectors of the heterogeneous vehicles in the platoon are independent of each other and lie in a closed real interval, that is,

$$\begin{aligned} &d_{ci} \in [0.01, 0.1], h_i \in [0.6, 0.8], \tau_{ai} \in [0.15, 0.2], \\ &\tau_{bi} \in [0.015, 0.02], \text{ and } \tau_{ci} \in [0.15, 0.2] \end{aligned} \tag{4.26}$$

$\forall\ i = 1, ..., n,\ \forall\ \mathbb{N} \setminus \{0\}$. The robust induced-$\mathcal{L}_2$ norm for the one vehicle look-ahead vehicular platoon using K given in (4.25) was also investigated. The robust induced-$\mathcal{L}_2$ norm in (4.22) satisfied the condition $\chi_\infty \leq 1$ and the corresponding pseudospectral abscissa defined in (4.21) is $\alpha = -0.1485$. In summary, the controller K given in (4.25) is also guaranteed to maintain *exponential* stability and *strict* $\mathcal{L}_2$ string stability as per Definition 4.4.2 for any number of vehicles in system (4.9) and for any combination within the platoon, given that the vehicle parameters are confined to the intervals in (4.26). A heuristics approach was utilised to design the controller K given in (4.25). This controller was obtained by optimising controller parameters for a finite set of vehicle parameters using the algorithm in Section 4.4.3. This set of vehicle parameters included the set in Table 4.2 and the set of vehicle parameters which tended to be the arguments for the worst-case induced $\mathcal{L}_2$ norm (χ_∞) in (4.22) when the robust string stability condition was violated.

4.6 Conclusions

The design problem of stabilising (identical) controllers that achieves strict $\mathcal{L}_2$ string stability for heterogeneous (parameter) vehicular platoons in the one vehicle look-ahead topology was considered. We proposed an approach to design the controllers satisfying the stability and performance requirements for the linearised third order heterogeneous vehicle plant models. The proposed

approach was implemented in MATLAB and the corresponding results were presented.

A scalable design approach to obtain (identical) decentralised controllers was also proposed for the case of the heterogeneous one vehicle look-ahead platoon, where the computational complexity is independent of the platoon size. We ensure that the achieved exponential stability and string stability properties are independent of the number of vehicles in the platoon, given that their parameters are confined to some real intervals. This improves the computational efficiency and scalability with the number of vehicles.

The network structure can also be exploited for the case where the heterogeneous (parameter) vehicles in a platoon (with one-vehicle look-ahead topology) have non-identical controllers. Then, using the same approach mentioned in this chapter, it is possible to design each controller (corresponding to a vehicle) independently. That is, we can decouple the control design problem (to satisfy both stability and string stability objectives) for each vehicle in the platoon. However, the computational costs involved in the controller design phase will depend on the number of vehicles.

Finally, note that all the algorithms presented in this chapter have been implemented in a publicly available software (Dileep and Michiels, 2018a).

Chapter 5

General conclusions

5.1 Summary

The design problem of a structured (decentralised, distributed, overlapping, or PID) controller for interconnected systems with time-delays has been addressed in this thesis with a focus on the decentralised control configuration. As a first step, a generic (non-conservative) frequency domain-based direct optimisation technique for the design of decentralised LTI controllers for continuous-time LTI systems modelled by DDAEs was presented in Chapter 2. This approach was grounded in necessary and sufficient stability conditions and imposed sparsity constraints in the controller parametrisation. Furthermore, a structure exploiting approach was proposed for networks of identical (sub-)systems and local controllers. By means of a case-study, the applicability to consensus type problems was shown, while also illustrating the flexibility of the modelling framework and control technique.

In Chapter 3, we presented an approach to design (input-output) stabilising decentralised controllers for generic MIMO plants which are robust against communication imperfections (such as model uncertainties, time-varying delays, aperiodic sampling, and asynchrony) and other input disturbances. The

approach was based on rewriting the networked system of the MIMO plant and sampled-data fixed-order controllers with time-delays as a feedback interconnection of a nominal (continuous-time) TDS and an uncertainty operator. That is, all the communication imperfections are concentrated at the (bounded) uncertainty operator in this feedback interconnection. Then, an input-output $\mathcal{L}_2$ stability criterion is proposed (using the small gain theorem). The closed-loop systems were modelled using DDAEs, which are flexible in modelling interconnected systems. Sparsity constraints were enforced in the parameterisation process within the optimisation to ensure that decentralised controllers are obtained. Additionally, we proposed a method to reduce some conservativeness in the result, which exploits the structure of the operator. Furthermore, the computational efficiency of the controller design algorithm is significantly improved in the case of a structured MIMO plant, where the plant is composed of (quasi-)identical subsystems, at the price that the local controllers need to be identical and the scaling approach to reduce conservatism is not applicable any more.

A scalable methodology was presented in Chapter 3 to design dynamic (LTI) fixed-order controllers for large-scale interconnected systems composed of quasi-identical subsystems connected through some delayed network. We concluded that using a direct optimisation approach and a decomposition (through network structure exploitation), one could design a stabilising decentralised controller independent of the number of nodes (or subsystems), by treating the network related eigenvalue parameter as a parameter subjected to bounded uncertainty. The implementation was based on the algorithm described in (Borgioli and Michiels, 2018) for the pseudospectral abscissa computation, which was briefly recalled in Chapter 2, and an extension of the algorithm in (Gumussoy and Michiels, 2011) to include the min-max optimisation problem of the robust-$\mathcal{H}_\infty$ norm, which was presented in Chapter 3.

Finally, the design problem of stabilising (identical) controllers that achieve strict $\mathcal{L}_2$ string stability for the application of heterogeneous (parameter) vehicular platoons in the one vehicle look-ahead topology was considered in Chapter 4. We proposed a scalable approach to design identical controllers satisfying the stability and performance requirements for linearised third order heterogeneous

vehicle models. The achieved exponential stability and string stability properties were independent of the number (and combination) of the vehicles in the platoon. The proposed approach was implemented in MATLAB and the corresponding results were presented. Here, we assumed that the vehicles can be modelled using DDAEs and that their parameters (corresponding to the heterogeneity) are confined to some real intervals.

Throughout the thesis, controllers were designed using non-conservative direct optimization techniques in the frequency domain, grounded in necessary and sufficient conditions for stability. The approach is flexible with respect to the structure that can be imposed on the controller. Hence, it is adequate to design decentralised, distributed, overlapping, or PID type controllers. However, issues related non-convexity and non-smoothness of the optimisation problem in general (especially for $\mathcal{H}_\infty$ norm) are still present as in the centralised setting. The non-smoothness is handled by using the special algorithm HANSO. With respect to the non-convexity, the algorithm can converge to local optima which are not global. The latter is mitigated by considering sufficiently large number of randomly generated (or user specified) starting points for the optimisation problem. In general, we assumed that the controllers to be designed were dynamic LTI controllers. However, the methodology presented in this thesis trivially extends to other classes of controllers, such as (decentralised) PID controllers, as shown in Section 2.2.

All the algorithms presented in this thesis have been implemented in publicly available software, see (Dileep and Michiels, 2018a), (Dileep and Michiels, 2018b) and (Dileep and Michiels, 2018c).

5.2 Future work

Some directions for future work were revealed during this work. They are as follows. First, the network topology was assumed to be time-invariant throughout this thesis. However, in many applications (such as power systems and platoon of drones), the network topology could be time-varying (which could also be switching), see (Cai and Ishii, 2014; Cheng et al., 2017; Popov

and Werner, 2012) and the references therein. Hence, the analysis and design of controllers or control strategies for systems with time-varying network topology is an open problem of interest. Note that some time-domain based tools (using LMI solvers) may be useful for the case of systems with switched topologies (Fiter et al., 2018; Hetel et al., 2017), and they could be combined with our approach. In this case, there may be some conservatism in the resulting conditions.

Second, network structure exploiting algorithms were presented in this thesis for the design of stable and robust controllers for LTI systems with constant delays. Exploitation of the network structure for a class of linear parameter-varying or time-varying systems is still an open problem. We may use a time domain-based approach to consider this problem. A starting point could be the results reported in (Fiter et al., 2018; Hilhorst et al., 2016; Pfifer and Seiler, 2015). Note that systems with time-varying network topology may be a special case of this problem.

Third, the frequency domain-based approach utilised for the (fixed-order controller design and) minimisation of spectral abscissa and $\mathcal{H}_\infty$ norm, in general, involves non-convex optimisation. That is, the final solution could be a local optima and, hence, it depends on the starting point. Another research direction includes finding a suitable starting point for such non-convex optimisation problems that could guarantee the convergence to a solution which is the global optimum. In (Monnet et al., 2016), a global optimisation approach is presented for the design of robust structured controllers for LTI systems without time-delays. The design problem is formulated as a min-max optimisation problem, and was solved using a branch and bound algorithm based on interval arithmetic.

Finally, this thesis focused on computationally efficient (structured) controller design methodologies for a given network topology. Another research problem could be the design of an optimal (in terms of stability or performance levels) network topology for interconnecting a given group of dynamical system (Fardad et al., 2014; Shafi et al., 2012). This problem may be framed as a discrete optimisation problem.

Appendix A

Frequently used network topologies

Series network topology - unidirectional coupling



Figure A.1: Series network topology - unidirectional coupling

In a series network, each node is connected to two neighbouring nodes except for the two nodes at the end of the series which are connected to (only) one subsystem. In the literature, it is also referred to as a line network, see (van Schuppen and Villa, 2014). For series network topology with unidirectional coupling (see Figure A.1), the adjacency matrix may take the form

$$A_M = \begin{bmatrix} 0 & \dots & 0 & 0 \\ 1 & \dots & 0 & 0 \\ \vdots & \ddots & \vdots & \vdots \\ 0 & \dots & 1 & 0 \end{bmatrix}. \tag{A.1}$$

The adjacency matrix A_M in (A.1) has a zero eigenvalue with algebraic multiplicity n.

Series network topology - bidirectional coupling



Figure A.2: Series network topology - bidirectional coupling

For a series network with bidirectional coupling (see Figure A.2), the adjacency matrix may take the form

$$A_M = \begin{bmatrix} 0 & 1 & 0 & \dots & 0 & 0 \\ 0.5 & 0 & 0.5 & \dots & 0 & 0 \\ 0 & 0.5 & 0 & \dots & 0 & 0 \\ \vdots & \vdots & \vdots & \ddots & \vdots & \vdots \\ 0 & 0 & 0 & \dots & 0 & 0.5 \\ 0 & 0 & 0 & \dots & 1 & 0 \end{bmatrix}. \tag{A.2}$$

The eigenvalues of A_M in (A.2) can be described using

$$\lambda_{ai} = \cos((i-1)\frac{\pi}{n-1}) \text{ for } i = 1, ..., n \text{ and } n \in \mathbb{Z}_0^+ \setminus \{1\}. \tag{A.3}$$

Ring network topology - unidirectional coupling

In a ring network, each node is connected to two other nodes. For the ring network topology with unidirectional coupling (see Figure A.3), the adjacency matrix may take the form

$$A_M = \begin{bmatrix} 0 & \dots & 0 & 1 \\ 1 & \dots & 0 & 0 \\ \vdots & \ddots & \vdots & \vdots \\ 0 & \dots & 1 & 0 \end{bmatrix}. \tag{A.4}$$

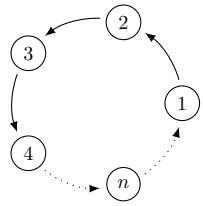

Figure A.3: Ring network topology - unidirectional coupling

The eigenvalues of A_M in (A.4) can be described (as taken from (Michiels and Nijmeijer, 2009)) using

$$\lambda_{ai} = e^{-j[2\pi(i-1)/n]} \text{ for } i = 1, ..., n \text{ and } n \in \mathbb{Z}_0^+.$$

Ring network topology - bidirectional coupling

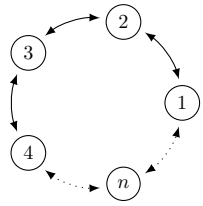

Figure A.4: Ring network topology - bidirectional coupling

For the ring network topology with bidirectional coupling (see Figure A.4), the adjacency matrix may take the form

$$A_M = \begin{bmatrix} 0 & 0.5 & 0 & \dots & 0 & 0.5 \\ 0.5 & 0 & 0.5 & \dots & 0 & 0 \\ 0 & 0.5 & 0 & \dots & 0 & 0 \\ \vdots & \vdots & \vdots & \ddots & \vdots & \vdots \\ 0 & 0 & 0 & \dots & 0 & 0.5 \\ 0.5 & 0 & 0 & \dots & 0.5 & 0 \end{bmatrix}. \tag{A.5}$$

The eigenvalues of A_M in (A.5) can be described described using

$$\lambda_{ai} = \cos(\frac{2\pi}{n}(i-1)) \text{ for } i = 1, ..., n \text{ and } n \in \mathbb{Z}_0^+ \setminus \{1, 2\}. \tag{A.6}$$

Fully connected network topology - all-to-all coupling

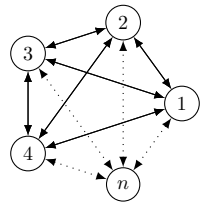

Figure A.5: Fully connected network topology

In a fully connected network (with equal weights), each node is connected to all the other nodes (see Figure A.5). Then, the adjacency matrix of this network topology may take the form

$$A_M = \begin{bmatrix} 0 & \frac{1}{n-1} & \frac{1}{n-1} & \cdots & \frac{1}{n-1} & \frac{1}{n-1} \\ \frac{1}{n-1} & 0 & \frac{1}{n-1} & \cdots & \frac{1}{n-1} & \frac{1}{n-1} \\ \frac{1}{n-1} & \frac{1}{n-1} & 0 & \cdots & \frac{1}{n-1} & \frac{1}{n-1} \\ \vdots & \vdots & \vdots & \ddots & \vdots & \vdots \\ \frac{1}{n-1} & \frac{1}{n-1} & \frac{1}{n-1} & \cdots & 0 & \frac{1}{n-1} \\ \frac{1}{n-1} & \frac{1}{n-1} & \frac{1}{n-1} & \cdots & \frac{1}{n-1} & 0 \end{bmatrix}. \tag{A.7}$$

The eigenvalues of A_M in (A.7) are 1 with algebraic multiplicity one and $-\frac{1}{n-1}$ with algebraic multiplicity $n-1$, where $n \in \mathbb{Z}_0^+ \setminus \{1\}$.

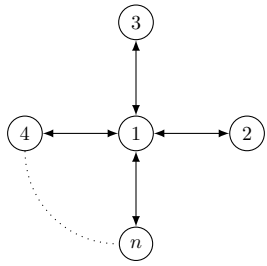

Figure A.6: Star network topology with bidirectional coupling

Star network topology - one-to-all coupling

In a star connected network, all the nodes are connected to one globally accessible node (see Figure A.6). Then, the adjacency matrix may take the form

$$A_M = \begin{bmatrix} 0 & \frac{1}{n-1} & \frac{1}{n-1} & \dots & \frac{1}{n-1} & \frac{1}{n-1} \\ 1 & 0 & 0 & \dots & 0 & 0 \\ 1 & 0 & 0 & \dots & 0 & 0 \\ \vdots & \vdots & \vdots & \ddots & \vdots & \vdots \\ 1 & 0 & 0 & \dots & 0 & 0 \\ 1 & 0 & 0 & \dots & 0 & 0 \end{bmatrix}. \tag{A.8}$$

The eigenvalues of A_M in (A.8) are 1 with algebraic multiplicity one, -1 with algebraic multiplicity one, and 0 with algebraic multiplicity $n-2$, where $n \in \mathbb{Z}_0^+ \setminus \{1\}$.

Appendix B

Small gain theorem

In this subsection, we recall the concept of small gain theorem from robust control theory. The system (1.5), with transfer function G and zero initial condition, can be viewed as an operator $\mathbf{G} : \mathcal{L}_2[0,\infty) \to \mathcal{L}_2[0,\infty)$ mapping the input space $w \in \mathcal{L}_2[0,\infty)$ to the output space $z \in \mathcal{L}_2[0,\infty)$. Note that we only consider causal systems. A system is said to be finite input-output $\mathcal{L}_2$ stable if it has a finite $\mathcal{L}_2$ gain, that is,

$$||\mathbf{G}||_{\mathcal{L}_2} = \inf\{\gamma : ||\mathbf{G}w||_{\mathcal{L}_2} \leq \gamma||w||_{\mathcal{L}_2} \ \forall \ w \in \mathcal{L}_2[0,\infty)\}. \tag{B.1}$$

Additionally, for LTI systems $||\mathbf{G}||_{\mathcal{L}_2} = ||G||_{\mathcal{H}_\infty}$. Given two causal systems with finite $\mathcal{L}_2$ gain $\mathbf{G} : \mathcal{L}_2[0,\infty) \to \mathcal{L}_2[0,\infty)$ and $\Delta : \mathcal{L}_2[0,\infty) \to \mathcal{L}_2[0,\infty)$, we consider the following feedback interconnection

$$\begin{aligned} z &= \mathbf{G}w + f, \\ w &= \Delta z + g, \end{aligned} \tag{B.2}$$

where $f, g \in \mathcal{L}_2[0,\infty)$ (see Figure B.1). The operator Δ is generally used in robust control theory to represent the uncertainties and perturbations that affect the nominal system $\mathbf{G}$ (system (1.5) with zero initial condition), and the signals f, g may also be used to consider some non-zero initial conditions for

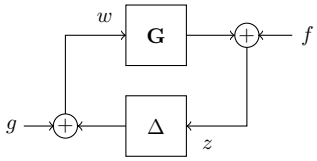

Figure B.1: The feedback interconnection of **G** and Δ.

the system (1.5) (Vidyasagar, 2002). The following small gain theorem holds, and its proof is given in (Fridman, 2014; Khalil, 2002).

Theorem B.0.1 *Assume that* **G** *and* Δ *are input-output* $\mathcal{L}_2$ *stable, and* **G** *is LTI. Then the mapping*

$$\begin{bmatrix} f \\ g \end{bmatrix} \longrightarrow \begin{bmatrix} w \\ z \end{bmatrix}, \tag{B.3}$$

is input-output $\mathcal{L}_2$ *stable if* $(||G||_{\mathcal{H}_\infty} \cdot ||\Delta||_{\mathcal{L}_2}) < 1$.

Consequently, the robust control design problem consists of synthesising a controller that minimises the $||G||_{\mathcal{H}_\infty}$ norm, which may also be interpreted as maximising the allowable $\mathcal{L}_2$ bound on the uncertainties or perturbations such that the input-output stability remains guaranteed.

Appendix C

Well posedness of the systems considered

In this section of appendix we refer to the Assumption 3.1 in (Gumussoy and Michiels, 2011) applied to the closed loop system (1.5) which reads as $\det(\tilde{U}^{\mathrm{T}} A_0 \tilde{V}) \neq 0$ where the columns of matrix $\tilde{U}$ and $\tilde{V}$ are the (minimal) basis for the right and left nullspace of E respectively,

$$\tilde{U}^{\mathrm{T}} E = 0 \text{ and } E\tilde{V} = 0.$$

This can be rephrased as the Assumption 1 mentioned in this paper, using the theorem below.

Theorem C.0.1 *Matrix $U^T(A_{p0} + B_{p1}D_cC_{p1})V$ being non-singular is equivalent to $\tilde{U}^T A_0 \tilde{V}$ being non-singular.*

Proof. We consider the following relations for U and V with $\tilde{U}$ and $\tilde{V}$ respectively,

$$\tilde{U}^{\mathrm{T}} = \begin{bmatrix} U^{\mathrm{T}} & 0 & 0 & 0 & 0 \\ 0 & I & 0 & 0 & 0 \\ 0 & 0 & I & 0 & 0 \\ 0 & 0 & 0 & 0 & I \end{bmatrix}; \qquad \tilde{V} = \begin{bmatrix} V & 0 & 0 & 0 \\ 0 & I & 0 & 0 \\ 0 & 0 & I & 0 \\ 0 & 0 & 0 & 0 \\ 0 & 0 & 0 & I \end{bmatrix}. \tag{C.1}$$

Using (2.9) and (C.1) we can write the expression

$$\bar{X} := \tilde{U}^{\mathrm{T}} A_0 \tilde{V} = \left[\begin{array}{c|ccc} U^{\mathrm{T}} A_{p0} V & U^{\mathrm{T}} B_{p1} & U^{\mathrm{T}} B_{p2} & 0 \\ \hline C_{p1} V & 0 & 0 & -I \\ 0 & 0 & -I & 0 \\ 0 & -I & 0 & D_c \end{array}\right]. \tag{C.2}$$

The matrix $\tilde{U}^{\mathrm{T}} A_0 \tilde{V}$ being invertible is equivalent to the block

$$\bar{X}_b := \begin{bmatrix} 0 & 0 & -I \\ 0 & -I & 0 \\ -I & 0 & D_c \end{bmatrix} \tag{C.3}$$

and the Schur complement $(\bar{X}/\bar{X}_b)$ of the block $\bar{X}_b$ of the matrix $\bar{X}$ being invertible. We can see that $\bar{X}_b$ is always invertible (independent of D_c) due to its structure. $\bar{X}/\bar{X}_b$ is invertible if

$$\begin{aligned} \bar{X}/\bar{X}_b &= U^{\mathrm{T}} A_{p0} V - \begin{bmatrix} U^{\mathrm{T}} B_{p1} & U^{\mathrm{T}} B_{p2} & 0 \end{bmatrix} \bar{X}_b^{-1} \begin{bmatrix} C_{p1} V \\ 0 \\ 0 \end{bmatrix} \\ &= U^{\mathrm{T}} A_{p0} V + U^{\mathrm{T}} B_{p1} D_c C_{p1} V \end{aligned} \tag{C.4}$$

is invertible. The proof is complete. □

Appendix D

Consensus problem in a ring network topology

In this section of the appendix we show that the closed-loop system (2.36)-(2.38) in a ring configuration has double zero eigenvalues, independent of the control.

Theorem D.0.1 *There always exist two zero eigenvalues for the closed-loop system of system (2.36) in ring network topology and their controller(s), irrespective of the controller parameters and the number of subsystems.*

Proof. The closed-loop system can be written in the DDAE form of (2.8) for $w \equiv 0$ using (2.7) and (2.36). For this, we consider the new state $x_i(t) =$

$$[\bar{\psi}_{pi}^{\mathrm{T}}(t)\ \nu_i^{\mathrm{T}}(t)\ \xi_i^{\mathrm{T}}(t)\ x_{ci}^{\mathrm{T}}(t)]^{\mathrm{T}}\ ,$$

$$\begin{bmatrix} I & 0 & 0 & 0 \\ 0 & 0 & 0 & 0 \\ 0 & 0 & 0 & 0 \\ 0 & 0 & 0 & I \end{bmatrix} \dot{x}_i(t) = \begin{bmatrix} A_g & 0 & 0 & 0 \\ 0 & -I & \hat{D}_c & \hat{C}_c \\ -C_g & 0 & -I & 0 \\ 0 & 0 & \hat{B}_c & \hat{A}_c \end{bmatrix} x_i(t) + \begin{bmatrix} 0 & B_g & 0 & 0 \\ 0 & 0 & 0 & 0 \\ 0 & 0 & 0 & 0 \\ 0 & 0 & 0 & 0 \end{bmatrix} x_i(t-\breve{\tau})$$

$$+ \begin{bmatrix} 0 \\ 0 \\ I \\ 0 \end{bmatrix} u_{ci}(t),$$

$$y_{ci}(t) = \begin{bmatrix} C_g & 0 & 0 & 0 \end{bmatrix} x_i(t). \tag{D.1}$$

Now we can bring the above equation, supplemented with (2.37) in a decoupled form as in (2.13), after the use of an appropriate transformation matrix,

$$\begin{bmatrix} I & 0 & 0 & 0 \\ 0 & 0 & 0 & 0 \\ 0 & 0 & 0 & 0 \\ 0 & 0 & 0 & I \end{bmatrix} \dot{\bar{x}}_i(t) = \left(\begin{bmatrix} A_g & 0 & 0 & 0 \\ 0 & -I & \hat{D}_c & \hat{C}_c \\ -C_g & 0 & -I & 0 \\ 0 & 0 & \hat{B}_c & \hat{A}_c \end{bmatrix} + \lambda_{ai} \begin{bmatrix} 0 & 0 & 0 & 0 \\ 0 & 0 & 0 & 0 \\ C_g & 0 & 0 & 0 \\ 0 & 0 & 0 & 0 \end{bmatrix} \right) \bar{x}_i(t)$$

$$+ \begin{bmatrix} 0 & B_g & 0 & 0 \\ 0 & 0 & 0 & 0 \\ 0 & 0 & 0 & 0 \\ 0 & 0 & 0 & 0 \end{bmatrix} \bar{x}_i(t-\breve{\tau}), \tag{D.2}$$

$i = 1, ..., n$. Based on the assumption that the system has a ring network topology, A_M contains an eigenvalue $1\ \forall\ n \in \mathbb{N} \setminus \{1\}$ at some value $i = k$ ($\lambda_{ak} = 1$). The k-th subsystem then takes the form

$$\begin{bmatrix} I & 0 & 0 & 0 \\ 0 & 0 & 0 & 0 \\ 0 & 0 & 0 & 0 \\ 0 & 0 & 0 & I \end{bmatrix} \dot{\bar{x}}_k(t) = \begin{bmatrix} A_g & 0 & 0 & 0 \\ 0 & -I & \hat{D}_c & \hat{C}_c \\ \boxed{0} & 0 & -I & 0 \\ 0 & 0 & \hat{B}_c & \hat{A}_c \end{bmatrix} \bar{x}_k(t) + \begin{bmatrix} 0 & B_g & 0 & 0 \\ 0 & 0 & 0 & 0 \\ 0 & 0 & 0 & 0 \\ 0 & 0 & 0 & 0 \end{bmatrix} \bar{x}_k(t-\breve{\tau}). \tag{D.3}$$

The above equation shows that the spectrum of system matrix A_g, which contains a double eigenvalue at zero, is part of the spectrum of the closed-loop system. The proof is complete. □

Remark. Theorem D.0.1 also holds true for other network typologies whose adjacency matrix has at least one eigenvalue equal to 1. ◇

Appendix E

Upper-bound for the operators

In this section of Appendix, we present the preliminary lemmas required to prove Lemma 3.3.1 followed by the proof itself. First, we generalise the proof of Lemma 1 in (Thomas et al., 2018). For this purpose, we define new sequences $\{b_l\}_{l\in\mathbb{Z}}$ in time to satisfy

$$\{b_l : b_{l+1} - b_l = \delta b_l,\ l \in \mathbb{Z}\}, \tag{E.1}$$

and $\delta b_l \in (0, \bar{\delta b}]\ \forall\ l \in \mathbb{Z},\ \bar{\delta b} \in \mathbb{R}^+$. Also, the sequences $\{c_l\}_{l\in\mathbb{Z}}$ satisfy

$$\{c_l : c_l = b_l + \delta c_l,\ l \in \mathbb{Z}\}, \tag{E.2}$$

and $\delta c_l \in [0, \bar{\delta c}]\ \forall\ l \in \mathbb{Z},\ \bar{\delta c} \in \mathbb{R}^+$. Also, we define a *general* bounded integral operator $\mathbf{\Delta}$ on $\mathcal{L}_{2e}(-\infty, \infty)$ that operates on the input based on the above sequences, that is

$$\hat{w}(t) = (\mathbf{\Delta}(\{b_l, c_l\}_{l\in\mathbb{Z}})\hat{z})(t) := \int_{b_l}^{t} \hat{z}(\theta)\mathrm{d}\theta, \quad \forall\ t \in [c_l, c_{l+1}),\ l \in \mathbb{Z}. \tag{E.3}$$

We abuse the notation for the operator as shown above, $\mathbf{\Delta}(\{b_l, c_l\}_{l\in\mathbb{Z}})$, to generalise it for any two sets of sequences that satisfy the above conditions as $\{b_l\}_{l\in\mathbb{Z}}$ and $\{c_l\}_{l\in\mathbb{Z}}$. Now we prove the following lemma for this *general* operator.

Lemma E.0.1 *The $\mathcal{L}_2$ induced norm of the operator $\mathbf{\Delta}(\{b_l, c_l\}_{l\in\mathbb{Z}})$ is upper-bounded by $\bar{\delta b} + \bar{\delta c}$, that is,*

$$||\mathbf{\Delta}(\{b_l, c_l\}_{l\in\mathbb{Z}})||_{\mathcal{L}_2} \leq \bar{\delta b} + \bar{\delta c}$$

Proof. By definition, we have

$$\hat{w}(t) = \int_{b_l}^{t} \hat{z}(\theta)\mathrm{d}\theta, \quad \forall\ t \in [c_l, c_{l+1}),\ l \in \mathbb{Z}. \tag{E.4}$$

Then by virtue of Jensen's inequality, we can write

$$\begin{aligned}
\hat{w}(t)^{\mathrm{T}}\hat{w}(t) &= \left(\int_{b_l}^{t} \hat{z}(\theta)\mathrm{d}\theta\right)^{\mathrm{T}} \left(\int_{b_l}^{t} \hat{z}(\theta)\mathrm{d}\theta\right), \\
&\leq (t - b_l)\int_{b_l}^{t} \hat{z}^{\mathrm{T}}(\theta)\hat{z}(\theta)\mathrm{d}\theta,\ \forall\ t \in [c_l, c_{l+1}), \\
&\leq (\bar{\delta b} + \bar{\delta c})\int_{b_l}^{t} \hat{z}^{\mathrm{T}}(\theta)\hat{z}(\theta)\mathrm{d}\theta,\ \forall\ t \in [c_l, c_{l+1}),
\end{aligned} \tag{E.5}$$

since we know that $t \in [c_l, c_{l+1})$

$$t - b_l \leq \overbrace{c_{l+1} - b_{l+1}}^{\leq \bar{\delta c}} + \overbrace{b_{l+1} - b_l}^{\leq \bar{\delta b}}\ \forall\ t\ \in [c_l, c_{l+1}),\ l \in \mathbb{Z}.$$

Substituting $\theta = t + p$ in the above equation and using the fact $t \in [c_l, c_{l+1})$, we get

$$\hat{w}(t)^{\mathrm{T}}\hat{w}(t) \leq (\bar{\delta b} + \bar{\delta c})\int_{-(\bar{\delta b}+\bar{\delta c})}^{0} \hat{z}^{\mathrm{T}}(t + p)\hat{z}(t + p)\mathrm{d}p. \tag{E.6}$$

Integrating both the sides with respect to t in (E.6), we get

$$\begin{aligned}\int_{-\infty}^{\infty} \hat{w}(t)^{\mathrm{T}}\hat{w}(t)\mathrm{d}t &\leq (\bar{\delta b}+\bar{\delta c})\int_{-\infty}^{\infty}\left(\int_{-(\bar{\delta b}+\bar{\delta c})}^{0}\hat{z}^{\mathrm{T}}(t+p)\hat{z}(t+p)\mathrm{d}p\right)\mathrm{d}t,\\ &\leq (\bar{\delta b}+\bar{\delta c})\int_{-(\bar{\delta b}+\bar{\delta c})}^{0}\left(\int_{-\infty}^{\infty}\hat{z}^{\mathrm{T}}(t+p)\hat{z}(t+p)\mathrm{d}t\right)\mathrm{d}p,\end{aligned} \tag{E.7}$$

where $\theta = t+p$, since $\theta \to \infty$ as $t \to \infty$ and $\theta \to -\infty$ as $t \to -\infty$, we have

$$\int_{-\infty}^{\infty} \hat{w}(t)^{\mathrm{T}}\hat{w}(t)\mathrm{d}t \leq (\bar{\delta b}+\bar{\delta c})\int_{-(\bar{\delta b}+\bar{\delta c})}^{0}\left(\int_{-\infty}^{\infty}\hat{z}^{\mathrm{T}}(\theta)\hat{z}(\theta)\mathrm{d}\theta\right)\mathrm{d}p. \tag{E.8}$$

Consequently, we have

$$||\hat{w}||_{\mathcal{L}_2}^2 \leq (\bar{\delta b}+\bar{\delta c})^2||\hat{z}||_{\mathcal{L}_2}^2, \tag{E.9}$$

hence proved. ∘

The idea underlying the proof of Lemma 3.3.1 is that the bounded operators on $\mathcal{L}_{2e}[0,\infty)$ considered in this paper can be seen as a special case of the operators on $\mathcal{L}_{2e}(-\infty,\infty)$ considered by the authors in (Thomas et al., 2018). To illustrate this, we define the new sequences $\{\hat{s}_l^i\}_{l\in\mathbb{Z}}$ in time to satisfy

$$\{\hat{s}_l^i : \hat{s}_{l+1}^i - \hat{s}_l^i = \hat{h}_l^i,\ l \in \mathbb{Z}\},\ i \in \{1,...,N\}, \tag{E.10}$$

$\hat{s}_k^i = s_k^i\ \forall\ k\ \in\ \mathbb{Z}_0^+$, and $\hat{h}_l^i \in (0,\bar{h}_i]\ \forall\ l \in \mathbb{Z}$. Also, the sequences $\{\hat{a}_l^i\}_{l\in\mathbb{Z}}$ satisfy

$$\{\hat{a}_l^i : \hat{a}_l^i = \hat{s}_l^i + \hat{\eta}_l^i,\ l \in \mathbb{Z}\},\ i \in \{1,...,N\}, \tag{E.11}$$

$\hat{a}_k^i = a_k^i\ \forall\ k\ \in\ \mathbb{Z}_0^+$, $\hat{\eta}_l^i \in [0,\bar{\eta}_i]\ \forall\ l \in \mathbb{Z}$, and $\hat{a}_l^i < 0\ \forall\ l \in \mathbb{Z}^-$. Using Lemma E.0.1, we know that $||\boldsymbol{\Delta}(\{\hat{s}_l^i,\hat{a}_l^i\}_{l\in\mathbb{Z}})||_{\mathcal{L}_2} \leq \bar{h}_i + \bar{\eta}_i$ for any input (with finite energy) to the operator. We define two new operators, an extension operator $\mathcal{D} : \mathcal{L}_{2e}[0,\infty) \to \mathcal{L}_{2e}(-\infty,\infty)$ such that

$$(\mathcal{D}\tilde{z})(t) := \begin{cases}\tilde{z}(t), & \forall\ t \in [0,\infty),\\ 0, & \forall\ t \in (-\infty,0),\end{cases} \tag{E.12}$$

and a restriction operator $\mathcal{R} : \mathcal{L}_{2e}(-\infty, \infty) \rightarrow \mathcal{L}_{2e}[0, \infty)$ such that $\tilde{z}(t) = (\mathcal{R}\hat{z})(t) := \hat{z}(t)\ \forall\ t \in [0, \infty)$, then, we have the following lemma.

Lemma E.0.2 *The following relation holds true,*

$$(\Delta_3^i \tilde{z})(t) = (\mathcal{R}\boldsymbol{\Delta}(\{\hat{s}_l^i, \hat{a}_l^i\}_{l\in\mathbb{Z}})\mathcal{D}\tilde{z})(t). \tag{E.13}$$

Proof. Using the fact that $\hat{a}_l^i < 0\ \forall\ l \in \mathbb{Z}^-$, we can write

$$(\boldsymbol{\Delta}(\{\hat{s}_l^i, \hat{a}_l^i\}_{l\in\mathbb{Z}})\mathcal{D}\tilde{z})(t) = \begin{cases} \int_{\hat{s}_l^i}^t \mathcal{D}\tilde{z}(\theta)\mathrm{d}\theta, & \forall\ t \in [\hat{a}_l^i, \hat{a}_{l+1}^i),\ l \in \mathbb{Z}_0^+ \cup \{-1\}, \\ 0, & \forall\ t \in (-\infty, \hat{a}_{-1}^i). \end{cases} \tag{E.14}$$

However, for the case in the above equation when $l = -1$ or $t \in [\hat{a}_{-1}^i, \hat{a}_0^i)$, we know that $\hat{a}_{-1}^i < 0 < \hat{a}_0^i$ then using (E.12) we have

$$\int_{\hat{s}_{-1}^i}^t \mathcal{D}\tilde{z}(\theta)\mathrm{d}\theta = \begin{cases} \int_0^t \tilde{z}(\theta)\mathrm{d}\theta, & \forall\ t \in [0, \hat{a}_0^i), \\ 0, & \forall\ t \in [\hat{a}_{-1}^i, 0), \end{cases} \tag{E.15}$$

then we can rewrite (E.14) as

$$(\boldsymbol{\Delta}(\{\hat{s}_l^i, \hat{a}_l^i\}_{l\in\mathbb{Z}})\mathcal{D}\tilde{z})(t) = \begin{cases} \int_{s_k^i}^t \tilde{z}(\theta)\mathrm{d}\theta, & \forall\ t \in [a_k^i, a_{k+1}^i),\ k \in \mathbb{Z}_0^+, \\ \int_0^t \tilde{z}(\theta)\mathrm{d}\theta, & \forall\ t \in [0, a_0^i), \\ 0, & \forall\ t \in (-\infty, 0), \end{cases} \tag{E.16}$$

hence proved. ∘

Proof of Lemma 3.3.1. From Lemmas E.0.1 and E.0.2 we directly have

$$||\Delta_3^i||_{\mathcal{L}_2} \leq ||\boldsymbol{\Delta}(\{\hat{s}_l^i, \hat{a}_l^i\}_{l\in\mathbb{Z}})||_{\mathcal{L}_2} \leq \bar{h}_i + \bar{\eta}_i,$$

or $||\Delta_3^i||_{\mathcal{L}_2} \leq \gamma_3^i\ \forall\ i \in \{1, ..., N\}$. Similarly, using Lemma E.0.1 and slightly modifying Lemma E.0.2 (by changing the sequences in (E.10)-(E.11) accordingly), it can also be shown that $||\Delta_1^i||_{\mathcal{L}_2} \leq \gamma_1^i$ and $||\Delta_2^i||_{\mathcal{L}_2} \leq \gamma_2^i,\ \forall\ i \in \{1, ..., N\}$. Hence, Lemma 3.3.1 has been proved. ∘

Bibliography

Alanis, A. Y. and Sanchez, E. N. (2017). Chapter 5 - neural observers with unknown time-delays. In Alanis, A. Y. and Sanchez, E. N., editors, *Discrete-Time Neural Observers*, pages 99 – 128. Academic Press.

Alavian, A. (2017). *Optimization-based Robustness and Stabilization in Decentralized Control*. PhD thesis, Department of Electrical and Computer Engineering, University of Maryland.

Alavian, A. and Rotkowitz, M. (2015a). Decentralized non-overshooting stabilization. In *2015 American Control Conference (ACC)*, pages 4785–4790.

Alavian, A. and Rotkowitz, M. (2015b). On the pole selection for h-infinity optimal decentralized control. In *2015 American Control Conference (ACC)*, pages 5471–5476.

Alavian, A. and Rotkowitz, M. C. (2013). Q-parametrization and an SDP for H-infinity-optimal decentralized control. *IFAC Proceedings Volumes*, 46(27):301 – 308.

Anthonis, J., Seuret, A., Richard, J., and Ramon, H. (2007). Design of a pressure control system with dead band and time delay. *IEEE Transactions on Control Systems Technology*, 15(6):1103–1111.

Apkarian, P. and Noll, D. (2006). Non-smooth H-infinity synthesis. *IEEE Transactions on Automatic Control*, 51(1):71–86.

Apkarian, P. and Noll, D. (2018). Structured H_∞-control of infinite-dimensional systems. *International Journal of Robust and Nonlinear Control*, 28(9):3212–3238.

Arioua, L., Marinescu, B., and Monmasson, E. (2014). Control of high voltage

direct current links with overall large-scale grid objectives. *IET Generation, Transmission Distribution*, 8(5):945–956.

Aström, K., Albertos, P., Blanke, M., Isidori, A., Schaufelberger, W., and Sanz, R. (2011). *Control of Complex Systems*. Springer London.

Bakule, L. (2008). Decentralized control: An overview. *Annual Reviews in Control*, 32(1):87 – 98.

Bapat, R. (2010). *Graphs and Matrices*. Universitext. Springer-Verlag London.

Barreau, M., Gouaisbaut, F., and Seuret, A. (2018). Static state and output feedback synthesis for time-delay systems. In *2018 European Control Conference (ECC)*, pages 1195–1200.

Bauer, N., Donkers, M., van de Wouw, N., and Heemels, W. (2013). Decentralized observer-based control via networked communication. *Automatica*, 49(7):2074 – 2086.

Bemporad, A., Heemels, M., and Vejdemo-Johansson, M. (2010). *Networked Control Systems*. Lecture Notes in Control and Information Sciences. Springer London.

Borgioli, F. and Michiels, W. (2018). Computing distance to instability for delay systems with uncertainities in the system matrices and in the delay terms. In *17th Annual European Control Conference (ECC)*.

Boyd, S., Balakrishnan, V., and Kabamba, P. (1989). A bisection method for computing the h-infinity norm of a transfer matrix and related problems. *Mathematics of Control, Signals and Systems*, 2(3):207–219.

Bragagnolo, M. C., Morărescu, I.-C., Daafouz, J., and Riedinger, P. (2016). Reset strategy for consensus in networks of clusters. *Automatica*, 65:53 – 63.

Bruinsma, N. A. and Steinbuch, M. (1990). A fast algorithm to compute the h-infinity-norm of a transfer function matrix. *Systems & Control Letters*, 14(4):287 – 293.

Burke, J., Henrion, D., Lewis, A., and Overton, M. (2006). HIFOO - a matlab package for fixed-order controller design and H-infinity optimization. *IFAC Proceedings Volumes*, 39(9):339 – 344. 5th IFAC Symposium on Robust Control Design.

Cai, K. and Ishii, H. (2014). Average consensus on arbitrary strongly connected digraphs with time-varying topologies. *IEEE Transactions on Automatic*

Control, 59(4):1066–1071.

Chen, W.-H. and Zheng, W. X. (2006). On improved robust stabilization of uncertain systems with unknown input delay. *Automatica*, 42(6):1067 – 1072.

Cheng, T., Kan, Z., Klotz, J. R., Shea, J. M., and Dixon, W. E. (2017). Event-triggered control of multiagent systems for fixed and time-varying network topologies. *IEEE Transactions on Automatic Control*, 62(10):5365–5371.

Col, L. D., Tarbouriech, S., and Zaccarian, L. (2018). H-infinity control design for synchronisation of identical linear multi-agent systems. *International Journal of Control*, 91(10):2214–2229.

D'Andrea, R. and Dullerud, G. E. (2003). Distributed control design for spatially interconnected systems. *IEEE Transactions on automatic control*, 48(9):1478–1495.

Darbha, S., Konduri, S., and Pagilla, P. R. (2019). Benefits of v2v communication for autonomous and connected vehicles. *IEEE Transactions on Intelligent Transportation Systems*, 20(5):1954–1963.

Davison, E. J. and Chang, T. N. (1990). Decentralized stabilization and pole assignment for general proper systems. *IEEE Transactions on Automatic Control*, 35(6):652–664.

Davison, E. J., Davison, D. E., and Lam, S. (2009). Multivariable three-term optimal controller design for large-scale systems. In *Proceedings of the 48h IEEE Conference on Decision and Control (CDC) held jointly with 2009 28th Chinese Control Conference*, pages 940–945.

Dileep, D., Borgioli, F., Hetel, L., Richard, J.-P., and Michiels, W. (2018a). A scalable design method for stabilising decentralised controllers for networks of delay-coupled systems. In *5th IFAC Conference on Analysis and Control of Chaotic Systems , Netherlands*.

Dileep, D., Fusco, M., Verhaegh, J., Hetel, L., Richard, J.-P., and Michiels, W. (2019). Achieving an L2 string stable one vehicle look-ahead platoon with heterogeneity in time-delays. In *European Control Conference, Naples, Italy*.

Dileep, D. and Michiels, W. (2018a). tds_hopt-cacc, a software tool to design CACC controller for heterogenous vehicular platoons through structure exploitation. Available at http://twr.cs.kuleuven.be/research/

software/delay-control/CACCproblem.zip.

Dileep, D. and Michiels, W. (2018b). tds_hopt-nse, a software tool for structured controller design for DDAEs with network structure exploitation. Available at http://twr.cs.kuleuven.be/research/software/delay-control/tds_hopt-nse.zip.

Dileep, D. and Michiels, W. (2018c). tds_hopt-nse v2, a software tool for sampled data structured controller design for DDAEs with network structure exploitation. Available at http://twr.cs.kuleuven.be/research/software/delay-control/tds_hopt-nse2.zip.

Dileep, D., Michiels, W., Hetel, L., and Richard, J.-P. (2018b). Design of robust structurally constrained controllers for mimo plants with time-delays. In *2018 European Control Conference (ECC)*, pages 1566–1571.

Dileep, D., Thomas, J., Hetel, L., Wouw, N. v. d., Richard, J.-P., and Michiels, W. (2020). Design of $\mathcal{L}_2$ stable fixed-order decentralised controllers in sampled data networks with time-delays. *European Journal of Control*.

Dileep, D., Van Parys, R., Pipeleers, G., Hetel, L., Richard, J.-P., and Michiels, W. (2018c). Design of robust decentralised controllers for MIMO plants with delays through network structure exploitation. *International Journal of Control*.

Donkers, M. C. F., Heemels, W. P. M. H., van de Wouw, N., and Hetel, L. (2011). Stability analysis of networked control systems using a switched linear systems approach. *IEEE Transactions on Automatic Control*, 56(9):2101–2115.

Erneux, T. (2009). *Applied Delay Differential Equations*. Surveys and Tutorials in the Applied Mathematical Sciences. Springer New York.

Fardad, M., Lin, F., and Jovanovic, M. R. (2014). Design of optimal sparse interconnection graphs for synchronization of oscillator networks. *IEEE Transactions on Automatic Control*, 59(9):2457–2462.

Feingesicht, M., Polyakov, A., Kerhervé, F., and Richard, J.-P. (2017). Siso model-based control of separated flows: Sliding mode and optimal control approaches. *International Journal of Robust and Nonlinear Control*, 27(18):5008–5027.

Ferguson, J., Donaire, A., Knorn, S., and Middleton, R. H. (2017). Decentralized control for L2 weak string stability of vehicle platoon. *IFAC-PapersOnLine*,

50(1):15012 – 15017. 20th IFAC World Congress.

Fiacchini, M. and Morarescu, I. (2016). Stability analysis for systems with asynchronous sensors and actuators. In *2016 IEEE 55th Conference on Decision and Control (CDC)*, pages 3991–3996.

Fiter, C., Korabi, T.-E., Etienne, L., and Hetel, L. (2018). *Stability of LTI Systems with Distributed Sensors and Aperiodic Sampling*, pages 63–82. Springer International Publishing.

Foley, C. and Mackey, M. C. (2009). Dynamic hematological disease: a review. *Journal of Mathematical Biology*, 58(1):285–322.

Fridman, E. (2002). Stability of linear descriptor systems with delay: a lyapunov-based approach. *Journal of Mathematical Analysis and Applications*, 273(1):24 – 44.

Fridman, E. (2014). *Introduction to Time-Delay Systems: Analysis and Control*. Systems & Control: Foundations & Applications. Springer International Publishing.

Fridman, E. and Shaked, U. (2002). An improved stabilization method for linear time-delay systems. *IEEE Transactions on Automatic Control*, 47(11):1931–1937.

Fujioka, H. (2007). Stability analysis of systems with aperiodic sample-and-hold devices. *IFAC Proceedings Volumes*, 40(23):310 – 315. 7th IFAC Workshop on Time Delay Systems TDS 2007, Nantes, France, 17–19 September, 2007.

Fujioka, H., Kao, C. Y., Almer, S., and Jonsson, U. (2005). Sampled-data H_∞ control design for a class of pwm systems. In *Proceedings of the 44th IEEE Conference on Decision and Control*.

Fusco, M., Semsar-Kazerooni, E., Ploeg, J., and van de Wouw, N. (2016). Vehicular platooning: Multi-layer consensus seeking. In *2016 IEEE Intelligent Vehicles Symposium (IV)*, pages 382–387.

Gao, F., Hu, X., Li, S. E., Li, K., and Sun, Q. (2018). Distributed adaptive sliding mode control of vehicular platoon with uncertain interaction topology. *IEEE Transactions on Industrial Electronics*, 65(8):6352–6361.

Gao, F., Li, S. E., Zheng, Y., and Kum, D. (2016). Robust control of heterogeneous vehicular platoon with uncertain dynamics and communication delay. *IET Intelligent Transport Systems*, 10(7):503–513.

Geromel, J. C., Bernussou, J., and de Oliveira, M. C. (1999). H2-norm optimization with constrained dynamic output feedback controllers: decentralized and reliable control. *IEEE Transactions on Automatic Control*, 44(7):1449–1454.

Graham, F. and Chung, F. (1996). *Spectral Graph Theory*. Regional conference series in mathematics. Conference Board of the mathematical sciences.

Gu, K., Kharitonov, V., and Chen, J. (2012). *Stability of Time-Delay Systems*. Control Engineering. Birkhäuser Boston.

Guanetti, J., Kim, Y., and Borrelli, F. (2018). Control of connected and automated vehicles: State of the art and future challenges. *Annual Reviews in Control*, 45:18 – 40.

Gumussoy, S. and Michiels, W. (2011). Fixed-order H-infinity control for interconnected systems using delay differential algebraic equations. *SIAM Journal on Control and Optimization*, 49(5):2212–2238.

Hale, J. K. and Verduyn Lunel, S. M. (2002). Strong stabilization of neutral functional differential equations. *IMA Journal of Mathematical Control and Information*, 19:5–23.

Helton, J. W. (1978). Orbit structure of the mobius transformation semigroup action onh-infinity (broadband matching). *Adv. in Math. Suppl. Stud.*, page 129–197.

Hetel, L., Fiter, C., Omran, H., Seuret, A., Fridman, E., Richard, J.-P., and Niculescu, S. I. (2017). Recent developments on the stability of systems with aperiodic sampling: An overview. *Automatica*, 76:309 – 335.

Hilhorst, G., Pipeleers, G., Michiels, W., Oliveira, R. C. L. F., Peres, P. L. D., and Swevers, J. (2016). Fixed-order linear parameter-varying feedback control of a lab-scale overhead crane. *IEEE Transactions on Control Systems Technology*, 24(5):1899–1907.

Hollot, C. V., Misra, V., and and, D. T. (2002). Analysis and design of controllers for aqm routers supporting tcp flows. *IEEE Transactions on Automatic Control*, 47(6):945–959.

Hristu-Varsakelis, D. and Levine, W. (2005). *Handbook of Networked and Embedded Control Systems*. Control Engineering - Birkhäuser. Birkhäuser Boston.

Ikeda, K., Shin, S., and Kitamori, T. (1993). Fault tolerance of decentralized

adaptive control. In *Proceedings ISAD 93: International Symposium on Autonomous Decentralized Systems*, pages 275–281.

Kao, C.-Y. and Lincoln, B. (2004). Simple stability criteria for systems with time-varying delays. *Automatica*, 40(8):1429 – 1434.

Kao, C.-Y. and Rantzer, A. (2007). Stability analysis of systems with uncertain time-varying delays. *Automatica*, 43(6):959 – 970.

Khalil, H. (2002). *Nonlinear Systems*. Pearson Education. Prentice Hall.

Kolmanovskii, V. and Myshkis, A. (1999). *Introduction to the Theory and Applications of Functional Differential Equations*. Mathematics and Its Applications. Springer Netherlands.

Kruszewski, A., Jiang, W. ., Fridman, E., Richard, J. P., and Toguyeni, A. (2012). A switched system approach to exponential stabilization through communication network. *IEEE Transactions on Control Systems Technology*, 20(4):887–900.

Lamnabhi-Lagarrigue, F., Annaswamy, A., Engell, S., Isaksson, A., Khargonekar, P., Murray, R. M., Nijmeijer, H., Samad, T., Tilbury, D., and den Hof, P. V. (2017). Systems and control for the future of humanity, research agenda: Current and future roles, impact and grand challenges. *Annual Reviews in Control*, 43:1 – 64.

Lavaei, J., Momeni, A., and Aghdam, A. G. (2008). A model predictive decentralized control scheme with reduced communication requirement for spacecraft formation. *IEEE Transactions on Control Systems Technology*, 16(2):268–278.

Li, S. E., Gao, F., Li, K., Wang, L., You, K., and Cao, D. (2018). Robust longitudinal control of multi-vehicle systems—a distributed h-infinity method. *IEEE Transactions on Intelligent Transportation Systems*, 19(9):2779–2788.

Li, S. E., Zheng, Y., Li, K., Wu, Y., Hedrick, J. K., Gao, F., and Zhang, H. (2017). Dynamical modeling and distributed control of connected and automated vehicles: Challenges and opportunities. *IEEE Intelligent Transportation Systems Magazine*, 9(3):46–58.

Li, X. and de Souza, C. E. (1997). Delay-dependent robust stability and stabilization of uncertain linear delay systems: a linear matrix inequality approach. *IEEE Transactions on Automatic Control*, 42(8):1144–1148.

Lunze, J. (1992). *Feedback control of large scale systems.* Prentice-Hall international series in systems and control engineering. Prentice-Hall.

Massioni, P. and Verhaegen, M. (2009). Distributed control for identical dynamically coupled systems: A decomposition approach. *IEEE Transactions on Automatic Control*, 54(1):124–135.

Massioni, P. and Verhaegen, M. (2010). A full block s-procedure application to distributed control. In *American Control Conference (ACC), 2010*, pages 2338–2343. IEEE.

McMillan, G. K. (2012). *Industrial Applications of PID Control*, pages 415–461. Springer London.

Meyer, C. (2000). *Matrix Analysis and Applied Linear Algebra:*. Other Titles in Applied Mathematics. Society for Industrial and Applied Mathematics.

Michiels, W. (2011). Spectrum-based stability analysis and stabilisation of systems described by delay differential algebraic equations. *IET Control Theory Applications*, 5(16):1829–1842.

Michiels, W., Fridman, E., and Niculescu, S.-I. (2009a). Robustness assessment via stability radii in delay parameters. *International Journal of Robust and Nonlinear Control*, 19(13):1405–1426.

Michiels, W., Hilhorst, G., Pipeleers, G., Vyhlídal, T., and Swevers, J. (2017). Reduced modelling and fixed-order control of delay systems applied to a heat exchanger. *IET Control Theory & Applications*, 11:3341–3352(11).

Michiels, W. and Niculescu, S. (2014). *Stability, Control, and Computation for Time-Delay Systems.* Society for Industrial and Applied Mathematics, Philadelphia, PA.

Michiels, W. and Nijmeijer, H. (2009). Synchronization of delay-coupled nonlinear oscillators: An approach based on the stability analysis of synchronized equilibria. *Chaos: An Interdisciplinary Journal of Nonlinear Science*, 19(3):033110.

Michiels, W., Vyhlídal, T., Ziték, P., Nijmeijer, H., and Henrion, D. (2009b). Strong stability of neutral equations with an arbitrary delay dependency structure. *SIAM Journal on Control and Optimization*, 48(2):763–786.

Mirkin, L. (2007). Some remarks on the use of time-varying delay to model sample-and-hold circuits. *IEEE Transactions on Automatic Control*, 52(6):1109–1112.

Mirkin, L., Rotstein, H., and Palmor, Z. (1999). H_2 and H_∞ design of sampled-data systems using lifting. part I: General framework and solutions. *SIAM Journal on Control and Optimization*, 38(1):175–196.

Monnet, D., Ninin, J., and Clement, B. (2016). A global optimization approach to structured regulation design under h-infinity constraints. In *2016 IEEE 55th Conference on Decision and Control (CDC)*, pages 658–663.

Morarescu, I.-C., Michiels, W., and Jungers, M. (2016). Effect of a distributed delay on relative stability of diffusely coupled systems, with application to synchronized equilibria. *International Journal of Robust and Nonlinear Control*, 26(7):1565–1582.

Ogata, K. (2010). *Modern Control Engineering*. Instrumentation and controls series. Prentice Hall.

Olfati-Saber, R. and Murray, R. M. (2004). Consensus problems in networks of agents with switching topology and time-delays. *IEEE Transactions on Automatic Control*, 49(9):1520–1533.

Oncu, S., Ploeg, J., van de Wouw, N., and Nijmeijer, H. (2014). Cooperative adaptive cruise control: Network-aware analysis of string stability. *IEEE Transactions on Intelligent Transportation Systems*, 15(4):1527–1537.

Overton, M. L. (2009). HANSO: a hybrid algorithm for non-smooth optimization. *Computer Science, New York University*.

Ozer, S. M. and Iftar, A. (2015). Decentralized controller design for time-delay systems by optimization. *IFAC-PapersOnLine*, 48(12):462 – 467.

Partington, J. R. and Bonnet, C. (2004). H-infinity and bibo stabilization of delay systems of neutral type. *Systems and Control Letters*, 52(3):283 – 288.

Pecora, L. M. and Carroll, T. L. (1998). Master stability functions for synchronized coupled systems. *Phys. Rev. Lett.*, 80:2109–2112.

Pfifer, H. and Seiler, P. (2015). Robustness analysis of linear parameter varying systems using integral quadratic constraints. *International Journal of Robust and Nonlinear Control*, 25(15):2843–2864.

Ploeg, J., Semsar-Kazerooni, E., Lijster, G., van de Wouw, N., and Nijmeijer, H. (2015). Graceful degradation of cooperative adaptive cruise control. *IEEE Transactions on Intelligent Transportation Systems*, 16(1):488–497.

Ploeg, J., Shukla, D. P., van de Wouw, N., and Nijmeijer, H. (2014a). Controller

synthesis for string stability of vehicle platoons. *IEEE Transactions on Intelligent Transportation Systems*, 15(2):854–865.

Ploeg, J., van de Wouw, N., and Nijmeijer, H. (2014b). Lp string stability of cascaded systems: Application to vehicle platooning. *IEEE Transactions on Control Systems Technology*, 22(2):786–793.

Popov, A. and Werner, H. (2012). Robust stability of a multi-agent system under arbitrary and time-varying communication topologies and communication delays. *IEEE Transactions on Automatic Control*, 57(9):2343–2347.

Prieur, C., Queinnec, I., Tarbouriech, S., and Zaccarian, L. (2018). *Analysis and Synthesis of Reset Control Systems*. now.

Qin, W. B., Gomez, M. M., and Orosz, G. (2017). Stability and frequency response under stochastic communication delays with applications to connected cruise control design. *IEEE Transactions on Intelligent Transportation Systems*, 18(2):388–403.

Rejeb, J. B., Morărescu, I.-C., and Daafouz, J. (2018). Control design with guaranteed cost for synchronization in networks of linear singularly perturbed systems. *Automatica*, 91:89 – 97.

Richard, J.-P. (2003). Time-delay systems: an overview of some recent advances and open problems. *Automatica*, 39(10):1667 – 1694.

Richard, J.-P. and Divoux, T. (2007). *Systèmes commandés en réseau*. IC2 Systèmes Automatisés. Hermès-Lavoisier.

Sabau, S., Oara, C., Warnick, S., and Jadbabaie, A. (2017). Optimal distributed control for platooning via sparse coprime factorizations. *IEEE Transactions on Automatic Control*, 62(1):305–320.

Samad, T. (2019). *IFAC Industry Committee Update, Initiative to Increase Industrial Participation in the Control Community*. Number 2 in Newsletters April 2019. IFAC.

Savastuk, S. K. and Siljak, D. D. (1994). Optimal decentralized control. In *Proceedings of 1994 American Control Conference - ACC '94*, volume 3, pages 3369–3373 vol.3.

Shafi, S. Y., Arcak, M., and El Ghaoui, L. (2012). Graph weight allocation to meet laplacian spectral constraints. *IEEE Transactions on Automatic Control*, 57(7):1872–1877.

Shamma, J. S. (1994). Robust stability with time-varying structured uncertainty. *IEEE Transactions on Automatic Control*, 39(4):714–724.

Shi, X. Q., Davison, D. E., Kwong, R., and Davison, E. J. (2016). Optimized decentralized control of large scale systems. In *2016 12th IEEE International Conference on Control and Automation (ICCA)*, pages 127–134.

Siljak, D. (2013). *Decentralized Control of Complex Systems*. Dover Publications.

Sipahi, R., Niculescu, S., Abdallah, C. T., Michiels, W., and Gu, K. (2011). Stability and stabilization of systems with time delay. *IEEE Control Systems Magazine*, 31(1):38–65.

Stankovic, S. S., Stanojevic, M. J., and Siljak, D. D. (2000). Decentralized overlapping control of a platoon of vehicles. *IEEE Transactions on Control Systems Technology*, 8(5):816–832.

Tannenbaum, A. (1980). Feedback stabilization of linear dynamical plants with uncertainty in the gain factor. *International Journal of Control*, 32(1):1–16.

Thomas, J., Hetel, L., Fiter, C., van de Wouw, N., and Richard, J. (2018). L2-stability criterion for systems with decentralized asynchronous controllers. In *2018 IEEE Conference on Decision and Control (CDC)*, pages 6638–6643.

Toscano, R. (2013). *Structured Controllers for Uncertain Systems: A Stochastic Optimization Approach*. Advances in Industrial Control. Springer London.

van Schuppen, J. and Villa, T. (2014). *Coordination Control of Distributed Systems*. Lecture Notes in Control and Information Sciences. Springer International Publishing.

Vidyasagar, M. (2002). *Nonlinear Systems Analysis*. Society for Industrial and Applied Mathematics, second edition.

Wang, C. and Nijmeijer, H. (2015). String stable heterogeneous vehicle platoon using cooperative adaptive cruise control. In *2015 IEEE 18th International Conference on Intelligent Transportation Systems*, pages 1977–1982.

Wang, M., Li, H., Gao, J., Huang, Z., Li, B., and van Arem, B. (2017). String stability of heterogeneous platoons with non-connected automated vehicles. In *2017 IEEE 20th International Conference on Intelligent Transportation Systems (ITSC)*, pages 1–8.

Wang, T., O'Neill, D., and Kamath, H. (2015). Dynamic control and optimization of distributed energy resources in a microgrid. *IEEE Transactions on Smart Grid*, 6(6):2884–2894.

Zames, G. (1966). On the input-output stability of time-varying nonlinear feedback systems–part ii: Conditions involving circles in the frequency plane and sector nonlinearities. *IEEE Transactions on Automatic Control*, 11(3):465–476.

Zames, G. (1981). Feedback and optimal sensitivity: Model reference transformations, multiplicative seminorms, and approximate inverses. *IEEE Transactions on Automatic Control*, 26(2):301–320.

Zecevic, A. I. and Siljak, D. D. (2004). Design of robust static output feedback for large-scale systems. *IEEE Transactions on Automatic Control*, 49(11):2040–2044.

Zegers, J. C., Semsar-Kazerooni, E., Fusco, M., and Ploeg, J. (2017). A multi-layer control approach to truck platooning: Platoon cohesion subject to dynamical limitations. In *2017 5th IEEE International Conference on Models and Technologies for Intelligent Transportation Systems (MT-ITS)*, pages 128–133.

Zeng, H., He, Y., Wu, M., and She, J. (2015). Free-matrix-based integral inequality for stability analysis of systems with time-varying delay. *IEEE Transactions on Automatic Control*, 60(10):2768–2772.

Özer, S. M. and İftar, A. (2015). Decentralized controller design for time-delay systems by optimization. *IFAC-PapersOnLine*, 48(12):462 – 467. 12th IFAC Workshop onTime Delay SystemsTDS 2015.

Zhang, B., Kruszewski, A., and Richard, J.-P. (2014). A novel control design for delayed teleoperation based on delay-scheduled lyapunov–krasovskii functionals. *International Journal of Control*, 87(8):1694–1706.

Zhang, X.-M., Wu, M., She, J.-H., and He, Y. (2005). Delay-dependent stabilization of linear systems with time-varying state and input delays. *Automatica*, 41(8):1405 – 1412.

Zheng, Y., Li, S. E., Wang, J., Wang, L. Y., and Li, K. (2014). Influence of information flow topology on closed-loop stability of vehicle platoon with rigid formation. In *17th International IEEE Conference on Intelligent Transportation Systems (ITSC)*, pages 2094–2100.

Curriculum vitae

Deesh Dileep

E-mail	: deesh.dileep@gmail.com
Date of Birth	: 16 July 1992
LinkedIn	: www.linkedin.com/in/deeshdileep/



Education

Mar. 2017 - Feb. 2020	Joint-Ph.D. at KU Leuven, Belgium & Centrale Lille, France.
Sep. 2014 - Aug. 2016	M.Sc. in Electrical Engineering (Intelligent Electrical Power Grids group) at TU Delft, Netherlands.
Sep. 2010 - Apr. 2014	B.E. in Electrical and Electronics Engineering at R. V. College of Engineering, Bangalore, India.

Experience

Apr. 2018 - Jun. 2018	Secondment at Dept. of Integrated Vehicle Safety, TNO, Helmond, Netherlands.
Oct. 2016 - Feb. 2017	Electrical design engineer at ESB International, Bahrain.
Jul. 2015 - Aug. 2016	Trainee (Internship & Master thesis) at TenneT TSO B.V., Arnhem, Netherlands.

List of publications

Journal

- *Design of stabilising fixed-order decentralised controllers for sampled-data network with time-delays.* D. Dileep, J. Thomas, L. Hetel, N. v. d. Wouw, J.-P. Richard and W. Michiels. European Journal of Control (2020).
- *Design of robust decentralised controllers for MIMO plants with delays through network structure exploitation.* D. Dileep, R. V. Parys, G. Pipeleers, L. Hetel, J.-P. Richard and W. Michiels. International Journal of Control (2018).

Proceedings of conference

- *Achieving an $\mathcal{L}_2$ string stable one vehicle look-ahead platoon with heterogeneity in time-delays.* D. Dileep, M. Fusco, J. Verhaegh, L. Hetel, J.-P. Richard and W. Michiels. European Control Conference 2019, Italy.
- *A scalable design method for stabilising decentralised controllers for networks of delay-coupled systems.* D. Dileep, F. Borgioli, L. Hetel, J.-P. Richard and W. Michiels. 5th IFAC Conference on Analysis and Control of Chaotic Systems 2018, Netherlands.
- *Design of robust structurally constrained controllers for MIMO systems with time-delays.* D. Dileep, W. Michiels, L. Hetel and J.-P. Richard. European Control Conference 2018, Cyprus.



FACULTY OF ENGINEERING SCIENCE
DEPARTMENT OF COMPUTER SCIENCE
NUMERICAL ANALYSIS AND APPLIED MATHEMATICS
Celestijnenlaan 200A box 2402
B-3001 Leuven